PB93143881

REACTIVITY OF SURFACE CARBONACEOUS INTERMEDIATES

TECHNISCHE UNIV. EINDHOVEN (NETHERLANDS)

19 JUN 1992

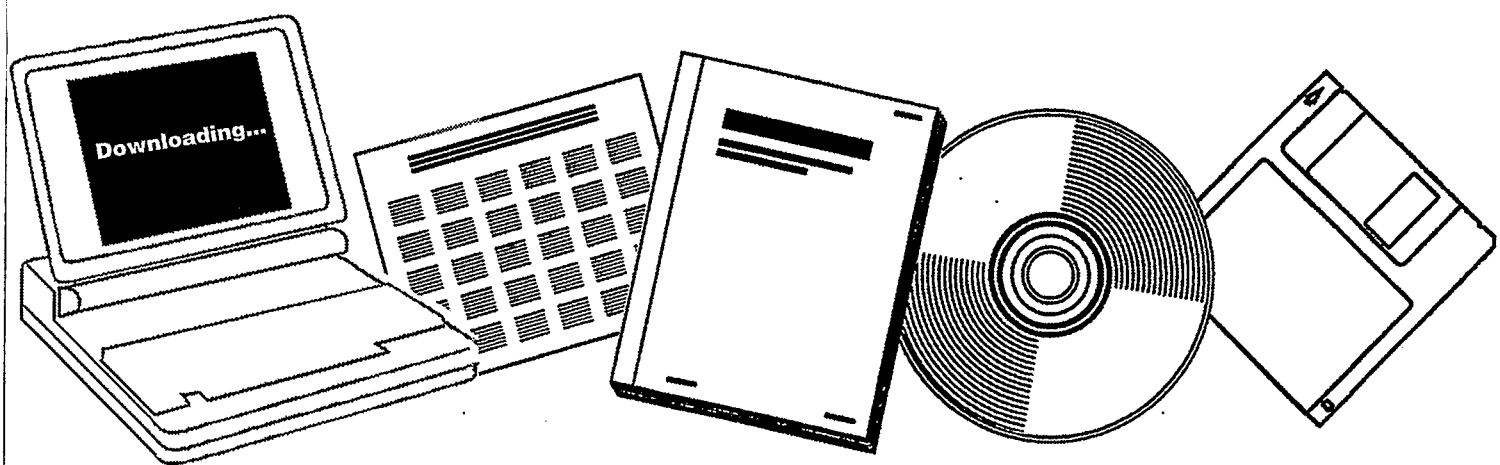

U.S. Department of Commerce
National Technical Information Service

One Source. One Search. One Solution.

NTIS

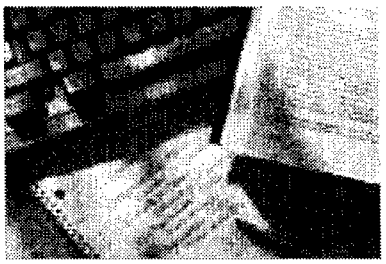

Providing Permanent, Easy Access to U.S. Government Information

National Technical Information Service is the nation's largest repository and disseminator of government-initiated scientific, technical, engineering, and related business information. The NTIS collection includes almost 3,000,000 information products in a variety of formats: electronic download, online access, CD-ROM, magnetic tape, diskette, multimedia, microfiche and paper.

Search the NTIS Database from 1990 forward

NTIS has upgraded its bibliographic database system and has made all entries since 1990 searchable on **www.ntis.gov.** You now have access to information on more than 600,000 government research information products from this web site.

Link to Full Text Documents at Government Web Sites

Because many Government agencies have their most recent reports available on their own web site, we have added links directly to these reports. When available, you will see a link on the right side of the bibliographic screen.

Download Publications (1997 - Present)

NTIS can now provides the full text of reports as downloadable PDF files. This means that when an agency stops maintaining a report on the web, NTIS will offer a downloadable version. There is a nominal fee for each download for most publications.

For more information visit our website:

www.ntis.gov

U.S. DEPARTMENT OF COMMERCE
Technology Administration
National Technical Information Service
Springfield, VA 22161

The Reactivity of Surface Carbonaceous Intermediates

Een studie naar de reactiviteit van oppervlakte kool gevormd uit CO en CH_4 op gedragen groep VIII metaalkatalysatoren.

PROEFSCHRIFT

ter verkrijging van de graad van doctor aan de Technische Universiteit Eindhoven, op gezag van de Rector Magnificus, prof. dr. J.H. van Lint, voor een commissie aangewezen door het College van Dekanen in het openbaar te verdedigen op vrijdag 19 juni 1992 om 16.00 uur

door

Tijs Koerts

geboren te Haarlem

druk: wibro dissertatiedrukkerij, helmond.

Dit proefschrift is goedgekeurd door de promotoren:

1e promotor: prof. dr. R.A. van Santen
2e promotor: prof. dr. V. Ponec

The research described in this thesis was carried out at the Schuit Institute of Catalysis, department of Inorganic Chemistry and Catalysis, Eindhoven University of Technology (P.O. Box 513, 5600 MB, the Netherlands) and was financially supported by the Dutch department of Fundamental Chemical Research (SON and NWO).

Stellingen behorende bij het proefschrift

The Reactivity of Surface Carbonaceous Intermediates

door

Tijs Koerts

Juni - 1992

1. Door het introduceren van transiente stappen bij reakties over heterogene katalysatoren, kunnen nieuwe (methaan) conversie routes gecreëerd worden.

   Hoofdstuk 6 en 7 van het bijbehorende proefschrift.

2. De directe omzetting van methaan naar ethaan, zoals voorgesteld door Belgued en anderen, is een ineffectieve manier om zeer zuivere methaan te voorzien van spoortjes ethaan en waterstof.

   Belgued M., Amariglio H., Pareja P., Amariglio A. & Saint-Juste J., *Nature*, **352**, 789 (1991).

3. De proeven zoals uitgevoerd door Takeuchi en Katzer, zijn niet geschikt om reaktieve kool aan te tonen op gedragen rhodium katalysatoren.

   Takeuchi A. & Katzer R., *J. Catal.*, **82**, 351 (1983).

4. De selectieve oxidatie van methaan met ozon naar formaldehyde bij 180 °C over bariumperoxide gepromoteerd met zilver, zoals beschreven in [1], is niet reproduceerbaar.

   [1] Holm M.M. & Reichl E.H., Fiat report nr. 1085, Office of military government for germany (U.S.), March 31 (1947).

Stellingen

5. De veronderstelling van Michalski en andere, dat bacterio-chlorophil *a* als zodanig niet in groene bacteriën voorkomt, is op niets gebaseerd.

Michalski T.J., Hunt J.E., Bouwmann M.K., Smith U., Bardeen K., Gest H., Norris J.R., & Katz J.J., *Proc. Natl. Acad. Sci. USA*, **84**, 2570-2574 (1987).

6. Bij het modeleren van de Si^{4+}/Si en Al^{3+}/Al intensiteitsverhouding bij hoekafhankelijke XPS, gaat Gries ten onrechte voorbij aan invloeden veroorzaakt door oppervlakte ruwheid.

Gries W.H., *J. Vac. Sci. Technol.*, **A7**, 1655 (1989).

7. Het meten van waterstofchemisorptie aan edelmetaalkatalysatoren op alumina en silica, na evacuatie bij hoge temperatuur, kan leiden tot afwijkende H/M waarden door oxidatie van het metaal door water of OH groepen.

Kip B.J., Duivenvoorden F.B.M., Koningsberger D.C. & Prins R., *J. Am. Chem. Soc.*, **108**, 5633 (1986).

8. De verplichting van SON om het bijwonen van een tweedaags-binnenlands congres gepaard te laten gaan met het schrijven van een verslag, gaat voorbij aan de doelstelling oio's en aio's op gelijke wijze te behandelen.

9. Het valt te betreuren dat geloofsconservatismen, belangrijke bewustwordingsprocessen, decennia lang kunnen vertragen.

10. Politieke partijen zouden het landsbelang nadrukkelijker moeten stellen boven dat van hun individuele partijbelangen.

..... daarover is al zoveel geschreven, daar heeft de waarheid geen kans meer.

M. Botwinnik

Voor Werner en Riet

Dankwoord

De 241.117 characters zoals die voor u gerangschikt liggen, zijn allerminst het resultaat van één promovendus. Met groot genoegen wil ik dan ook alle mensen bedanken die mij de afgelopen vier jaar praktisch en geestelijk hebben bijgestaan, om dit boekje tot stand te brengen.

Allereerst wil ik mijn eerste promotor Rutger van Santen bijzonder bedanken. Hij heeft mij altijd weten te stimuleren en veel van zijn ideeën zijn in dit boekje terug te vinden. Vladimir Ponec komt niet alleen dank toe voor zijn precieze correcties die hij als tweede promotor heeft aangebracht maar ook voor het helpen opzetten van het onderzoek dat ten dele geïnspireerd is op het werk in zijn vakgroep. Professor Marin wil ik hartelijk bedanken voor het aandachtig doorlezen en corrigeren van het proefschrift en voor het lenen van de 'puls-kar' waar samen met Han van Kasteren zeer leuke resultaten mee zijn behaald. Hans Niemantsverdriet, bedankt voor het goede kommentaar op mijn boekje en de plezierige ervaringen die zich tot in Amerika toe uitstrekken.

Joop wil ik bijzonder bedanken, zonder jouw hulp was mijn promotie nooit begonnen of geëindigd; ik heb zeer veel geprofiteerd van je technische inzichten en praktische ervaring. Wout jij wordt hartelijk bedankt, omdat je je 'gouden handen' ook voor mij liet werken.

Leo, bijzonder bedankt voor de vele discussies en analyses van metingen; je wist altijd direct aan te geven waar de fout zat! Marius, ik heb het zeer gewaardeerd dat je vier jaar lang, nooit te beroerd was om computer-commando's en de juiste syntaxis van mijn Fortran-routines uit je mouw te schudden. Ad, hartelijk bedankt voor het gebruik van je programma's en de hulp bij het uitvoeren van de ASED berekeningen. Dik van Langeveld en Luc Nonneman, jullie hebben mij zeer geholpen met het uitvoeren van mijn eerste transiënte proeven met rhodium katalysatoren.

De studenten die mij geholpen hebben bij het uitvoeren van de vele metingen wil ik allen hartelijk bedanken: de afstudeerders Wim Welters, Mark Deelen, Gert-Jan Kock, Cor Vermeiden en Jef Willigers; de 'p3-ers': M.J. de Fauw, R.A. de Haan, R.C. Hutermans, G.M. Verschelling, B. Groenendaal en S.

Vrijland en de 'p2-ers': E.A. Verlangen, F.J. Smedema, M. van Stekelenburg, A. Toonders, F. Moers, P.J. Deckers, S. Krijnen en S. Frings.

Peter en Anja Wijnen wil ik hartelijk bedanken voor de bijdrage die mijn verblijf bij DuPont in Wilmington tot een zeer aangename tijd hebben gemaakt; Leo Manthers en Jan Leroe voor de mij geboden mogelijkheid tot uitvoeren van TAP metingen bij DuPont; Jos voor het zeer nauwkeurig uitvoeren van de IR metingen; Jean-Paul voor het uitvoeren van de LEIS metingen; Arthur voor de XPS metingen die je voor mij hebt verricht en Mark de Boer voor het maken van de vanadium/silica kat, en in het bijzonder voor de goede vriendschap de afgelopen negen jaar.

Verder wil ik alle mensen van zowel de 'oude' en 'nieuwe' koffiegroep alsmede de 'borrel-bezoekers' bijzonder bedanken, voor hun gezelschap.

Op speciale wijze komt Astrid dank toe, die er als geen ander voor gezorgd heeft, dat ik mijn promotie als een zeer plezierige tijd heb kunnen ervaren.

Tenslotte dank ik mijn ouders, jullie hebben mij altijd zeer goed gesteund.

Contents

Chapter 1 Introduction 1

Chapter 2 Reactivity of CO on vanadium-promoted rhodium catalysts as studied with transient techniques 11

Chapter 3 Transient response study of CO insertion into CH_x surface intermediates on a vanadium promoted rhodium catalyst 33

Chapter 4 The reactivity of surface carbon from carbonmonoxide on vanadium promoted rhodium catalysts 51

Chapter 5 The reaction path for recombination of surface CH_x species 61

Chapter 6 Hydrocarbon formation from methane by a low temperature two step reaction sequence 73

Chapter 7 Homologation of olefins with methane on transition metal catalyst 93

Chapter 8 General conclusions 111

Samenvatting 115

Curriculum Vitae 119

1

Introduction

GENERAL

This thesis concerns the general aspects of carbon-carbon bond formation. This is an important elementary reaction step, which is of potential or practical use in the catalytic cycle of many reactions. The formation of a carbon-carbon bond often implies the production of more valuable products. Examples can be found in a wide area of catalytic reactions of current interest, proceeding via different intermediates:

- Direct routes for methane conversion as oxidative coupling and pyrolysis form carbon-carbon bonds from radicals in the gas phase.
- The chain growth in the Fischer-Tropsch reaction occurs by recombination of surface carbonaceous intermediates on metal catalysts.
- The coupling of methanol molecules to gasoline using acid ZSM-5 zeolites, is another route for C_1 oligomerization. Also alkylation reactions can be performed on zeolites with a carbenium ion as reaction intermediate.
- In homogeneous catalytic systems carbon-carbon bond formation is widely used in oligomerization and polymerization reactions. Further homogeneous hydroformylation reactions can form carbon-carbon bonds between olefins and CO. In homogeneous systems, organometallic complexes can form reaction intermediates.
- Homogeneous super-acids are claimed for their ability to form carbon-carbon bonds in e.g. the ethylation of methane to propane.
- Platinum clusters in zeolites are able to initiate a carbon-carbon bond within an adsorbed n-hexane molecule, resulting in benzene.

Carbon-carbon bond formation in acid and base catalysis is relatively well understood. Protons e.g. catalyse olefin polymerization, alkylation and dehydration of methanol to olefins and aromatics. Typical base catalysed reactions are classical organic reactions as aldol condensation.

In this study the microscopic aspects of carbon-carbon bond formation reactions on heterogeneous metal catalysts will be considered. This elementary step is still not completely understood. Two reactions are studied in detail. The first being carbon-carbon bond formation in CO hydrogenation as occurring in Fischer-Tropsch like reactions. The second concerns carbon-carbon bond formation in the transition metal catalysed conversion of methane into higher hydrocarbons.

SYNTHESIS GAS CONVERSION

Gasoline is a very important fuel and although reformulated, it is not likely to be replaced in the near future. The oil crises in the seventies demonstrated the dependence of the western countries on the large crude sources in the middle east countries. To become less dependent from the instability in that region, a general route for the creation of gasoline and other products via synthesis gas was developed (see Fig. 1). Also the analysis of the world energy sources indicated that, sooner or later, methane or coal have to be used for the production of gasoline, instead of the limited available crude oil.

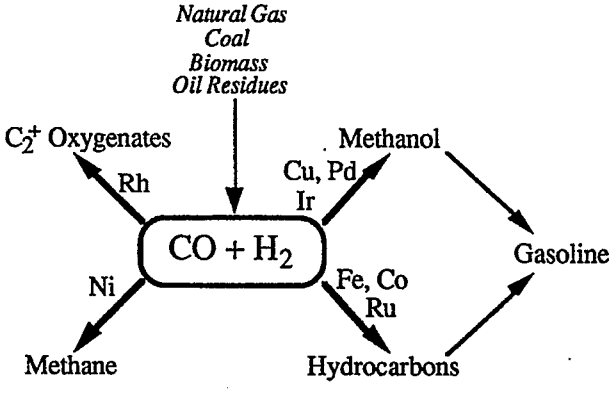

Figure 1. General route for the conversion of carbon containing materials via synthesis gas to products.

Coal and methane, which are world wide available in very large quantities, can be converted by steam reforming or selective oxidation into synthesis gas. Synthesis gas owes its name to the ability to be converted selectively into different products when using the right catalyst and reaction conditions. It can be transformed into methane over a nickel catalyst, into methanol using a copper/sink catalyst, into hydrocarbons using the Fischer-Tropsch reaction and into oxygen containing products with two or more carbon atoms, over rhodium based catalysts. Subsequently methanol and hydrocarbons can be converted into gasoline using zeolites.

The conversion of synthesis gas is related to the use of bimetallic catalysts. Bimetallic catalysts are of great fundamental interest. The mechanism according to which two metals can create a more active catalyst than the two separate metals, has still many open questions.

Use of oxidic promoters

The bimetallic catalysts, as often used in synthesis gas conversion, consist of an active noble metal of the group (Pt, Ir, Pd, Rh, Ru, Ni or Co) that is promoted or supported on a less noble metal of the group II to VII including Fe. Especially in selective hydrogenation reactions such bimetallic catalyst systems are often used. Selective hydrogenation of CO to oxygenated products over group VIII transition metals, is related to the addition of oxidic metal promoters. Methanol producing catalyst based on copper [1] iridium [2] or paladium [3], have high selectivity when promoted by metal oxides. The production of higher oxygenates from synthesis gas over rhodium based catalyst, as considered in this study, is also related to the use of oxygen containing promoters.

When this study was started, the conversion of synthesis gas to ethanol and ethanal over rhodium based catalysts, had been extensively studied [4-7]. It was well established that for high oxygenate selectivity, oxidic metal promoters are necessary (see ref's 5-39 chapter 2). It was also known that high selectivities for oxygenated products (<60%) could only be obtained at low conversion, so that the yield per pass was limited. This made the reaction less attractive for commercial purposes. However, the role of the oxygenate promoter remained a matter of great interest from fundamental point of view. Although many promoter effects have been reported, the working of the promoter in terms of changes in the rate of elementary reaction steps was not well understood [8].

Promoter effects

Structure effects. Through the addition of a promoter the catalyst morphology can be changed. More open active surfaces can be stabilized or catalyst dispersion can be changed, which can increase the catalyst performance. A very intriguing problem is the so called Small Metal Support Interaction (SMSI) [9]. This is a name for the observation that catalysts consisting of a noble metal supported on metals like TiO_2 and V_2O_5 show a suppressed CO or H_2 chemisorption capacity after reduction at temperatures around 400 °C. This was explained by the migration of sub-oxides ($TiO_{(2-x)}$, $V_2O_{(5-x)}$) over the metal particle [10,11] and by electronic effects [12]. Other structure effects are reviewed by Van Santen [13].

Electronic effects. Electrostatic effects around promoter ions can induce changes in the bondstrength of adsorbed molecules [8,14-16]. Further a decrease

in the local work function induced by alkali promoters has been observed [17]. It has also been suggested that a promoter donates electronic density to a metal particle, which increases its Fermi level [18]. This can result in an increased 'backdonation' into the $2\pi^*$ orbital of an adsorbed CO molecule, lowering the stretch frequency of CO [19].

Directs interaction with adsorbates. Oxidic metal promoters can have direct interactions with adsorbed surface species. A well known example is the observation of the so called 'tilted CO' using Infra Red spectroscopy [20-22]. Tilted CO is proposed to be adsorbed with its carbon atom to a noble metal and with its oxygen end to a promoter. Another example is the stabilization of oxygenated intermediates induced by metal oxide promoters [23-25]. Further 'hydrogen spillover' can be classified as such an effect; the transition metal promoter is supposed to act as a dynamic hydrogen reservoir for hydrogen that is dissociated by the noble metal.

Modification of the active phase. It has been suggested that the production of oxygenated products like methanol and ethanol from synthesis gas, is related to the presence of noble metal ions [26-28]. A less noble transition metal is able to create such active centres. Also mixed stoichiometric compounds (metal bronzes) can be formed that can have intrinsic activity.

METHANE CONVERSION

Methane is world wide available in large quantities and is a useful fuel, but very difficult to transport over long distances. Therefore interest exists to transform methane in better transportable and more valuable products. The most well known routes for methane conversion are summarized in figure 2.

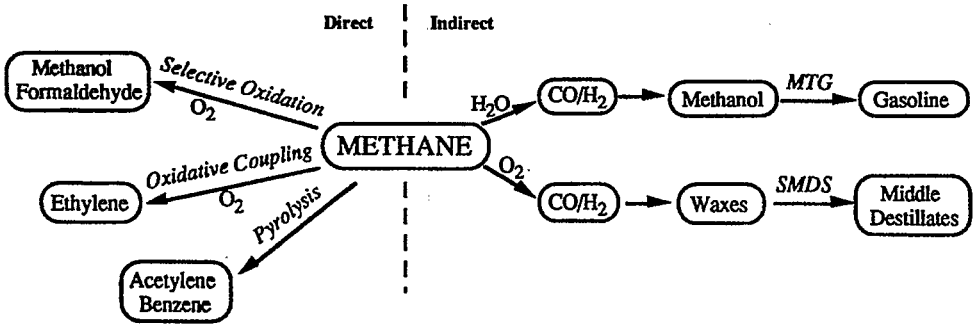

Figure 2. Scheme of direct (1 step) and indirect (multiple step) routes of methane conversion to products.

- Direct selective oxidation of methane to methanol and formaldehyde is of interest because it eliminates one or two conversion steps compared to the route via synthesis gas. The main problem in selective oxidation is the relative rapid consecutive oxidation of the products to CO and CO_2, limiting the overall yield. Selective methane oxidation routes are reviewed by Pitchai and Klier [29], by Foster [30] and by Pasquon [51].

- Oxidative coupling of methane to ethene is reviewed in references [31-33] and can be performed for a short time with yields up to 25 %. Despite tremendous efforts, this yield has hardly increased the last couple of years and the development of stable catalysts remains a problem.

- Methane pyrolysis occurs at temperatures above 1200 °C, by radicals in the gas phase and is not truly catalytic [34]. The main problem is to prevent graphite formation. The yields of this route are limited to about 12 %.

- Until now only two commercial indirect routes have been realized for methane transformation, using conversion via synthesis gas into hydrocarbons [35]. In 1985 Mobil build a plant in New Zealand to convert methane via synthesis gas and methanol into gasoline [36,37]. In 1991 Shell build a plant in Malaysia for the transformation of methane via synthesis gas and the Fischer-Tropsch reaction into middle destillates and other fuels [38,39]. Because of the laboriousness of these methane conversion processes, consisting of at least three steps, new routes for methane conversion remain of great interest.

The problem of methane conversion is related to that of C-H activation in alkanes [40]. Methane is thermodynamically very stable, it has a noble gas like configuration with strong tetrahedral C-H bonds, which lack from polarity. Therefore most of the methane conversion routes require high operation temperatures. Selective C–H activation in small alkanes has been realized at low temperatures using organometal complexes [41,42]. The instability of such complexes limits reaction to low temperature were the catalyst activity is low.

Most of the methane conversion reactions, use reagents like water, oxygen or chlorine. These oxidants are corrosive, while chlorine has a large draw back because of its poisonousness. The use of pure oxygen, as in the Shell middle destillate synthesis process, is expensive: oxygen has to be separated cryogenical from air. The oxygen atoms result in the final products CO_2 and H_2O. Also when water is used in steam reforming, the production of synthesis gas is expensive: up to 80% of the total costs of the methane conversion route is due to synthesis gas formation [43]. This means that methane conversion routes into hydrocarbons, that can circumvent the high conventional operation temperatures, and do not require expensive oxidants, are of world wide interest.

SCOPE OF THIS THESIS

As the title indicates this thesis will concentrate on the reactivity of surface carbon, adsorbed on group VIII transition metal catalysts. Adsorbed carbonaceous intermediates are important reaction intermediates in reactions like metathesis [44], catalytic reforming [45], steam reforming [46], Fischer-Tropsch synthesis [47], hydrogenolysis [48] and isomerization [49,50]. The state of the adsorbed intermediates are of great importance to both practical and fundamental aspects of heterogeneous catalysis.

This study is restricted to carbonaceous intermediates on group VIII transition metal catalysts, which are formed from relative simple molecules as CO and CH_4. The dissociative adsorption of these molecules is widely studied on single crystals (ref's [52-55] for CO and ref's [56-64] for CH_4). Surface C_1 fragments can be formed also from dissociative adsorption of CH_2N_2 [65,66], CH_3NO_2 [67,68], chloro-methanes [69] and methyliodide [70]. In these references the reactivity for carbon-carbon bond formation of the carbonaceous surface species was shown.

This thesis will mainly concentrate on the C_1 surface intermediate, that has been shown to be a reaction intermediate in the Fischer-Tropsch reaction [71,72]. Figure 3 shows the different elementary reactions that such a CH_x surface intermediate can proceed.

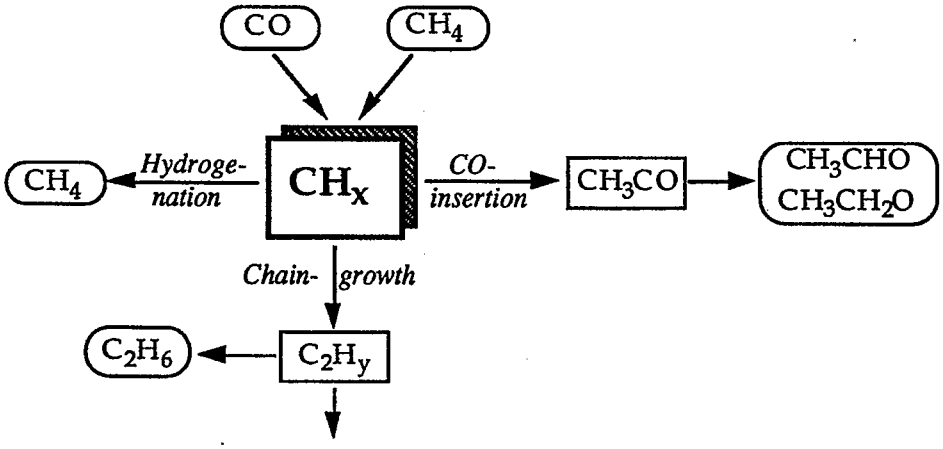

Figure 3. Different elementary reaction steps that an adsorbed CH_x intermediate can proceed during synthesis gas conversion.

The central CH_x intermediate can either be hydrogenated to methane, it can recombine with another surface C_1 fragment initiating chaingrowth and it can undergo CO insertion. It is an important reaction intermediate because its

reactivity for these different elementary reaction steps partially determines the selectivity for methane, hydrocarbons and oxygenates respectively. In this thesis we will analyse the influence of a metal promoter on the kinetics of the CH_x intermediate for these steps.

In fact the study concentrates on two main point:

What is the role of a vanadium promoter on the intrinsic reactivity of adsorbed surface intermediates for different elementary reaction steps on a rhodium catalyst?

Ponec [8] indicated recently that although the overall selectivity of promoted rhodium catalysts is very well documented, the extend of promotion of different reaction steps has not been understood. In this study supported rhodium has been chosen as metal catalyst because it is very sensitive for CO dissociation, and all the three elementary reaction steps from figure 3 are able to proceed on this catalyst. Vanadium is chosen as a model promoter because of its well known influence on the catalyst performance [73-80]. The influence of this promoter on the elementary reaction steps: CO dissociation, CO insertion, C_1 hydrogenation and chaingrowth propagation, will be analysed in the chapters 2, 3 and 4.

How does the reactivity of surface carbon from methane compare with that of surface carbon from CO and how can we convert methane to higher hydrocarbons?

It will be shown that from CO a very reactive surface C_1 intermediate can be formed that can produce hydrocarbons upon hydrogenation. We have investigated if a similar surface intermediate can be formed from methane. If we are able to produce such a reactive intermediate from methane, we can try to let it react to interesting products. This would supply new routes for methane conversion, as will be demonstrated in the chapters 6 and 7.

APPROACH

Transient techniques

In heterogeneous catalysis one normally operates under steady state conditions, with the great advantage of working continually. However, in this thesis mainly non steady state techniques are used like: ITKA (isotopic transient kinetic analysis), TPR (temperature programmed reduction), PSRA (pulse surface reaction rate analysis) and TPSR (temperature programmed

hydrogenation). Such transient techniques are able to demonstrate in situ the intrinsic reactivity of reactants. They also can be useful to catalyst characterization and to unravel changes in the rates of elementary reaction steps. Further it will be shown that when introducing transient steps, in special cases, new reactions can be made feasible (chapter 6 and 7).

Quantum chemical calculations using the ASED method

Practical analytical methods are limited in their detection when molecules are approached to close. Then theoretical calculations can become useful. To analyse the reactivity of the central CH_x fragments up to orbital level, quantum chemical calculations are applied using the ASED method. This Atom Superposition and Electron Delocalization Molecular Orbital theory is a modified Extended Hückel method [81-85]. The use of this semi empirical method is especially explored to predict trends in reactivity as a function of the metal d-valence electron occupation.

LITERATURE

1. Chinchen G.C., Denny P.J., Jennings J.R., Spencer M.S. and Waugh K.C., *Appl. Catal.*, **36**, 1 (1988).
2. Van Gruijthuijsen L., private communications.
3. Poutsma M.L., Elek L.F., Ibarbia P.A., Risch A.P. and Rabo J.A., *J. Catal.*, **52**, 157 (1978).
4. Bhasin M.M. and O' Conner G.L., Belgian Patent 824,822 to Union Carbide Corp. (1975).
5. Bhasin M.M., Belgian Patent 824,823 to Union Carbide Corp. (1975).
6. Ellgen P.C. and Bhasin M.M., US Patent 4,014,913 to Union Carbide Corp. (1977).
7. Ellgen P.C., Bartley W.J., Bhasin M.M. and Wilson T.P., *Adv. Chem.*, **178**, 147 (1979).
8. Ponec V. in *'New trends of CO activation'* (ed. L. Guzci) Elsevier Amsterdam, Studies in Surf. Sci. and Catal., **64**, 117 (1991).
9. Tauster S.J., Fung S.C. and Garten R.L., *J. Am. Chem. Soc.*, **100**, 170 (1978).
10. Levin M., Salmeron M., Bell A.T. and Somorjai G.A., *Surf. Sci.*, **169**, 123 (1986).
11. Bell A.T., in *'Catalyst design- progress and perspectives'* (ed. L.L. Hegedus), Wiley, New York, p.118 (1987).
12. Martens J.H.A., Prins R., Zandbergen H. and Koningsberger D.C., *J. Phys. Chem.*, **92**, 1903 (1988).
13. Van Santen R.A., *Surf. Sci.*, **6**, 251 (1991).
14. Nørskov J.K., *Physica*, **127 B**, 193 (1984).
15. Anderson A.B. and Awad Md.K., *J. Am. Chem. Soc.*, **107**, 7854 (1985).
16. Van Santen R.A., in *Proc. 8th Int. Conf. Catal.*, (Springer-Verlag, Berlin1984), vol. IV, p. 97.
17. Mross W.D., *Catal. Rev., -Sci. Eng.*, **25**, 591 (1983).
18. Weimer J.J., Umbach E. and Menzel D., *Surf. Sci.*, **155**,132 (1985).
19. Fleisch T.H., Hicks R.F. and Bell A.T., *J. Catal.*, **87**, 398 (1984).
20. Lavalley J.C., Saussey J., Lamotte J., Breault R., Hindermann J.P. and Kiennemann A., *J. Phys. Chem.*, **19**, 5941 (1990).
21. Ichikawa M., Hoffmann P.E. and Fukuoka A., *J. Chem. Soc., Chem. Comm.*, **18**, 1395 (1989).

22. Fukuoka A., Kimura T., Rao L-F. and Ichikawa M., *Catal. Today*, 6, 55 (1989).
23. Kikuzono Y., Kagami S., Naito S., Ouishi T. and Tamaru K., *Farad. Disc., Chem. Soc.*, 72, 143 (1981).
24. Orita H., Naito S. and Tamaru K., *J. Catal.*, 112, 167 (1988).
25. Bastein A.G.T.M., Ph.D. Thesis, Leiden University (1988).
26. Katzer J.R., Sleight A.W., Gajarde P., Michel J.B., Gleason E.F. and McMillan S., *Farad. Disc., Chem. Soc.*, 72, 121 (1981).
27. Van der Lee G. and Ponec V., *Catal. Rev., -Sci. Eng.*, 29, 183 (1987).
28. Iwasawa Y., Hayasaka T. and Ogasawata S., *Chem. Lett.*, 1982, 131.
29. Pitchai R. and Klier R., *Catal. Rev., -Sci. Eng.*, 28, 13 (1986).
30. Foster N.R., *Appl. Catal.*, 19, 1, (1985).
31. Amenomiya Y., Goledzinowski M., Birss V., Galsuszka J. and Sanger A. R., *Catal. Rev. - Sci. Eng.*, 32, 63 (1990).
32. Anderson J.H., *Appl. Catal.*, 47, 177 (1989).
33. Lunsford J.H., in *'New trends of CO activation'* (ed. L. Guzci). Studies in Surf. Sci. and Catal., 61, 3 (1991), Elsevier, Amsterdam.
34. Zwet, van der G. P., Hendriks, P. A. J. M. and van Santen, R. A., *Catal. Today*, 4, 365 (1989).
35. Rostrup-Nielsen J.P. in *'Catalysis, Science and Technology'* vol. 5 (eds Anderson and Boudart), Springer, Berlin (1984).
36. Chang C.D. and Silvestri A.J., *J. Catal.*, 47, 249 (1977).
37. Chang C.D. and Silvestri A.J., *J. Chemtech.*, 17, 624 (1987).
38. Sie S.T., Senden M.M.G. and Wechem van H.M.H., *Catal. Today*, 8, 371 (1991).
39. Eilers J., Posthuma S.A. and Sie S.T., *Catal. Lett.*, 7, 253 (1990).
40. Bearns M., *Nachr. Chem. Tech. Lab.*, 33, 292 (1985).
41. Crabtree R.H., *Chem. Rev.*, 85 245 (1985).
42. Bergman R.G., *Science*, 223, 4639 (1984).
43. Michel S., Linde A.G. and Hoëllriegelskreuth W., *Hydrocarbon Processing*, 68, 37 (1989).
44. Jørgensen K.A. and Schiøtt B., *Chem. Rev.*, 90, 1483 (1990).
45. Van Hook J.P., *Catal. Rev., -Sci. Eng.*, 21, 1 (1980)
46. Sinfelt J.H., Horwitz Z.H. and Rohrer J.C., *J. Catal.*, 48, (1962).
47. Pichler H., *Adv. in Catal.*, 4, 271 (1952).
48. Leconte M., Theolier A., Rojas D. and Basset M.J., *J. Am. Chem. Soc.*, 106, 1141 (1984).
49. Sachtler W.M.H., *Far. Disc. Chem. Soc.*, 72, 7 (1981).
50. Gault F.G., *Adv. Catal.*, 30, 1 (1981).
51. Pasquon I., *Catal. Today*, 1, 297 (1987)
52. Gorodetskii V.V. and Nieuwenhuys B., *Surf. Sci.*, 105, 299 (1981).
53. Yates Jr. J.T., Williams E.D. and Weinberg W.H.,*Surf. Sci.*, 91, 562 (1980).
54. Castner P., and Somorjai G.A., *Surf. Sci.*, 83, 60 (1979).
55. Castner P., and Somorjai G.A., *Surf. Sci.*, 103, L134 (1981).
56. M.B. Lee, Q.Y. Yang, S.L. Tand and S.T. Ceyer, *J. Chem. Phys.*, 85, 1693 (1986).
57. Beckerle J.D., Yang Q.Y., Johnson A.D. and Ceyer S.T., *J. Chem. Phys.*, 86, 7236 (1987).
58. M.T. Tavares, C.A. Bernardo, I. Alstrup, J.R. Rostrup-Nielson, *J. Catal.*, 100, 545 (1986).
59. Brass S.G. and G. Ehrlich, *Surf. Sci.*, 187, 21 (1987).
60. Sun Y.K. and Weinberg W.H., *J. Vac. Sci. Technol., A*, 8, 2445 (1990).
61. Schoofs G.R., Arumainayagam C.R., McMaster M.C. and Madix R.J., *Surf. Sci.*, 215, 1 (1989).
62. Sault A. G. and Goodman D. W., *Advances in Chem. Phys.*, 76, 153 (1989).
63 Rettner C. T., Pfnür H. E. and Auerbach D. J., *Phys. Rev. Lett.*, 54, 2716 (1985).
64. Kay B. D. and Coltrin M. E., *Surf. Sci.*, 198, L375 (1988).

65. Petit R.C. and Brady R., *J. Am. Chem. Soc.*, **102**, 6181 (1980).
66. Petit R.C. and Brady R., *J. Am. Chem. Soc.*, **103**, 1287 (1981).
67. Cavalcanti F.A.P., Oukac R., Wender I. and Blackmond D.G., *J. Catal.*, **123**, 260 (1990).
68. Cavalcanti F.A.P., Oukac R., Wender I. and Blackmond D.G., *J. Catal.*, **128**, 311 (1991).
69. Van Barneveld W.A.A. and Ponec V., *J. Catal.*, **88**, 382 (1984).
70. Williams J.A., Blackmond D.G., Wender I., Energy Res. Abstr. 1986, 11(16) Abstr. No. 35420 (1985).
71. Biloen P. and Sachtler W. M. H., *Adv. Catal.*, **30**, 165 (1981).
72. Wojeciechowski B.W., *Catal. Rev., -Sci. Eng.*, **30**, 629 (1988).
73. Kowalski J., Van der Lee G. and Ponec V., *Appl. Catal.*, **19**, 423 (1985).
74. Turlier P., Praliaud H., Moral P., Martin G.A. and Dalmon J.A., *Appl. Catal.*, **19**, 287 (1985).
75. Nakajo T., Sano K., Matsuhira S. and Arakawa H., *Chem. Lett.*, **1986**, 1557.
76. Van der Lee G., Schuller B., Post H., Favre T.L.F. and Ponec V., *J. Catal.*, **98**, 522 (1986).
77. Bastein A.G.T.M., Luo H.Y., Mulder A.A.J.P. and Ponec V., *Appl. Catal.*, **38**, 241 (1988).
78. Kip B.J., Smeets P.A.T., Wolput van J.H.M.C., Zandbergen H., Grondelle van J. and Prins R., *Appl. Catal.*, **33**, 157 (1987).
79. Kip B.J., Ph.D. Thesis, Eindhoven (1987).
80. Johnston P., Joyner R.W., Pudney P.D.A., Shipiro E.S. and Williams B.P., *Farad. Disc. Chem. Soc.*, **89**, 91 (1990).
81. Anderson A.B., Grimes R.W. and Hong S.Y., *J. Phys. Chem.*, **91**, 4245 (1987).
82. Anderson A.B., *J. Phys. Chem.*, **62**, 1187 (1975).
83. De Koster A., Ph. D. Thesis, Eindhoven (1990).
84. Saillard J-Y., Hoffmann R., *J. Am. Chem. Soc.*, **106**, 2006 (1984).
85. Anderson A.B. and Nichols J.A., *J. Am. Chem. Soc.*, **108**, 1385 (1986).

2

Reactivity of CO on vanadium-promoted rhodium catalysts as studied with transient techniques.

ABSTRACT

The effect of vanadium promotion on the kinetics of CO methanation on silica-supported rhodium catalysts was probed. Transient model experiments as temperature programmed surface reaction spectroscopy and pulse surface reaction rate analysis were used to unravel changes in rates of elementary reaction steps. CO dissociation is the rate-limiting step in the overall methanation reaction. The rate of CO dissociation is found to be enhanced by vanadium. The activation energy is lowered from 90 kJ/mol for Rh/SiO_2 to 65 kJ/mol for the promoted catalyst. The activation energy for CO dissociation is a strong function of the CO surface coverage on the unpromoted catalyst, while it is not on the vanadium promoted catalyst. This leads to a mechanism explaining the effect of the vanadium promoter according to the creation of free sites necessary for CO dissociation.

CO adsorption at temperatures above 250 °C results in very reactive surface carbonaceous intermediates that can be hydrogenated to methane at temperatures as low as -15 °C. This reactive surface carbon can be incorporated into higher hydrocarbons.

This chapter will be published in *Journal of Catalysis*, 133, (1992) with co-authors Wim J.J. Welters and Rutger A. van Santen.

INTRODUCTION

Rhodium has a special place in the group VIII metals in relation to synthesis gas conversion. Upon CO hydrogenation it is able to produce reaction products both from dissociated and undissociated CO. On the right and below rhodium in the periodic system, metals such as iridium, paladium and platinum are located that have poor activity in CO dissociation and they can produce methanol from synthesis gas. On the left and above rhodium the metals ruthenium, cobalt and iron, have high activity for CO dissociation and are known to be good metals for the Fischer-Tropsch reaction. Rhodium is an intermediate metal that is just able to dissociate CO at elevated temperatures. CO dissociation on rhodium catalysts is a nice probe to study the effects of the catalyst morphology and promoters.

After the exploration of the formation of C_2^+ oxygenates from synthesis gas over rhodium catalysts by Bhasin et al [1-4], many promoters have been added to the catalyst to improve its performance. Especially the addition of oxidic promoters has been shown to increase both selectivity and activity of oxygen containing products like methanol, acetic acid, ethanal and ethanol. The typical promoters used in this work are Ti [5-10], V [11-18], Mn [14,19-23], Fe [6,24-30], Co [31,32], Zr [5,33,34], Mo [35,36], Mg [10,37,38], La [9,16,39,40] and Ce [41,42]. In these studies mainly the influence of the promoter on the overall catalytic performance is reported while it remains unclear to what extent the promoter increases CO dissociation, CO insertion or hydrogenation of different reaction intermediates. From the many studies to find rhodium based catalyst with high yields for C_2^+ oxygenated products from synthesis gas, it became obvious that the selectivity for these products can only be high when working at low conversion. This resulted in a loss of interest for this reaction from commercial point of view. However the role of the promoter in such bimetallic catalysts is of great fundamental interest, and can have implications for other bimetallic systems. In this study vanadium is chosen as a model promoter because it enhances both activity and selectivity for ethanol formation. Here we concentrate on the influence of the vanadium promoter on the activity for CO dissociation on a rhodium catalyst.

CO dissociation has been studied on rhodium single crystals with different surface techniques, showing that CO dissociation is impossible or very slow on flat surfaces like f.c.c. (111) [43-45]. The introduction of steps and kinks [46-48] or alkali co-adsorption [49] can enhance the rate of CO dissociation. Nieuwenhuis et al [43] and Joyner [50] however, found that CO dissociation is impossible under UHV conditions indicating that at very low pressures, CO prefers to desorb above to dissociate.

Small rhodium particles supported on silica allow CO dissociation at temperatures above 250 °C as reported by Solymosi and Erdöhelyi [51]. Many articles deal with the influence of the support on CO dissociation in relation to catalytic activity in synthesis gas conversion [52-56]. Ichikawa et al [57] proposed that the influence of the carrier or promoter is related to its acid/basic properties. Acid metals promote CO dissociation and basic metals promote CO insertion. Further the metal particle size can be a factor of importance for CO dissociation. Sachtler and Ichikawa [58] showed that blocking atoms on group VIII metals are able to decrease the rate for CO dissociation that is a structure sensitive reaction. CO dissociation needs a metal ensemble of at least 5-7 free metal surface atoms [59] as indicated with quantum chemical calculations. This implies that metal particles below 15 Å will show decreased CO dissociation activity. Further it has been proposed from infra red measurements [60] that bridge adsorbed CO is the favoured configuration for CO dissociation on supported rhodium catalysts.

Sachtler et al [61] suggested a mechanism explaining the promotion of CO dissociation by oxidic transition metals. Chemisorbed CO is activated through an interaction of its oxygen end bending to an oxophilic promoter. Using infrared spectroscopy others [27,29,42,62,63] have suggested the observation of such 'tilted' adsorbed CO. Ichikawa et al [27] suggested that multi-valent reduced transition metals are able to dissociate CO in a redox mechanism. Reduced transition-metal M^{n+} ions can be oxidised to $M^{(n+2)+}$ by oxygen supplied by dissociated CO. Subsequent reduction occurs by CO or H_2 to form again M^{n+}.

It is difficult to study the process of CO dissociation in isolation at steady state synthesis gas conversion because many processes occur at the same time. Therefore we studied the kinetics of CO dissociation on (vanadium-promoted) rhodium catalysts with two transient model experiments. The first is Temperature Programmed Surface Reaction spectroscopy (TPSR) [64-66]. The second technique: Pulse Surface Reaction rate Analysis (PSRA), as has been extensively used by Mori and co-workers [67-77].

EXPERIMENTAL

Catalyst preparation

A 3 wt.% rhodium catalyst was prepared by incipient wetness impregnation of an aqueous solution of $RhCl_3$ on pre-shaped Grace 332 type silica, 300 m^2/g, mesh size 75-125, pore volume=1.6 ml/g. This silica contains 0.02% Na, 0.0005% K and 0.044% Fe. After impregnation, the catalyst was dried overnight at 110 °C. The catalyst was reduced 24 hours at 350 °C in a flow of 30% H_2 in N_2. The temperature was raised with 2 °C/min. After cooling to room temperature the

catalyst was passivated by pulsing oxygen in the nitrogen flow. To compare Rh and RhV catalysts with the same particle size vanadium was added by post impregnation from a solution of NH_4VO_3 in water. The ratio Rh/V was 3 on a molar basis. The catalyst was again dried at 110 °C. The low amount of added vanadium resulted in a catalyst system in which the CO chemisorption capacity is hardly influenced by the reduction temperature.

Another 4.7 wt.% rhodium catalyst was prepared by wet impregnation of $RhCl_3$ on Aerosil 200 type silica (200 m^2/g). After reducing and passivating, vanadium was added to this system by wet post impregnation with a solution of $VOCl_2$ in a mixture of 50% ethanol and 50% 5M·HCl (Rh/V=2 on a molar basis). For both catalyst systems the amount of added vanadium was chosen in such a way that the CO chemisorption capacity was reduced by about fifty percent.

Methods

For each experiment 300 mg of the catalyst was placed in the reactor tube (i.d. = 10 mm) and was reduced in situ between 300 and 450 °C in a flow of about 8% hydrogen in helium. At the first reduction the temperature was raised not faster than 5 °C/min. This prevented the catalyst from sintering. The experiments were performed in a reactor flow system (see fig.1). The reaction gases were analysed on line by a Quadrupole Mass Spectrometer (type: pga 100 from Leybold). The mass spectrometer monitored 8 masses at a sample frequency of 1 sec.

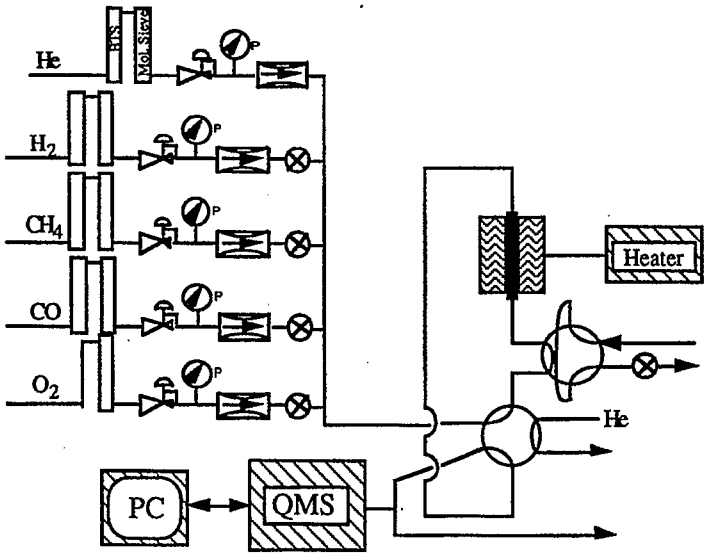

Figure 1. *Scheme of the pulse reactor flow system with on line detection with a quadrupole mass spectrometer.*

All gases were oxygen purified with a BTS column (reduced copper). Water was extracted from the gases using a molecular sieve. An extra molecular sieve column was added for the hydrogen and helium gases, which could be cooled at liquid nitrogen temperature to reduce the water concentration below ppm level. In all cases the carrier gas was helium.

CO chemisorption was performed from a flow of 55 ml/min of 0.5% CO in He at 1 atmosphere. From the consumed amount of CO the catalyst metal dispersion was calculated.

Temperature Programmed Surface Reactions spectroscopy (TPSR) experiments were performed after the creation of surface species from CO. The flow was 20 ml/min of 7.5% hydrogen in helium while the temperature was raised with 5 or 10 °C/min. The formation of methane, water and carbon dioxide as well as CO desorption, could be monitored on line in one experiment as a function of the temperature.

During Pulse Surface Reaction rate Analysis (PSRA) experiments a volume of 0.19 ml of 3 atmosphere of 5% CO in He was pulsed into a flow of 50 ml/min 3% hydrogen in helium. At a fixed temperature the reactivity of pulsed CO to methane was measured.

Unless stated otherwise, the experiments were performed with the catalyst systems prepared on Grace type silica. These catalysts had a higher dispersion, their preparation was more reproducible and consisted of a well defined mesh size.

CHARACTERIZATION

Metal particle size

The rhodium particle size of the unpromoted catalysts was determined by Transmission Electron Microscopy (TEM) as well as by CO chemisorption. The rhodium particle size in the rhodium/vanadium systems could only be determined from TEM because vanadium co-adsorption reduces CO chemisorption by an effect commonly referred to as Strong Metal Support Interaction (SMSI) [78].

The particle size as determined by TEM is in good agreement with that obtained with chemisorption for the unpromoted rhodium catalysts on Grace silica. The rhodium particle size measured by TEM was the same with or without vanadium on the Grace-supported catalyst (in contrast with CO chemisorption, CO/Rh = 0.55 and 0.22 respectively) as shown in Table 1.

Table 1. Particle size analysis with CO chemisorption and TEM measurements.

Catalyst	Carrier	CO/Rh [1], () [3]	Rh Particle size [2]
3% Rh	Grace 332	0.55 , (20 Å)[3]	22 Å
Rh/V=3	Grace 332	0.26 , (53 Å)[3]	22 Å
4.7% Rh	Aerosil 200	0.30 , (45 Å)[3]	35 Å
Rh/V=2	Aerosil 200	0.12 ,(125 Å)[3]	50 Å

1 Mol CO chemisorbed per mol rhodium.

2 From TEM measurements.

3 Calculated particle size from CO chemisorption using a pyramid model assuming that every surface rhodium atom adsorbs one CO molecule.

Temperature Programmed Reduction

On the RhV catalyst supported on Grace-type silica, small amounts of vanadium were not in contact with the rhodium, as indicated by Transition Electron Microscopy. This was suggested also from Temperature Programmed Reduction TPR (fig. 2) measurements.

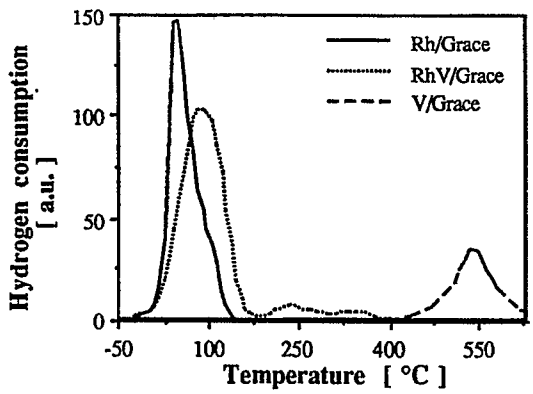

Figure 2. Temperature programmed reduction of Rh/Grace (straight line), RhV/Grace (dotted line) and V/Grace (dashed line).The temperature was raised at 7.8 °C/min in a flow of 4% hydrogen in argon. Before TPR the catalysts were calcined at 350 °C.

Most of the vanadium compound is reduced at the same temperature as the rhodium particles, suggesting a very good interaction between the vanadium and the rhodium metal particles. This result is in good agreement with Kip et al [18,79] and Ponec and co-workers [66,80] who measured TPR spectra as a function of the vanadium content in respectively $Rh_2O_3/V_2O_5/Al_2O_3$ and

$Rh_2O_3/V_2O_5/SiO_2$ catalysts. Some of the vanadium, about 15%, is reduced at higher temperature between 160 and 400 °C. This second peak may be due to a vanadium compound that has no interaction with the rhodium metal particles, although the reduction temperature of vanadium on Grace is higher: around 500 °C. The difference in reduction temperature may be induced by the smaller, more defect-rich vanadium particles, that can be reduced at lower temperature [81]. Also spillover hydrogen dissociated by the rhodium particles, can be the reason of the lower reduction temperature of the vanadium compound.

The rhodium metal particles are reduced at a higher temperature in the vanadium-promoted system, which also indicates their close contact with the promoter.

Ethylene Hydrogenolysis

An interesting surface morphology characterization probe is the hydrogenolysis of ethene to methane. Carbon-carbon bond cleavage is known to be a structure sensitive reaction [82,83]. Metal ensembles of a certain size are needed for the formation of methane from ethene and hydrogen. Figure 3 shows the activity for the rhodium and rhodium-vanadium catalyst for this reaction.

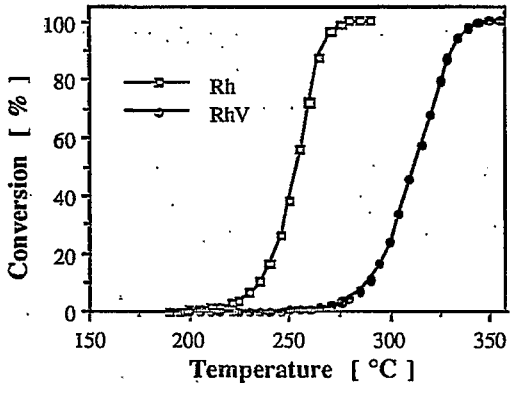

Figure 3. Hydrogenolysis of ethene to methane on a Rh/Grace and RhV/Grace catalyst in a flow of 56 ml/min of 9 % hydrogen and 1.6 % ethene in helium, as a function of the temperature.

The rate of the hydrogenolysis reaction is obviously reduced by the vanadium promoter. However, the activation energy is the same for the two catalyst systems, suggesting a decrease in the number of metal ensembles with large enough size for hydrogenolysis. It confirms the presence of the vanadium promoter adsorbed on the surface of the rhodium metal particles. So the vanadium oxide precipitates preferentially on the rhodium metal particles

instead of on the silica support during post-impregnation or is transported onto the rhodium during reduction.

Infra-red spectroscopy

The extent to which adsorbed CO is activated by a metal catalyst as well as the different adsorption sites, can be nicely studied with infra spectroscopy. Figure 4 shows the infra-red absorbance spectrum of CO adsorbed at room temperature on the rhodium and rhodium vanadium catalyst.

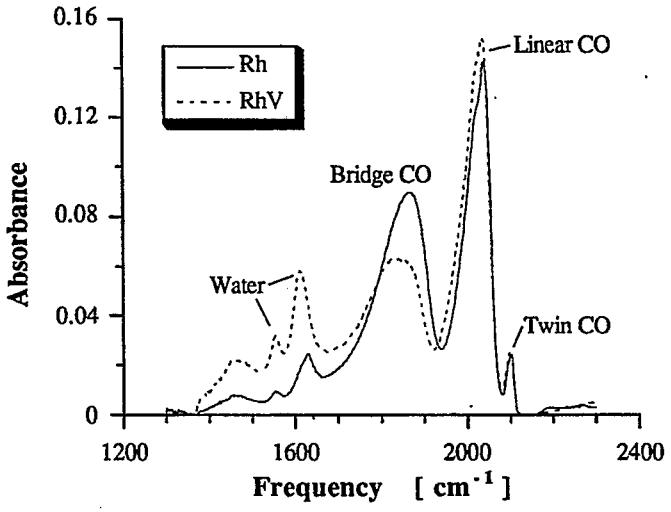

Figure 4. Infra-Red absorbance spectra of CO adsorbed at room temperature on the Rh and RhV catalyst on Grace-type silica. CO was adsorbed at 20 mbar; spectra are taken with dynamic vacuum.

The absorbance spectra show that CO is bonded both bridged, linearly and as twin CO on the Rh and RhV catalyst. The Vanadium hardly change the position of the frequencies. On the rhodium catalyst more bridged CO is present; vanadium co-adsorption shifts CO a little from the bridge to linear adsorption sites. The peaks around 1600 cm^{-1} are from water and not from tilted CO as indicated from measurements with labelled $^{13}C^{18}O$.

Synthesis gas conversion

Finally the catalysts were characterized by their catalytic performance with respect to the synthesis-gas conversion reaction. Activity and selectivity were measured under differential conditions (conversion < 1%), after one hour of steady state reaction at 200 °C in a flow of 15 ml/min (H_2/CO=2). The results are presented in table 2.

Table 2. Activity and selectivity during synthesis gas reaction at 200 °C.

Catalyst	Rh/Grace	RhV/Grace	Rh/Aer. 3	RhV/Aer. 3
CO Conversion %	0.21	0.80	0.22	0.85
Activity 1	0.18	0.70	0.15	0.52
Methane selectivity % 2	28	24	50	23
C_2^+ hydrocarbon select. 2	18	22	16	21
Ethanol selectivity 2	32	36	7.1	39
Ethanal selectivity 2	12	4.2	22	5.1
Other oxo's selectivity 4	10	13.8	4.8	12

1 Activity in : mmol CO converted per mol surface Rh per second.

2 Selectivities expressed in carbon efficiency.

3 Aer. = Aerosil 200 type silica.

4 Selectivity of other oxygen containing products than ethanol or ethanal.

The differences in selectivities between the Grace 332 and Aerosil 200 type silica for the unpromoted catalysts has been noticed by Nonneman et al [84,85] who ascribed this to impurities in the silica. The Grace 332 carrier contains in addition to silica, Na 0.04 %, CaO < 0.005 % and Fe_2O_3 < 0.01 %. The catalytic activity is increased by about a factor of four due to vanadium promotion on both types of silica support, while the 'oxo-selectivity' is changed from ethanal to ethanol.

RESULTS AND DISCUSSION

Pulse Surface Reaction rate Analysis

During steady state synthesis gas reaction many elementary reaction steps occur at the same time. Under such conditions it is not clear which one is the rate limiting step. Especially at high pressure the surface is covered with a lot of different species. These conditions do not allow a well defined study of CO dissociation. Using Pulse Surface Reaction rate Analysis (PSRA), the surface condition is well known. Before pulsing CO the rhodium catalyst has a well reduced surface. During PSRA experiments the following processes take place: CO adsorption, CO dissociation and subsequent hydrogenation of adsorbed oxygen and carbon. CO adsorption on the clean reduced metal particles is very fast and not activated. The second step CO dissociation, is slow compared with hydrogenation of carbon as will be shown later. The use of PSRA to unravel changes in the rate of reaction steps in CO hydrogenation has been extensively demonstrated by Mori and co-workers [67-77]. They showed that the rate of CO dissociation, k_{CO}, is much smaller than k_{CH_x} the rate of surface CH_x

hydrogenation, at the small CO pulses applied. Therefore one can calculate Turn Over Frequencies for CO dissociation from PSRA curves.

The rates of methane formation as determined by PSRA as a function of the temperature are presented in fig. 5. The amount of pulsed CO corresponds with an average coverage of 10-20 % of the catalyst surface. However most of the CO will be adsorbed in the beginning of the catalyst bed due to the CO sticking coefficient near unity. No CO slipped through the catalyst bed.

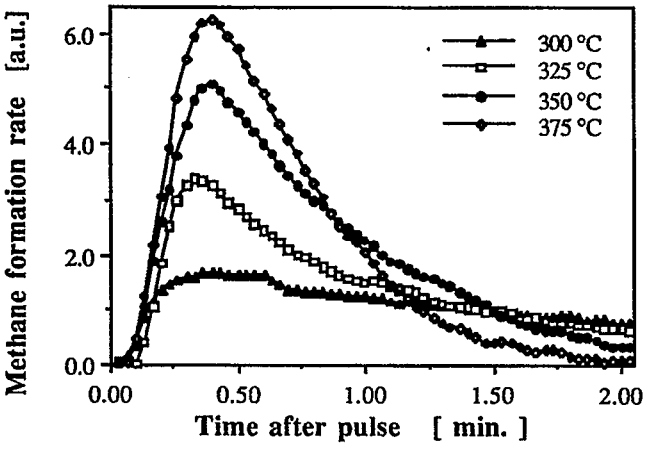

Figure 5. Methane formation from a short CO pulse in a diluted hydrogen flow over a Rh/Aerosil catalyst at different temperatures.

The rate of methane formation is faster at high temperature as indicated by the higher and steeper curve in fig. 5. The methane formation rate is considered to be first order in adsorbed CO, what can be expected for adsorbed surface species. The methane formation rate as a function of time can therefore be written in the form of equation (1) in which k is the reaction coefficient in sec^{-1} for CO dissociation.

$$r_{CH_4}(t) = p_{H_2}^{\beta} \Theta_{CO_{t=0}} k e^{-kt} \qquad (1)$$

The value of β lies between 1 and 2, and is not important to the fit as long as the p_{H_2} is kept constant during the experiment. From the curve $\ln(r_{CH_4})$ versus the time t, the reaction coefficient k is obtained from the slope. However, this line is only straight in the decreasing part of the curve (for the fit the data points are taken in the decreasing part when 75% of the maximum height is achieved).

If desired, the whole PSRA curves can be fitted by taking the performance of the reactor system into account. Equation (2) describes the methane formation curves wherein the reactor is considered as a continuously stirred tank reactor.

$$r_{CH_4}(t) = A\left[e^{-kt} - e^{-t/\tau}\right] \qquad (2)$$

The factor A is a function of k, $P_{H_2}\,\Theta_{CO_{t=0}}$ and τ. The mean residence time in the reactor τ can be measured in a separate experiment in which a CO pulse is given over a silica catalyst bed. It appeared to be 5 seconds. The results of both fit procedures are shown in fig. 6.

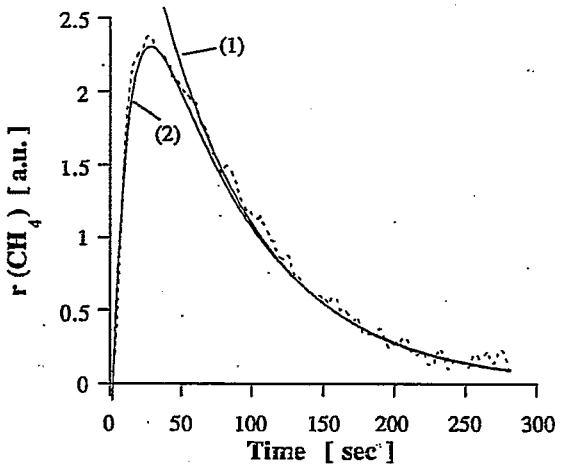

Figure 6. Different fit procedures for a PSRA curve. Dotted line: PSRA data at 350 °C on a rhodium catalyst; line 1: exponential fit according to equation (1); line 2: fit according to equation (2).

The fitted k-values as found with the two procedures differ only two percent for this case, indicating that the reactor does not disturb the transient response at response times above 50 seconds.

The values of the reaction rate constants as deduced with equation 1 for the Rh and RhV catalyst systems, are shown, in the Arrhenius plot of fig. 7. From this figure it is clear that the CO dissociation rate is greatly enhanced by vanadium promotion. The activity is increased by more than a factor of 10. The activation energy for CO dissociation is lowered from 90 kJ/mol to 65 kJ/mol by the vanadium promoter. This agrees well with the results obtained by Mori and co-workers. They noticed that vanadium promotion on a ruthenium catalyst decreased the activation energy for CO dissociation [68].

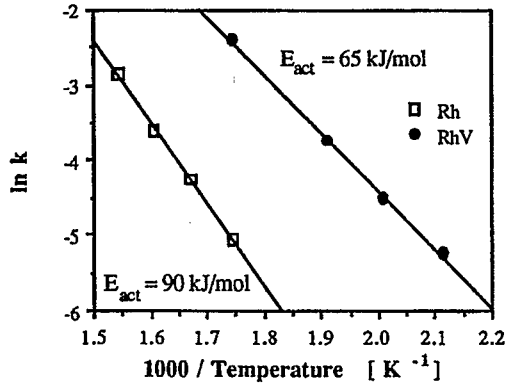

Figure 7. Arrhenius plot from PSRA data for CO dissociation on Rh/Aerosil 200 and Rh,V/Aerosil 200; k-values are the reaction coefficients in (sec^{-1}).

Temperature Programmed Surface Reaction

The ability of adsorbed CO to dissociate can be studied also with TPSR. The rate of methane formation from CO adsorbed at room temperature, as a function of temperature is described by the curves of Fig 8.

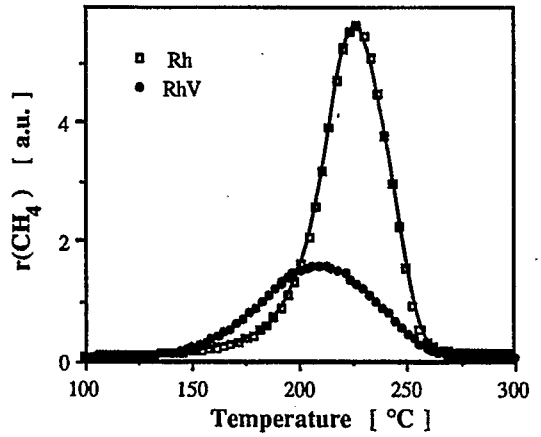

Figure 8. Temperature programmed hydrogenation of adsorbed CO on the Rh/Grace and the RhV/Grace catalyst.

During the hydrogenation of adsorbed CO, methane and water are the only products. The curve shape of the formation of water and methane as a function of the temperature, are the same. This indicates that water and methane formation have the same rate-limiting step in CO hydrogenation: CO

dissociation. This was concluded also for CO hydrogenation over nickel catalysts by McCarty and Wise [65]. The total area below the RhV curves is less than under the unpromoted catalyst because the CO chemisorption capacity is reduced by the vanadium. Characteristic in these plots is the lower temperature for the maximum methane formation rate of the vanadium-promoted catalyst [66]. Not withstanding the lower number of adsorbed CO molecules on the RhV system, the reaction rate of methane formation is higher at low temperatures. One may conclude that the vanadium promoter enhances the rate of CO dissociation. The rate of methane formation (r_{CH_4}) in the TPSR curves can be described by equation (3) [86,87], as a function of the surface CO coverage (Θ_{CO}), the effective frequency factor (ν_{eff}) and the activation energy E_{act}.

$$r_{CH_4}(T,\Theta_{CO}) = \nu_{eff(\Theta_{CO})}\,\Theta_{CO}\,e^{-Eact/RT} \qquad (3)$$

When Θ_{CO} is assumed to be constant in a small temperature range in the beginning of the curve, it is possible to convert these data into an Arrhenius plot and derive an activation energy.

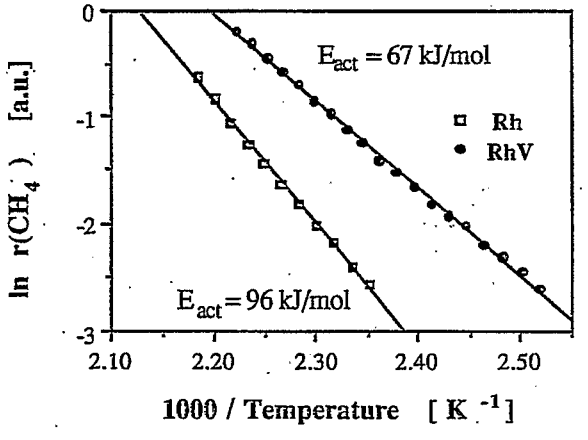

Figure 9. Arrhenius plot from TPSR data for the Rh/Grace and the Rh,V/Grace catalyst.

Also from fig. 9 it appears that the CO methanation activity is increased by vanadium promotion. The activation energy is decreased from 96 to 67 kJ/mol which is in good agreement with the activation energy derived from PSRA data. Although the size of the rhodium metal ensembles are decreased by vanadium promotion, as shown with hydrogenolysis and CO chemisorption, the rate of CO dissociation is increased. Vanadium promotion generates new sites for CO dissociation with a higher reaction coefficient.

Influence of CO surface coverage

With TPSR the activation energy for CO dissociation can be determined under well defined conditions. The activation energy for this step was studied as a function of the surface coverage of CO. Different homogeneous CO surface coverages on a rhodium catalyst were created by adsorbing a mono-layer of CO and removing subsequently a known part of the CO by hydrogenation. By monitoring the amount of methane formed, the CO coverage is determined.

The TPSR curves of fig. 10a show that under 200 °C the methanation rate can be increased by decreasing the surface coverage of CO from 1 to 0.5. Also the temperature at which methane formation is maximal, decreases when Θ_{CO} decreases, indicating that CO dissociation is easier at low CO coverages on the rhodium catalyst. Figure 10b shows the Arrhenius plots from TPSR data as a function of the initial surface coverages of CO using formula (3).

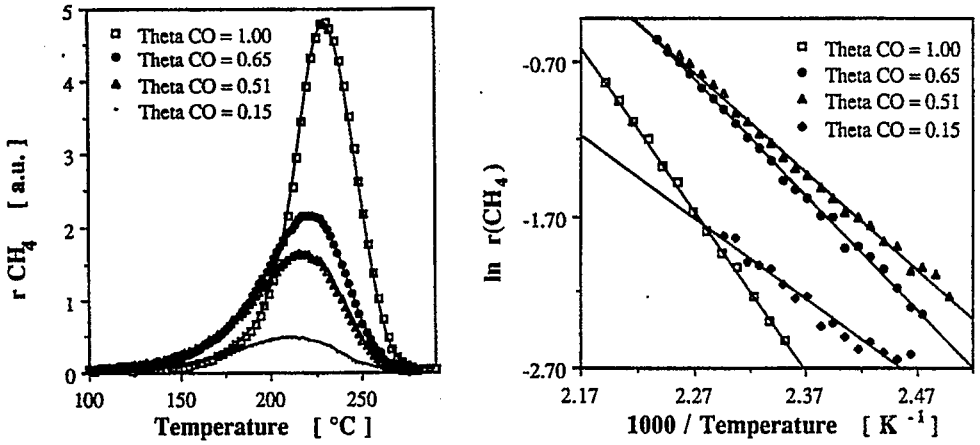

Figure 10. TPSR curves obtained with different initial surface coverages of CO. a: TPSR curves. b: Arrhenius plot.

The activation energy for CO dissociation is clearly a function of the surface coverage of CO. At low surface coverage (Θ_{CO}=0.15) the measured activation energy is 45 kJ/mol while it increases to about 90 kJ/mol at the CO coverage of a mono layer. CO dissociation needs a free metal ensemble. From quantum chemical calculations it was suggested that at least 5 free metal atoms are necessary for successful separation of the CO bond. Especially the moving oxygen atom needs space and free rhodium atoms to bind with [88,89]. At high CO coverages the metal ensembles used are small resulting in a high activation energy for CO dissociation. At full CO coverage always a little CO desorption is detected, before CO dissociation occurs on the rhodium catalyst.

The overall effect of vanadium co-adsorption on the rate of CO dissociation is very similar to the effect of a decreasing CO coverage. In both cases the activation energy for CO dissociation is found to be decreased. On the vanadium promoted catalyst the activation energy for CO dissociation appeared to be rather independent of the CO surface coverage. From these observations a new mechanism for the promotion of CO dissociation is proposed. The vanadium promoter supplies a new kind of oxygen vacancy, necessary for CO dissociation. It is possible that V_2O_3 generates additional sites that can interact with the oxygen atom from CO. In this way the vanadium promoter would act as a structural promoter creating free sites for CO dissociation. It has been suggested that SMSI promoters are able to suppress CO chemisorption on the rhodium metal near the vanadium promoter by electronic effects [90]. This is consistent with our model that suggests a local larger free metal ensemble close to the vanadium promoter enhancing CO dissociation.

The hypothesis of an alternative oxygen vacancy is close to the ideas of Sachtler and Ichikawa [57] and Levin et. al. [58] who suggested that V_2O_3 can interact with adsorbed CO through an interaction with the oxygen end of CO, weakening the CO bond. Such tilted CO has been observed on bimetallic catalysts with infra red spectroscopy. However on our promoted catalyst no tilted CO is present between 30 and 400 °C (see fig. 4). The observed infra red frequencies of bridge, linear and twin adsorbed CO are not significantly changed by vanadium promotion.

The function that describes the dependence of the activation from the CO surface coverage on the unpromoted rhodium catalyst can be estimated from fig. 10b. A second order approximation of the activation energy as a function of the CO coverage, is given in the empirical equation (4).

$$E_{act}(\Theta_{CO}) = 43.64 - 1.48\,\Theta_{CO} + 46\,\Theta_{CO}^2 \quad (kJ/mol) \qquad (4)$$

Knowing the activation energy as a function of the surface coverage the functions (3) and (4) can be used to calculate the relative rate for CO dissociation at any temperature and CO coverage. Figure 11 shows this plot from which it appears that there is an optimum CO surface coverage for methanation, at a specified temperature. The CO surface surface coverage, at which CO dissociation activity is highest, is 0.2 at 100 K and is slightly increasing at higher temperatures to 0.33 at 1000 K. If the aim is to create rhodium catalysts with optimum methanation performance, one should try to realize this coverage.

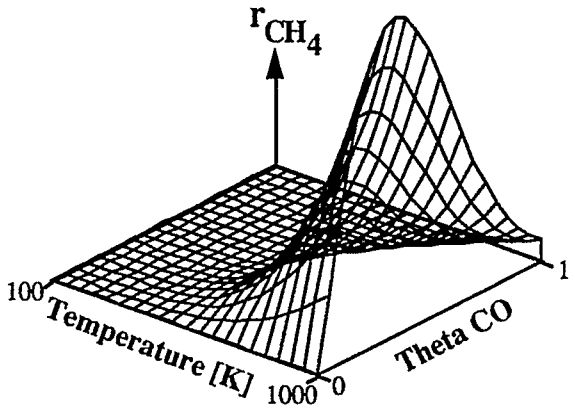

Figure 11. Calculated methanation activity of adsorbed CO on the rhodium catalyst as a function of surface coverage and temperature according to equation 3 and 4.

Influence of the hydrogen partial pressure

The influence of the hydrogen partial pressure on the activation energy for CO dissociation on the unpromoted rhodium catalyst was studied using TPSR. At a higher hydrogen pressure the surface coverage of hydrogen is supposed to increase because surface hydrogen is in equilibrium with gas phase hydrogen. TPSR spectra were measured at the same flow, varying the hydrogen partial pressure in a hydrogen helium mixture. The results are shown in the Arrhenius plot of fig. 12.

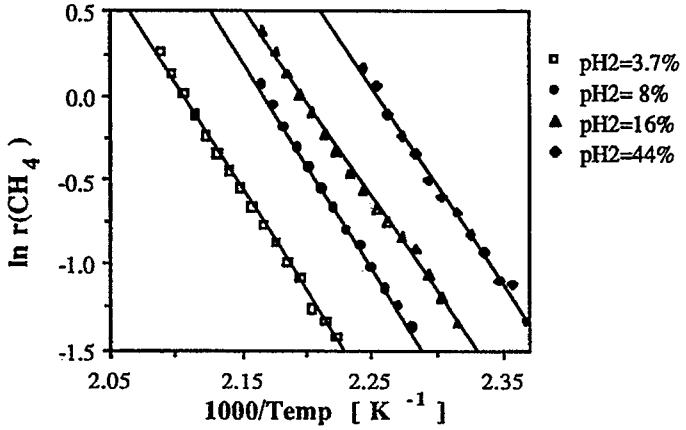

Figure 12. Arrhenius plot from TPSR curves with different hydrogen partial pressures on the rhodium/Grace catalyst. Squares: p_{H_2} = 37 mbar; circles: p_{H_2} = 80 mbar; triangles: p_{H_2} = 160 mbar; diamonds: p_{H_2} = 440 mbar.

From fig. 12 it appears that the activation energy for methanation is not a strong function of the hydrogen partial pressure. This is in agreement with the idea that CO dissociation is the rate limiting step in CO methanation. However at higher hydrogen pressure the rate of the reaction increases. Figure 12 shows that this is due to the creation of an increased number of active sites. High hydrogen pressures will result in a higher concentration of dissociated hydrogen on the rhodium surface. This leads to a faster removal of the surface oxygen species remaining after CO dissociation. This results in a larger number of free rhodium surface sites that can be used for CO dissociation. Some authors have indicated that the dissociation of CO [67,91,92] and CO_2 [93] is enhanced by hydrogen via 'hydrogen assisted CO dissociation'. Two alternative mechanisms has been mentioned for this hydrogen effect (see fig. 13).

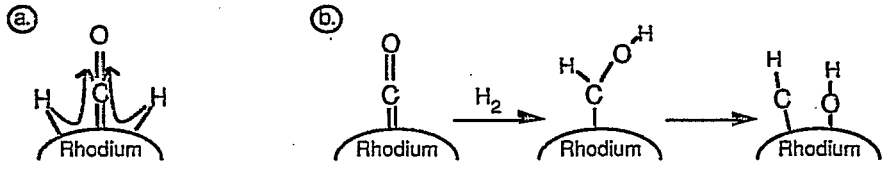

Figure 13. Suggested mechanism for hydrogen assisted CO dissociation in the literature. a: Solymosi et al [91]. b: Vannice [103,104].

In the mechanism shown in fig. 13b hydrogen is supposed to attack the double bonding of CO resulting in an ethoxy like intermediate. Biloen and Sachtler [94] demonstrated from kinetic analysis that this reaction path is not likely to occur. In the mechanism proposed by Solymosi (fig. 13a) hydrogen is supposed to increase the 'back donation' by donating electrons via the metal into the antibonding $2\pi^*$ orbital of CO, resulting in a lower CO stretch frequency as observed with infra red spectroscopy. However according to both mechanisms the activation energy for CO dissociation is supposed to decrease. This is not true and therefore we do not think that these effects exist. The enhanced hydrogenation at higher hydrogen pressures is mainly due to a large number of sites.

Hydrogenation of surface carbon

TPSR can be used also to study the reactivity of surface species that are formed from CO decomposition. CO dissociation can occur during CO adsorption at elevated temperatures. Figure 14 shows such a plot in which the hydrogenation activity of surface species created from CO adsorption at 400 °C is shown. CO was adsorbed from a pulse of 10 minutes from a flow of 50 ml/min of 0.5 % CO in helium. During CO adsorption CO_2 formation was observed from both the Boudouard reaction and the water gas shift reaction, as shown from

$C^{18}O$ adsorption experiments. After adsorption the catalyst was quickly cooled in a helium flow to 50 °C.

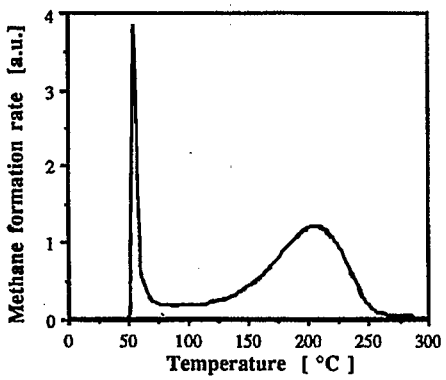

Figure 14. TPSR of surface species formed from CO adsorption at 400 °C on the Rh/Grace catalyst.

During the adsorption of CO at 400 °C a very reactive carbonaceous surface species is formed that can be hydrogenated towards methane at 50 °C. Even at -15 °C methane formation was detected upon hydrogenation. This highly reactive carbon species is created by CO dissociation at temperatures above 250 °C. The high rate of hydrogenation of surface carbon is consistent with CO dissociation to be the rate limiting step in CO methanation. The second peak in the TPSR of figure 14 is at the temperature where non-dissociated CO reacts. This peak can therefore be described to undissociated CO that is still present on the catalyst surface. This was confirmed by additional FT/IR experiments in which adsorbed CO was still visible after a temperature treatment at 400 °C.

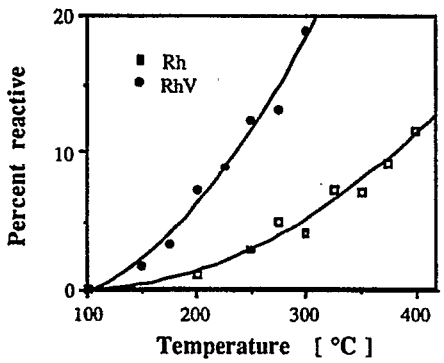

Figure 15. Fraction of reactive carbon formed from CO as a function of the CO adsorption temperature, for the Rh and the RhV/Aerosil catalyst.

Integrating the first and second peak from fig. 14 it is possible to define a fraction reactive carbon to total species that can be hydrogenated. Formation of methane below 100 °C is considered as contributed by reactive carbon; below this temperature no methane is produced during a TPSR of at room temperature adsorbed CO (fig. 7). The influence of the vanadium-promoter on the relative amount of reactive surface carbon formed was investigated at different CO adsorption temperatures (see fig. 15).

The fraction of reactive carbon formed from CO is a function of the adsorption temperature. Its formation is an activated process. The fraction reactive carbon produced from CO is increased by vanadium promotion and the temperature of initial formation is lowered by 50 °C. This again indicates a faster CO dissociation rate on the vanadium-promoted catalyst. Reactive carbon can be created also from CO adsorbtion at room temperature and subsequent heating of the catalyst. The fraction of reactive surface carbon formed in this way, is less than that formed from CO adsorption from the gas phase. The effective activation energy for CO dissociation is less in the last case, and is equal to that for dissociation of the chemisorbed state minus the heat of adsorption [95].

The incorporation of reactive carbon into C_2^+ hydrocarbons is of interest. Efstathiou and Bennett [96] showed that the surface concentration of reactive C_α carbonaceous species can vary from 2 to 6 % during synthesis gas reaction on supported rhodium catalysts. We have seen that vanadium can increase this value due to an enhanced rate of CO dissociation [97,102]. However, comparing intrinsic reactivity for carbon-carbon bond formation between these carbidic surface species, it is important that the surface coverages are the same on the two catalysts. This is possible by choosing the right CO adsorption temperature from fig. 15. We generated a surface coverage of about 14% on a Rh and RhV catalyst. Subsequently, the formation of higher hydrocarbons can be initiated by flowing 15 ml/min of $H_2/CO=2$ at 200 °C over the catalyst. The initial concentration of hydrocarbons formed as a function of time was measured with time based GC analysis. We have compared the incorporation of reactive surface carbon from CO into hydrocarbons, with hydrocarbon formation from synthesis gas without pre-deposition. Methane to pentane product formation appeared to be higher after pre-deposition of surface carbon on both the rhodium and rhodium-vanadium catalyst. When a synthesis gas reaction was started after CO adsorption at 400 °C and subsequent removal of reactive carbon with hydrogen at 50 °C, no extra initial C_2^+ hydrocarbon formation was observed. This indicates that the reactive carbidic surface carbon can be incorporated in a synthesis gas reaction. Especially these reactive C_α surface species show high affinity for C-C bond formation on rhodium catalysts [97,98]. This was also demonstrated with labelled ^{13}CO on nickel by Araki and Ponec [99] and on cobalt and ruthenium by

Biloen et al [94,100,101]. They deposited ^{13}C carbon by ^{13}CO decomposition, which could be rapidly incorporated into hydrocarbons under synthesis conditions.

CONCLUSION

Both TPSR and PSRA show that CO dissociation on rhodium catalysts is enhanced by vanadium promotion. This is due to a reduction of the apparent activation energy by about 27 kJ/mol. While the activation energy for CO dissociation is independent of the hydrogen partial pressure, it is a strong function of the CO surface concentration. From this dependence it is possible to estimate the optimum surface coverage for methanation. It is found to be weakly temperature dependent is about 0.2 - 0.3 for the rhodium catalyst investigated.

The activation energy for CO dissociation depends strongly on the number of free sites. Therefore enhanced rates for CO dissociation in the presence of reduced vanadium patches, can be due to more free rhodium surface or to the supply of a new kind of oxygen vacancies, increasing the rate of CO dissociation.

Dissociative CO adsorption at temperatures above 250 °C produces a very reactive carbidic surface species. Its formation is enhanced by co-adsorption of vanadium. This carbidic type carbon species can be incorporated into hydrocarbons under synthesis gas conditions.

LITERATURE

1. Bhasin M.M. and O' Conner G.L., Belgian Patent 824,822 to Union Carbide Corp. (1975).
2. Bhasin M.M., Belgian Patent 824,823 to Union Carbide Corp. (1975).
3. Ellgen P.C. and Bhasin M.M., US Patent 4,014,913 to Union Carbide Corp. (1977).
4. Ellgen P.C., Bartley W.J., Bhasin M.M. and Wilson T.P., *Adv. Chem.*, **178**, 147 (1979).
5. Kawai M., Uda M. and Ichikawa M., *J. Phys. Chem.*, **89**, 1654 (1985).
6. Henrion A., Ewald H. and Miessner H., *Appl. Catal.*, **62**, 23 (1990).
7. Meriaudeau P., Ellstad H. and Naccache C., *J. Mol. Catal.*, **17**, 219 (1982).
8. Monchida I., Ikeyama N., Ishibashi H. and Fujitsu H., *J. Catal.*, **110**, 159 (1988).
9. Bond G.C. and Richards D.G., *Appl. Catal.*, **28**, 303 (1986).
10. Katzer J.R., Sleight A.W., Gajardo P., Michel J.B., Gleason E.F. and McMillan S., *Farad. Disc.*, **72** (8), 1 (1981).
11. Johnston P., Joyner R.W., Pudney P.D.A., Shipiro E.S. and Williams B.P., *Farad. Disc. Chem. Soc.*, **89**, 91 (1990).
12. Kowalski J., Van der Lee G. and Ponec V., *Appl. Catal.*, **19**, 423 (1985).
13. Turlier P., Praliaud H., Moral P., Martin G.A. and Dalmon J.A., *Appl. Catal.*, **19**, 287 (1985).
14. Nakajo T., Sano K., Matsuhira S. and Arakawa H., *Chem. Lett.*, 1986, 1557.
15. Van der Lee G., Bastein A.G.T.M., Boogert J. van den, Sculler B., Luo H-Y. and Ponec V., *J. Chem. Soc., Faraday Trans. I*, **83**, 2103 (1987).
16. Van der Lee,G., Schuller B., Post H., Favre T.L.F. and Ponec V., *J. Catal.*, **98**, 522 (1986).
17. Bastein A.G.T.M., Luo H.Y., Mulder A.A.J.P. and Ponec V., *Appl. Catal.*, **38**, 241 (1988).
18. Kip B.J., Smeets P.A.T., Wolput van J.H.M.C., Zandbergen H., Grondelle van J. and Prins R., *Appl. Catal.*, **33**, 157 (1987).
19. Bartley W.J., Ellgen P.C. and Bhasin M.M., *Adv. Chem. Ser.*, **178**, 147 (1979).
20. Wilson T.P.,Kasai P.H. and Ellgen P.C., *J. Catal.*, **69**, 193 (1981).

21. Berg F.G.A. van den, Glezer J.H.E. and Sachtler W.M.H., *J. Catal.*, 93, 340 (1985).
22. Lisitsyn A.S., Stevenson S.A. and Knözinger H., *J. Mol. Catal.*, 63, 201 (1990).
23. De Jong K.P., Glezer J.H.E., Kuipers H.P.C.E., Knoester A. and Emeis C.A., *J. Catal.*, 124, 520 (1990).
24. Bhasin M.M., Bartley W.J., Ellgen P.C. and Wilson T.P., *J. Catal.*, 54, 120 (1978).
25. Fukuoka A., Kimura T., Kosugi N., Kurod H., Minai Y., Sakai Y., Tominaga T. and Ichikawa M., *J. Catal.*, 126, 434 (1990).
26. Arakawa H., Fukushima T., Ichikawa M., Natsushita S., Takeuchi K., Matsuzaki T. and Sugi Y., *Chem. Lett.*, 1985, 881.
27. Ichikawa M., Hoffmann P.E. and Fukuoka A., *J. Chem. Soc., Chem. Comm.*, 18, 1395 (1989).
28. Fukuoka A., Kimura T., Rao L-F. and Ichikawa M., *Catal. Today*, 6, 55 (1989).
29. Ichikawa M. and Fukushima T., *J. Phys. Chem.*, 89, 1564 (1985).
30. Niemantsverdriet J.W., Lauwers S.P.A., Van Grondelle J. an Van der Kraan A.M., Proc. 9th Int. Conf. Catal., Calgary, vol 2, 674 (1988).
31. Van 't Blik H.F.J., Van Zon JBAD, Huizinga T., Vis J.C., Koningsberger D.C. and Prins R., *J. Phys. Chem.*, 87, 2264 (1983).
32. Van 't Blik H.F.J., Ph. D. Thesis, Eindhoven (1984).
33. Iizuka T., Tanaka Y. and Tanabe K., *J. Catal.*, 76, 1 (1983).
34. Mazzocchia C., Tempesti E., Gronchi P., Giuffré L. and Zanderighi L., *J. Catal.*, 111, 345 (1988).
35. Trunschke A., Böttcher H., Fukuoka A., Ichikawa M. and Miessner H., *Catal. Lett.*, 8, 221 (1991).
36. Jackson S.D., Brandreth B.J. and Winstanley D., *Appl. Catal.*, 27, 325 (1986).
37. Efstathiou A.M., *J. Mol. Catal.*, 69, 41 (1991).
38. Poels E.K., Mangnus P.J., Van Welzen J. and Ponec V., *8th I.C.C.*, Berlin, vol II, 59 (1984).
39. Underwood R.P. and Bell A.T., *Appl. Catal.*, 21, 157 (1986).
40. Underwood R.P., Thesis, Berkeley, CA (1986).
41. Kiennemann A., Breault R., Hindermann J.P. and Laurin M., *J. Chem. Soc., Faraday Trans. I*, 83, 2119 (1987).
42. Lavalley J.C., Saussey J., Lamotte J., Breault R., Hindermann J.P. and Kiennemann A., *J. Phys. Chem.*, 19(15), 5941 (1990).
43. Gorodetskii V.V. and Nieuwenhuys B., *Surf. Sci.*, 105, 299 (1981).
44. Yates Jr. J.T., Williams E.D. and Weinberg W.H.,*Surf. Sci.*, 91, 562 (1980).
45. Castner P., and Somorjai G.A., *Surf. Sci.*, 83, 60 (1979).
46. Castner P., and Somorjai G.A., *Surf. Sci.*, 103, L134 (1981).
47. Li X.Q.D. and Vanselow R., *Catal. Lett.*, 2, 113 (1989).
48. Marbrow R.A. and Lambert R.M., *Surf. Sci.*, 67, 489 (1977).
49. Crowel J.E., Tysoe W.T. and Somorjai G.A., *J. Phys. Chem.*, 89, 1598 (1985).
50. Joyner. R.W., Personal Communications.
51. F. Solymosi and A. Erdöhelyi, Surf. Sci., 110, L630 (1981).
52. Mochida I., Ikeyama N., Ishibashi H. and Fulitsu H., *J. Catal.*, 110, 159 (1988).
53. Gilhooley K., Jackson S.D. and Rigby S., *Appl. Catal.*, 21, 349 (1986).
54. Erdöhelyi A. and Solymosi F., *J. Catal.*, 84, 446 (1983).
55. Haller G.L., Resasco D.E. and Rouco A.J., *Far. Disc. Chem. Soc.*, 72, 1 (1981).
56. Ichikawa M., Fukushima T. and Shikakura K., 8th ICC Berlin, vol. 2, 69 (1984).
57. Sachtler W.M.H. and Ichikawa M., *J. Phys. Chem.*, 90, 4752 (1986).
58. Levin M.E., Salmeron M., Bell A.T. and Somorjai G.A., *Surf. Sci.*, 169, 123 (1986).
59. De Koster A., Jansen A.P.J., Geerlings J.J.C. and Van Santen R.A., *Farad. Disc.*, 87, 263 (1989).
60. Fujimoto K., Kameyama M. and Kung T., *J. Catal.*, 61, 7 (1980).
61. Sachtler W.M.H., Shriver D.F., Hollenberg W.B. and Lang A.F., *J. Catal.*, 92, 429 (1985).
62. Guglielminotti E., *J. Catal.*, 120, 287 (1989).
63. Stevenson S.A., Lisifsin A. and Knözinger H., *J. Phys. Chem.*, 94, 1576 (1990).
64. Low G.G. and Bell A.T., *J. Catal*, 57, 397 (1979).

65. McCarty J.G. and Wise H., *J. Catal.*, **57**, 406 (1979).
66. Bastein A.G.T.M., Ph.D. Thesis, Leiden (1988).
67 Mori T., Masuda H., Imal H., Miyamota A., Hasebe R., Murakami Y., *J. Phys. Chem.*, **87**, 3648 (1983).
68. Mori T., Miyamoto M., Takahashi N., Fukagaya M., Niizuma H., Hattori T. and Murakami Y., *J. Chem. Soc.,Chem Comm.*, **1984**, 678.
69. Mori Y., Mori T., Miyamoto M., Hattori T. and Murakami Y., *Appl. Catal.*, **66**, 59 (1990).
70. Taniguchi S., Mori T., Mori Y., Miyamoto M., Hattori T. and Murakami Y., *J. Catal.*, **116**, 108 (1989).
71. Mori T., *Catal. Lett.*, **7**, 151 (1990).
72. Mori T., Miyamoto A., Takahashi N., Fukagaya M., Hattori T., Murakami Y., *J. Phys. Chem.*, **90**, 5197 (1986).
73. Mori T., Niizuma H., Takahashi N., Hattori T. and Murakami Y., *J. Phys. Chem.*, **90**, 103 (1986).
74. Mori T., Masuda H. and Imai H., *J. Mol. Catal.*, **25**, 263 (1984).
75. Mori T., Miyamoto A., Takahashi N., Niizuma H., Hattori T. and Murakami Y., *J. Catal.*, **102**, 199 (1986).
76. Mori Y., Mori T., Miyamoto A., Takahashi N., Hattori T. and Murakami Y., *J. Phys. Chem.*, **93**, 2039 (1989).
77. Mori Y., Mori T., Hattori T. and Murakami Y., *Appl. Catal.*, **55**, 225 (1989).
78. Tauster S.J., Fung S.C. and Garten R.L., *J. Am. Chem. Soc.*, **100**, 170 (1978).
79. Kip B.J., Thesis, Eindhoven (1987).
80. Van den Berg F.A.G., Thesis, Leiden (1983).
81. Vogt E.C.T., De Boer M., Van Dillen A.J., Geus J.W., *Appl. Catal.*, **40**, 255 (1988).
82. Hartog A.G. den, Deuz M., Jongerius F. and Ponec V., *J. Mol. Catal.*, In press.
83. Burton J.J., *Cat. Rev. -SCI. ENG.*, **9**, 209 (1974).
84. Nonneman L.E.Y., Bastein A.G.T.M., Ponec V. and Burch R., *Appl. Catal.*, **68**, L23 (1990).
85. Nonneman L.E.Y. and Ponec V., *Catal. Lett.*, **7**, 197 (1990).
86. Falconer J.L. and Schwarz J.A., *Catal. Rev. -Sci. Eng.*, **25(2)**, 141-227 (1983).
87. Jong A.M. de and Niemantsverdriet J.W., *Surf. Sci.*, **223**, 355-365 (1990).
88. Van Santen R.A. and De Koster A., in "*New trends in CO activation*" ed L. Guczi, *Studies in Surface scienc,64* , 30 (1991).
89. De Koster A. and Van Santen R.A., *Surf. Sci.*, to be published.
90. Martens J.H.A., Prins R., Zandbergen H. and Koningsberger D.C., *J. Phys. Chem.*, **92**, 1903 (1988).
91. Solymosi F., Tombáckz I. and Cocksis M., *J. Catal.*, **75**, 78 (1982)
92. Siddall J.H., Miller M.L. and Delgass W.N., *Chem. Eng. Comm.*, **83**, 261 (1989).
93. Henderson M.A. and Worley S.D, *J. Phys. Chem.*, **89**, 1417 (1985).
94. Biloen P. and Sachtler W.M.H., *Adv.in Catal.*, **30**, 165 (1981).
95. Santen R.A. van, Koster A. de and Koerts T., *Catal. Lett.*, **7**, 1 (1990).
96. Efstathiou A.M. and Bennett C.O., *J. Catal.*, **120**, 118 (1989).
97. Koerts, T. and Van Santen, R.A. *Catal. Lett.*, **6**, 49 (1990).
98. Koerts T. and Van Santen R.A., *J. Mol. Catal.*, (1992) in press.
99. Araki M. and Ponec V., *J. Catal.*, **44**, 439 (1976).
100. Biloen P., Helle J.N. and Sachtler W.M.H., *J. Catal.*, **58**, 95 (1979).
101. Sachtler W.M.H., Biloen P. and Helle J.N., *Proc. Int. Conf. Heterog. Catal.*, Varna (1979).
102. Koerts T., Welters W.J.J., Santen R.A. van, Nonneman L.E.Y. and Ponec V.,in "*Natural gas Conversion*", (Holmen A., Jens K-J. and Kolboe S.), Elsevier, Amsterdam 1990.
103. Vannice M.A., *J. Catal.*, **37**, 462 (1975).
104. Vannice M.A., *Catal. Rev. -Sci. Eng.*, **14**, 153 (1976).

3

Transient response study of CO insertion into CH_x surface intermediates on a vanadium promoted rhodium catalyst.

ABSTRACT

The rate of CO insertion into surface CH_x species was investigated on a silica-supported rhodium and rhodium/vanadium catalyst. Isotopically labelled ^{13}CO was used in a transient kinetic experiment under steady state conditions. A main conclusion is that vanadium promotion does not effect the reaction coefficient of CO insertion. From temperature programmed surface reaction measurements the surface concentration of CH_x species during steady-state reaction was determined. This concentration is increased by the vanadium promoter co-adsorption. Combining these data with the selectivity and activity in synthesis gas to oxygenate conversion, a model is derived from which reaction rates of elementary steps and surface concentrations are calculated. Ethanal formation appears to occur at two distinguishable sites. Vanadium promotion decreases the desorption rate of ethanal, enhances the hydrogenation rate to ethanol, and increases the surface concentration of oxygenated intermediates.

This chapter will be published in *Journal of Catalysis*, 133 (1992), with co-author Rutger A. van Santen.

INTRODUCTION

The formation of oxygenated compounds such as ethanol and ethanal from synthesis gas is of significant fundamental interest [1-2]. Supported rhodium catalyses this reaction. Oxidic promoters like Mn_2O_3, FeO_x, V_2O_3, HfO_2 and TiO_2 have been shown to increase the selectivity for ethanol formation [3-7]. In this chapter the influence of a vanadium promoter on the reaction rate of some elementary steps is analysed.

Mechanism

In the mechanism of the ethanol and ethanal formation, generally three main elementary reaction steps can be distinguished: CO dissociation, CO insertion into surface CH_x fragments and hydrogenation of surface intermediates. It is difficult to describe quantitatively how these steps are individually influenced by oxidic promoters from the overall performance in synthesis gas conversion. In chapter two it was demonstrated that CO dissociation is promoted by the vanadium promoter. CO dissociation results in adsorbed oxygen and carbon. The oxygen adsorbed atom is removed as CO_2 or H_2O and the surface carbon is supposed to be partially hydrogenated to a CH_x fragment. This is an important intermediate because it can react towards methane, it can recombine with other carbon fragments supporting chain growth or it can undergo CO insertion resulting in an oxygen containing intermediate.

In this chapter we shall concentrate on the influence of the vanadium promoter on CO insertion into adsorbed CH_x fragments and the subsequent hydrogenation to ethanal and ethanol. CO insertion is a key reaction step in the formation of C_2^+ oxygenates from synthesis gas as well as in hydroformylation reactions [7a-7c, 38]. The value of x in the CH_x species during CO insertion is equal to 3 or 2 [8] because only then the metal-carbon interaction is relative low [9]. CO insertion leads to an intermediate that can produce ethanol and ethanal.

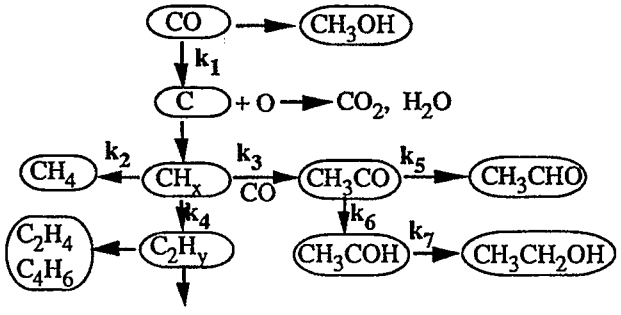

Figure 1. Elementary reaction scheme for synthesis gas conversion into oxygenates [10-15].

The intermediates involved in the formation of oxygenates from synthesis gas have been extensively studied but some controversy remained. Orita et al [10] claimed that the formation of ethanal occurs from an acetate species as reaction intermediate. Underwood and Bell [11], Mazzochia et al [11a] and Kiennemann et al [12] showed that ethanal is the precursor for ethanol formation. Jackson et al [13] suggested that different reaction intermediates are responsible for ethanol and ethanal formation, because according to him ethanal formation is much faster than ethanol formation. This was deduced from experiments in which ^{13}CO was pulsed in a synthesis gas flow. Contrary to this interpretation, Ichikawa and Fukushima [14] showed, by a reaction of ^{13}CO and $^{13}CH_3OH$ with synthesis gas, that ethanal and ethanol can be generated from a common reaction intermediate. Fukushima et al [15] indicated this reaction intermediate as an acyl species, with FT-IR spectroscopy. In addition to such a reaction intermediate a second oxygenated reaction intermediate must be proposed in the reaction mechanism of fig. 1 which can be an ethoxy species as indicated by the same authors [15]. This intermediate was also proposed by Agarwal et al [16], who studied the hydrogenation of ethanal to ethanol. They argued that ethanal is adsorbed on the catalytically active surface through the oxygen atom and is hydrogenated to an intermediate that is bounded by its hydroxy carbon atom to the metal surface. Although it remains unclear whether the first oxygenated reaction intermediate (CH_3CO) is adsorbed as an acyl species or as acetate, and whether the second oxygenated intermediate (CH_3COH) is bonded through a carbon atom or an oxygen atom to the surface, the transient data show that at least two different reaction intermediates must be postulated.

Influence of promoters

The influence of promoters on the rate of CO dissociation has been studied extensively [17-19]. Both alkali and oxygen-containing transition metals can enhance the rate of CO dissociation. The enhanced CO dissociation rate, as demonstrated for vanadium promotion [20,21], will increase the overall activity of a rhodium catalyst with respect to the synthesis gas conversion reaction. Much less is known about the effect of promoters on the CO insertion rate into adsorbed CH_x species. Fukuoka et al [22,23] recently suggested a mechanism for iron promoted rhodium catalysts, in which tilted adsorbed CO molecules resulted in an enhanced activity for CO insertion. From activity measurements, Chuang et al concluded that CO insertion is favoured by small metal ensembles, which could be created by blocking silver atoms [24] or by co-adsorbed sulfur [25]. Results on CO insertion activity obtained from ethene addition to synthesis gas resulting in propanol [26-29], must be interpreted cautiously. Ethylene addition also changes the surface concentration of reaction intermediates, which may

effect selectivities. Orita et al [10] showed that potassium promoter could supply reactive oxygen, which can be used to stabilize acetate species. This was also shown for acyl species by FT-IR measurements with vanadium-promoted rhodium by Fukushima et al [30,15]. Also Boujana et al [31] noticed a stabilized acetyl species when a promoter was added to a paladium catalyst. A relation has been proposed between the stabilization of oxygenated intermediates and an improved selectivity for ethanol formation. Despite all these suggestions, a direct study of the reactivity of adsorbed CH_x fragments with CO has not yet been performed. Here we report on a study of the CO insertion step under steady state conditions using transient kinetic experiments.

Transient kinetic analysis

Steady State Isotopic Transient Kinetic Analysis (SSITKA) is a powerful tool to analyse reaction rates of elementary steps as shown by Happel [31a-31c], Bennett [31d], Biloen [32,33], Goodwin [34,35], Bell [36] and Delgass [37]. Without changing the steady state conditions it is possible to determine surface concentrations of reaction intermediates and their residence time on the catalyst surface. Also the heterogeneity of the surface can be analysed, as is shown for the formation of ethanal.

The effect of vanadium promotion on a silica supported rhodium catalyst was studied for the reaction of surface CH_x and CO to an adsorbed CH_3CO intermediate and its subsequent hydrogenation. The enhancement of CO dissociation by vanadium promotion [39] complicates direct analysis of the transient data. In order to circumvent this we analysed the incorporation rate of ^{13}C from CO, into the carbonyl group of ethanal and into the hydroxy-carbon group of ethanol during a step-wise change from ^{12}CO synthesis gas to labelled ^{13}CO synthesis gas.

$$5\,H_2 + 2\,CH_x + 2\,{}^{13}\underline{C}O \rightarrow CH_3{}^{13}\underline{C}HO + CH_3{}^{13}\underline{C}H_2OH \qquad (1)$$

The ^{13}C carbon atoms (underlined) in ethanal and ethanol are from undissociated CO, and the rate of incorporation should be independent of the rate of CO dissociation. The incorporation of these ^{13}C atoms can be determined by analysing mass spectra.

The rate of appearance of ^{13}CO in products will not only depend on the rate of CO insertion, but also on the rate of hydrogenation of the adsorbed CH_3CO intermediates and on their subsequent rate of desorption. To analyse the interactions of ethanal and ethanol precursors with the catalyst, we carried out Temperature Programmed Desorption (TPD) experiments. The hydrogenation rate of surface intermediates was studied in a separate experiment, in which ethanal was hydrogenated to ethanol.

The results are analysed using a model in which the influence of the vanadium promoter is described in terms of changes in reaction rates of the elementary steps and surface concentrations of reaction intermediates. In order to do so the surface concentration of adsorbed CH_x intermediate must be known. The concentrations were estimated from separate Temperature Programmed Surface Reaction (TPSR) experiments, using the observation that the reactivity of adsorbed CH_x intermediates in hydrogenation is much higher than that of adsorbed CO [39,40].

EXPERIMENTAL

Catalyst

A 3 wt.% rhodium catalyst was made by pore volume impregnation of pre-shaped Grace 332 type silica (surface area=300 m^2/gram, pore volume = 1.65 ml/g, mesh size=100) with an aqueous solution of $RhCl_3$. After reduction at 350 °C for 16 hours and passivation at room temperature, vanadium was added by post impregnation of a solution of amonia-metavanadate. On the promoted catalyst the molar-ratio of rhodium:vanadium was 3. The amount of CO that can be chemisorbed on the promoted catalyst system, was insensitive for the reduction temperature. The vanadium promoter covered the rhodium particles as deduced from CO chemisorption and other techniques [39]. From transmission electron microscopy photographs it was concluded that the rhodium particles have the same size on both catalysts.

method

Before each experiment, the catalyst was reduced in situ at 350 °C for at least one hour. Catalytic reaction was carried out with 500 mg of the catalyst in a flow of 15 ml/min of synthesis gas (H_2/CO=2) at 210 °C. All experiments were done after one hour of steady state synthesis gas reaction.

With TPSR the surface concentration of reactive surface carbon species during synthesis gas reaction was determined. After the synthesis gas reaction the reactor was quickly cooled to 100 °C in a helium flow, while CH_x intermediates as well as CO remained adsorbed. At 100 °C only the reactive CH_x intermediates produce methane in a reaction with hydrogen. On raising the temperature surface carbon monoxide and graphitic carbon are hydrogenated to methane. The amount of methane produced at 100 °C divided by the total amount of methane produced in a TPSR experiment, was used as an estimate for the concentration of adsorbed surface CH_x intermediates.

For the transient kinetic experiment a reactor system was used, connected to a mass spectrometer. All dead volumes were minimised. The dead volume of

the reactor above the catalyst was filled with quartz. Just above the reactor a four way valve could switch from normal synthesis gas to ^{13}C labelled synthesis gas. After the catalyst bed a small tube led to a multi-position 16 way loop valve (type ST16 Chrompack). This valve contained 16 loops of 0.3 ml that could be placed in turn into the reaction gas flow. By switching this valve, 15 loops of reaction gases could be stored. It was kept at 110 °C. To obtain well defined response data without disturbing the steady state, it is important that the pressures are the same in the two flow sets before switching. The pressure drop of the catalyst bed (normally about 0.18 atm.) was also created in the second flow by a needle valve. The system is schematically presented in figure 2.

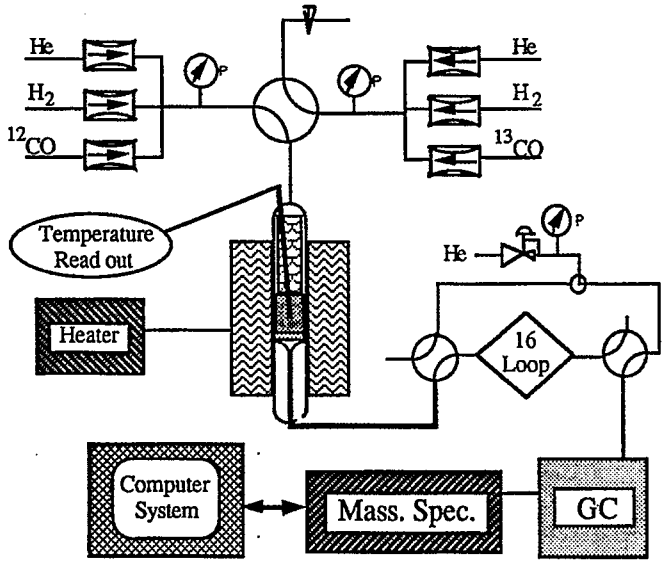

Figure 2. Schematic presentation of the time based GC-MS equipment as used for the isotopic transient experiment.

The temperature in the catalyst bed was measured by a thermocouple in a quarts capillary. After one hour of steady state reaction, the synthesis gas was switched to labelled ^{13}CO (MSD isotopes, 99.3% ^{13}C). 15 Loops were filled with reaction gas during the first ten minutes after the switch. Afterwards the stored gases were pulsed into a gas chromatograph on a widebore plot q column of 13 meter (Ø = 0.53 mm). All components, except methane, hydrogen and CO, were separated in a temperature programmed GC run from 30 to 180°C. The widebore column was connected by a glass press-fit coupling with a capillary column of 3 meter length that introduced the components into a high resolution mass spectrometer (AMD MMH1, Harpstedt Germany [41]). Every 1.5 second all masses between 10 and 50 atomic mass units were measured. The data were

stored in a computer system and evaluated afterwards, with a DP 1.05 program. From the fragment ions in the mass spectrum it was possible to calculate the fraction of labelled ^{13}C in the carbonyl group of ethanal from masses 29 and 30, and in the hydroxy-carbon group of ethanol from masses 31 and 32. Corrections were made for the natural fragmentation of the products, the oxygen and nitrogen background and the natural abundance of ^{13}C of 1.1 %. The transient experiment was duplicated, with similar results.

The hydrogenation of ethanal to ethanol was tested in a micro-flow reactor (i.d. of 10 mm). A flow of 58 ml/min of 2% ethanal and 8.5% hydrogen in helium was passed over 300 mg of the reduced catalysts at different temperatures. The products were analysed with a gas chromatograph (Chrompack, CP 9000), using a widebore plot q column of 25 meter (Ø = 0.53 mm). The TPD experiments were carried out in the same reactor system. The catalyst was saturated with ethanal or ethanol by adsorption in a helium flow of 56 ml/min at 110°C. After flushing for 30 minutes in helium the reactor was cooled to 40 °C and the TPD was started in a helium flow of 20 ml/min. The temperature was raised at 5 °C/min while every two minutes the desorbing products were analysed with the GC.

RESULTS

The activity and selectivity of the catalysts during the steady state synthesis gas reaction are presented in table 1.

Table 1. Activity and product distribution during synthesis gas reaction at 210 °C (H_2/CO=2, 1 atm.) of the rhodium and the rhodium vanadium catalyst.

		Selectivity percent				
Catalyst	Activity [1]	Ethanal	Ethanol	Methane	C_2^+ H.C.	oxo's [2]
Rh	0.27	7.18	18.9	42.0	25.0	6.9
RhV	1.00	2.28	22.8	36.3	29.8	8.8

[1] Activity expressed as mmol CO converted per surface metal atom per second.

[2] Products containing one ore more oxygen atoms other than ethanal and ethanol.

As previously noticed [20,21,38,39] the vanadium promoter shifts the selectivity from ethanal to ethanol. The activity per surface rhodium atom is about four times increased.

The transient response curves of the incorporation of ^{13}C into ^{13}CO to produce $CH_3{}^{13}CHO$ and $CH_3{}^{13}CH_2OH$ for the rhodium and rhodium-vanadium catalyst are presented in the figures 3a and 3b.

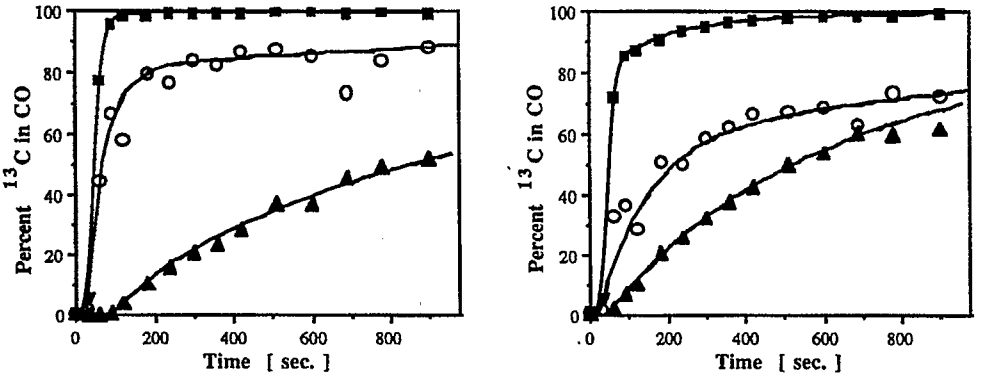

Figure 3. Appearance of ^{13}C from ^{13}CO in carbon monoxide (squares), the carbonyl group of ethanal (open circles) and in the hydroxy-carbon group of ethanol (triangles). Left: Rh. Right: Rh-V.

The disappearance with time of the fraction of ^{12}C in the above mentioned carbon atoms of ethanal and ethanol for the Rh and RhV catalysts is shown in figure 4 on a logarithmic scale.

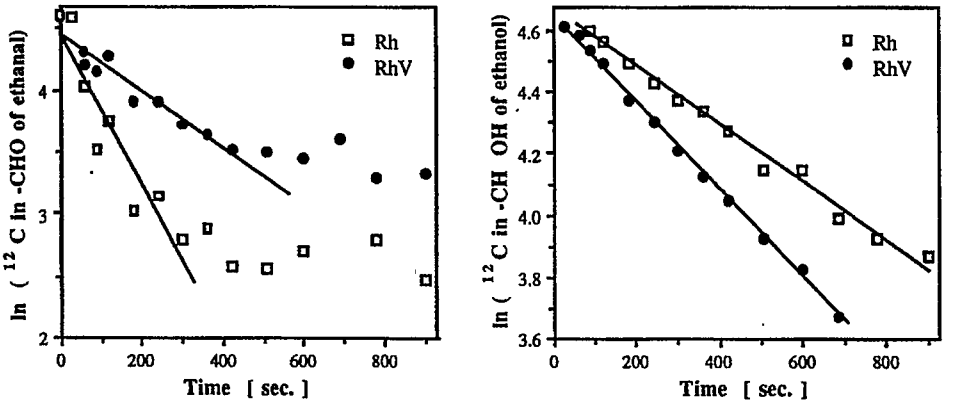

Figure 4. The disappearance of ^{12}CO in C_2 -oxygenates compared on the rhodium and rhodium-vanadium catalyst. a: Ethanal. b: Ethanol.

The presence of the vanadium promoter slows the rate of ^{13}C O incorporation into ethanal while it is enhanced for incorporation in ethanol.

Differences in the interaction of ethanal and ethanol with the silica support follow from the Temperature Programmed Desorption experiments in figure 5.

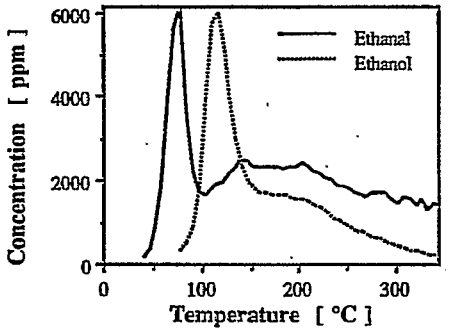

Figure 5. Temperature programmed desorption of ethanal and ethanol from silica. (Ethanol concentration has been multiplied with 3).

Ethanal and ethanol TPD experiments from the Rh and RhV catalysts were carried out; ethanol desorbs at a little higher temperature than ethanal.

To compare the reactivity coefficients of CO insertion on the Rh and RhV catalysts, the surface concentration of reactive surface carbon has to be known. Therefore a temperature programmed surface reaction was done after one hour of synthesis gas reaction at 200 °C, and subsequent cooling in helium to 50 °C (fig. 6).

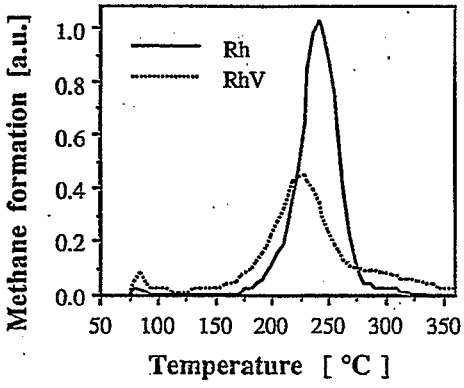

Figure 6. Temperature programmed hydrogenation of surface species, formed during one hour of synthesis gas reaction.

The total amount of surface species that can be hydrogenated on the RhV catalyst is about half of that on the Rh catalyst, due to partial coverage of the rhodium particles by the promoter. The concentration of reactive carbon species is determined from the amount of methane produced at 100 °C divided by total

amount of methane formed (up to 400 °C) and is 0.34% for the Rh catalyst and 1.4% for the RhV. The low concentration of the reactive C_α carbonaceous intermediates on the rhodium catalyst during synthesis gas reaction corresponds well with the amount found by Efstathiou and Bennett [40].

Finally we analysed the influence of the vanadium promoter on the hydrogenation of ethanal to ethanol in a separate experiment. The activity and selectivity as well as the order in ethanal and hydrogen are presented in table 2 and figure 7.

Table 2. Activity and selectivity for hydrogenation of ethanal to ethanol at 110 °C.

Catalyst	Activity TOF[1]	Ethanol Selectivity %	Order in Hydrogen	Order in Ethanal	deactivation % per hour
Rh/SiO_2	0.11	65	1.70	-0.5	4
RhV/SiO_2	0.97	93	0.80	-0.4	1

1 mol converted ethanal per surface rhodium atom per second.

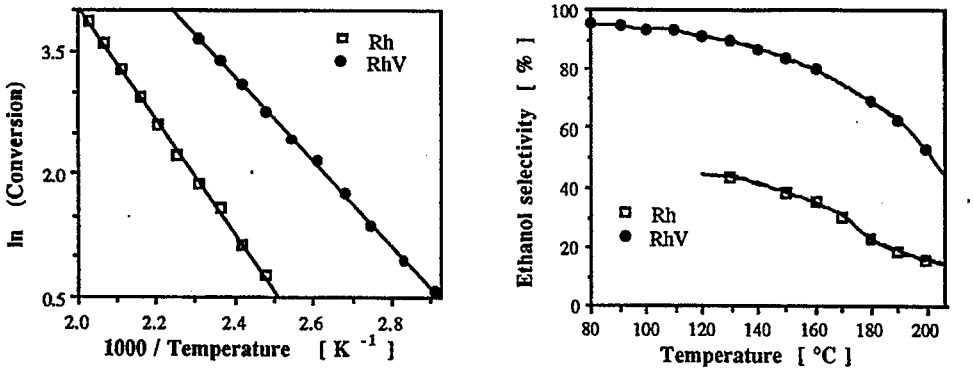

Figure 7. Hydrogenation of ethanal to ethanol on the Rh and RhV catalyst. a:Arrhenius plot (left). b:Selectivity (right).

It can be seen that both activity and selectivity to ethanol are greatly increased by the vanadium promoter. The activation energy for ethanal conversion is hardly changed: 44 kJ/mol for Rh and 43 kJ/mol for RhV.

DISCUSSION

The ratio of the rate of incorporation of ^{13}CO into ethanol and ethanal, correspond well with that measured by Jackson et al [13] on Rh/SiO_2. They pulsed labelled $C^{18}O$ into a synthesis gas flow, and measured the incorporation into ethanal and ethanol. They noted that the incorporation into ethanal is fast

while the incorporation into ethanol was so slow that it could not be observed. However this does not prove that ethanal and ethanol are formed from different reaction intermediates as they suggested.

A semi-logarithmic plot of the normalised isotopic transient data is expected to be linear. This appeared to be true for the ethanol production (fig. 4b). However, for the formation of ethanal, a clear deviation exists from straight line behaviour (fig. 4a) at higher response times. This indicates that different active sites exist. Analysing the curve in more detail can give information about the reactivity coefficients of the different sites. The total rate of a first order surface reaction, taking place on a non homogeneous surface, consisting of sites with different reaction coefficients, can be modelled as a sum of exponentials. The distribution of the rate constant k can in principle be calculated by fitting the transient curve with the expression (2).

$$\text{Rate} = \Theta_0 \Sigma_i (x_i k_i e^{-k_i t}) \qquad (2)$$

Θ_0 is the total surface coverage, x_i is the fraction with reactivity k_i. De Pontes et al [36] derived a general deconvolution to extract the function x(k), from the plots in figure 3. For less well defined data one also can model the transient data using equation (2). Fixed k_i values were chosen and the amplitudes x_i were fitted using a Marquardt routine. The k-value distributions derived in this way for the Rh and RhV catalyst are shown in figure 8. The incorporation rate calculated from this figure is shown as the fit in the figures 3a and b.

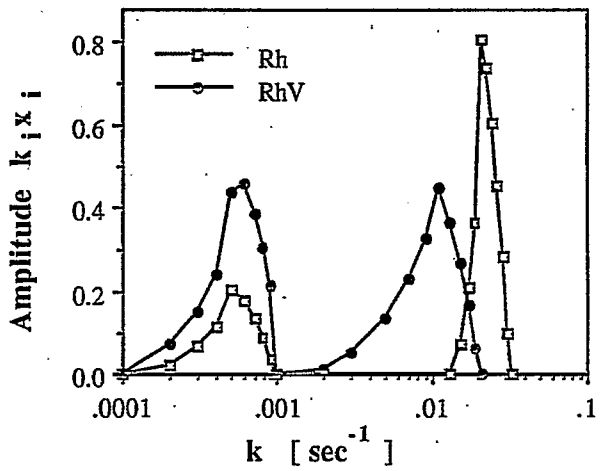

Figure 8. The k-value distribution from SSITKA data for the formation of ethanal, on a Rh and RhV catalyst.

One can conclude that ethanal formation occurs at least at two different sites. Vanadium promotion decreases the reactivity of the active sites and increases the fraction of stabilized ethanal intermediates that desorb only slowly as ethanal.

To obtain quantified information from the plots in figure 3a and 3b, in terms of elementary reaction rates, we used the kinetic scheme as shown in figure 1. Also the surface concentrations of the reaction intermediate CH_3CO and CH_3COH can be calculated and left within the reaction coefficients k. The hydrogen pressure dependence of each elementary step is not explicitly considered. Our analysis implicitly assumes that the hydrogen partial pressure and coverage was constant during the experiment. The concentration of the two important oxygenated reaction intermediates from figure 1, are written as $I_1 \equiv \Theta_{CH_3CO}$ and $I_2 \equiv \Theta_{CH_3COH}$. To extract the k values, the corresponding equations have to be derived. For incorporation of ^{13}C into the aldehyde group of ethanal according to the mechanism from figure 1, one can write the rate equations (3) and (4).

$$\frac{dCH_3{}^{13}CHO}{dt} = r_5\, {}^{13}I_1 \qquad (3)$$

$$\frac{d{}^{13}I_1}{dt} = k_3\, \Theta_{CH_3}^{\alpha}\, \Theta_{{}^{13}CO}^{\beta} - (k_5 + k_6)\, {}^{13}I_1 \qquad (4)$$

The reaction orders α and β of the surface intermediates are assumed to be one. The integration of (4) results in (5) when the fraction of surface ^{13}CO is taken the same as that of the gas phase and follows: $\Theta_{^{13}CO}(t) = [\, 1 - e^{-\gamma t}\,]$

$${}^{13}I_1(t) = \frac{k_3\, \Theta_{CH_3}}{k_5 + k_6}\, [\, 1 - e^{-(k5 + k6)t}\,] - \frac{k_3\, \Theta_{CH_3}}{\gamma - (k_5 + k_6)}\, [\, e^{-(k5 + k6)t} - e^{-\gamma t}\,] \qquad (5)$$

In this equation γ is introduced as a correction for the non-ideal switch from ^{12}CO to ^{13}CO, the value of which can be deduced from the experimental data in figures 3a and 3b. For relative large γ (step wise change from ^{12}CO to ^{13}CO) the second part of this equation becomes zero. The measured γ values were 0.05 for the Rh and 0.03 sec^{-1} for the RhV experiment while the dead time for response was 27 sec. The scrambling between adsorbed ^{12}CO and ^{13}CO gas is rapid, as concluded by Yates et al [42], and therefore the fraction of ^{13}CO in the gas phase is the same as that of adsorbed CO.

The rate of ^{13}CO incorporation into the aldehydic group of ethanal follows from the equations (3) and (5).

$$CH_3{}^{13}CHO(t) = \frac{k_5 k_3 \Theta_{CH_3}}{k_5 + k_6}\left[1 - e^{-(k5 + k6)\,t}\right] - \frac{k_5 k_3 \Theta_{CH_3}}{\gamma - (k_5 + k_6)}\left[e^{-(k5 + k6)\,t} - e^{-\gamma t}\right] \quad (6)$$

The incorporation of ^{13}C into the hydroxy-carbon group of ethanol can be deduced in the same way according to the mechanism of figure 1.

$$\frac{d^{13}CH_3CH_2OH}{dt} = k_7\, {}^{13}I_2(t) \quad (7)$$

$$\frac{d^{13}I_2}{dt} = k_3\, {}^{13}I_1(t) - k_7\, {}^{13}I_2(t) \quad (8)$$

The solution for $I_2(t)$ is presented in (9) assuming $\gamma >> k_5+k_6$, which is valid because the incorporation of ^{13}C in CO is much faster than that in ethanol as shown in fig. 3.

$${}^{13}I_2(t) = \frac{k_6 k_3 \Theta_{CH_3}}{k_7(k_5+k_6)}\left[1 - \frac{k_7}{k_5+k_6-k_7}e^{-(k5+k6)t} - \left(1 - \frac{k_7}{k_5+k_6-k_7}\right)e^{-k7t}\right] \quad (9)$$

Equation (7) and (9) produce the desired equation (10) for the rate of appearance of ^{13}C into ethanol.

$$CH_3{}^{13}CH_2OH(t) = \frac{k_6 k_3 CH_3}{k_5 + k_6}\left[1 - K\, e^{-(k5+k6)\,t} - (1-K)\, e^{-k7t}\right] \quad (10)$$

$$\text{with } K = \frac{k_7}{k_5+k_6-k_7}$$

For the analysis of the rate constants according to equation 6 and 10 only the high reactivity coefficients for ethanal formation are taken into account. The experimental data of ^{13}C incorporation into ethanol is fitted with formula (10). The fitted curves are shown in figure 3b. The resulting k-values: k_5+k_6 and k_7, are presented in table 3. At high response times the calculated ethanal curve becomes a little higher than the measured one (fig. 3b). This can be corrected if the slow sites for ethanal formation are also taken into account in r_5 in equation (9). However at residence times lower than 750 seconds, the transient data can be fitted very well. The agreement achieved, supports the mechanism suggested. The rate parameters determined from these fits are presented in table 3.

The reaction-rate constants k_3, k_5, k_6 and k_7 as well as the surface concentration of the reaction intermediates I_1 and I_2 can be calculated for both the rhodium and the vanadium promoted catalyst from a more complete analysis. Therefore, six independent equations have to be solved. The necessary information is obtained from the selectivities and turn over numbers from table

1 and the surface concentration of CH_x intermediates that has been estimated with TPSR. The first two equations are (6) and (10). The other equations can be solved using the steady state conditions (11-14).

$$\frac{k_5}{k_6} = \frac{\text{ethanal selectivity}}{\text{ethanol selectivity}} \tag{11}$$

$$k_3 \Theta_{CO} \Theta_{CH_x} = I_1 (k_5 + k_6) \tag{12}$$

$$I_1 k_5 = \text{TOF selectivity ethanal} \tag{13}$$

$$I_2 k_7 = \text{TOF selectivity ethanol} \tag{14}$$

The Turn Over Frequencies from table 1 are used in equation (13) and (14). The resulting rate parameters for the rhodium and vanadium-promoted rhodium catalyst are presented in table 3.

Table 3. Changes in reaction rates and surface concentrations of C_2O intermediates by vanadium promotion at 210 °C.

	k_3 [1]	k_5 [1]	k_6 [1]	k_7 [1]	ΘC_2O [2]	ΘC_2OH [2]
Rh	22	5.7	15	0.83	0.003	0.06
RhV	20	0.95	10	1.2	0.024	0.18
RhV/Rh	0.9	0.17	0.7	1.5	7.2	3.0

1 k is the reaction coefficient in 10^{-6} sec^{-1}.

2 Surface concentration Θ is the fraction of the rhodium surface covered.

Residence times of surface intermediates may be affected due to chemical interaction of C_2O or C_2OH intermediates with the silica support. Especially the following equilibrium has to be considered:

$$\text{Si-OH} + HOCH_2CH_3 \Leftrightarrow SiOC_2H_5 + H_2O \tag{15}$$

To ensure that the long residence time of ethanol intermediates is not due to a great buffer of C_2OH intermediates adsorbed on the silica carrier, TPD experiments were carried out. In figure 5 it is shown that most of the chemisorbed ethanal and ethanol would desorb below 210 °C, the reaction temperature during steady state experiments. Moreover, during synthesis gas reaction, the concentration of water is about 3 times greater than that of ethanol, which shifts the equilibrium of equation 15 to the left. So it is unlikely that long residence times of ethanol are due to an interaction with the silica support. However, it can not be excluded that for ethanal desorption, the unreactive sites

for ethanal formation are due to an interaction with the silica support, because some ethanal desorption occurs also at temperatures above 210 °C (see figure 8).

The reaction coefficients for CO insertion from table 3 on the Rh and RhV catalyst differ by only 10%. CO insertion is fast compared with the hydrogenation steps and is therefore not rate limiting. This reaction step can be considered to be in local equilibrium because the reverse reaction, the decomposition of a C_2O intermediate to CO and CH_x, is also fast on rhodium catalysts. This follows from TPD experiments by Davis and Barteau [43]. Co-adsorption of vanadium makes the CH_x fragments a little less reactive for CO insertion. The enhancement of the CO insertion by oxidic promoters, as measured in homogeneous catalysis [44,45], is not found for the discussed heterogeneous RhV system. Our results indicate that the enhancement of hydroformylation activity as observed for oxidic promoted rhodium catalyst [53,14] is not due to an enhanced CO insertion, but due to an enhanced hydrogenation activity and due to the stabilization of oxygenated intermediates.

An increase in the selectivity towards more C_2-oxygenates through oxidic promotion is not due to an enhanced CO insertion activity, but can be due to a stabilization of oxygenate intermediates. This shifts the CO insertion equilibrium to adsorbed oxygenates. Further, oxo-selectivity can be increased through a decrease in the reactivity of the CH_x intermediates towards methane as discussed before [46]. The stabilization of the C_2O intermediates appears from the increased surface concentration of these surface species through vanadium promotion. The stabilization of acetate species during synthesis gas reaction, has been observed with Infra Red spectroscopy [47,48]. However Orita et al [47] mentioned that not all the observed acetate species are reaction intermediates because they do not disappear upon hydrogenation. Also Bastein [48] could not estimate which part of the reaction intermediates reacts towards ethanol or ethanal. The same, is valid for the FT-IR work of Fukushima et al for acyl species [15]. In our experiment we only account for those CH_3CO species that are true reaction intermediates because they are calculated from the TOF. For the mechanism of acetate stabilization, Orita et al [10] showed that one oxygen atom of the support is needed. In a similar way it can be proposed that vanadium can act as an oxygen donor, which can increase the number of stabilized oxygenated intermediates. Also the ionic V-O bonds can influence the metal particles resulting in a more polar rhodium surface. This can result in stronger adsorbed oxygen-containing intermediates.

Orita et al [10] suggested that acetate species are located at the support near the rhodium metal particles. The high surface coverage of oxygenated reaction intermediates as calculated in table 3, also suggests that at least part of these

species are not located on the rhodium particles. Especially in the presence of vanadium, the high surface concentration of oxygenated intermediates suggests that CH_3CO species are possibly located on the vanadium or on the silica support near the rhodium particles. From the heterogeneity in the residence time of ethanal intermediates one can speculate that the reactive ethanal species are located on the rhodium particles while the less reactive ones are slowly desorbing from the silica support. This was also suggested by Arakawa et al [50] who noted two different acetate species with in situ IR spectroscopy during synthesis gas conversion at 50 atm at 260 °C.

Table 3 shows that during the synthesis gas reaction the hydrogenation rate is increased by vanadium promotion as was also found for cerium oxide promotion by Kiennemann et al [12], for molybdenum promotion by Jackson et al [51], and Trunschke et al [54], and for tungsten promotion by Bhore et al [52]. The enhanced hydrogenation activity is more obvious from the separate hydrogenation experiment of ethanal to ethanol (fig 7a and 7b). From these figures it appears that the hydrogenation activity is increased by a factor of 9 without changing the activation energy. The enhanced activity seems to be due to a greater number of active hydrogenation sites. The reaction order upon the hydrogenation of ethanal to ethanol is slightly negative in ethanal and positive in the hydrogen pressure, suggesting a stronger adsorption of ethanal than hydrogen. Remarkable is the decrease in the reaction order in hydrogen pressure from 1.7 to 0.8 through the vanadium promoter. This can be due to stronger adsorbed hydrogen. This effect is in agreement with effects indicated as 'spillover hydrogen' as reported in the references [51,52]. Also the selectivity for methane formation is decreased during ethanal hydrogenation. This effect is due to the smaller size of rhodium metal ensembles on the RhV system because the vanadium promoter is on top of the rhodium particles. This decreases the rate of C-C bond fission, which is known to be dependant on large metal ensembles. This idea is also confirmed by the reduced activity in hydrogenolysis of ethene (to methane) through vanadium on this catalyst, as reported in references [38,49].

CONCLUSION

The influence of vanadium promotion on the kinetics of several elementary reaction steps was studied by a Steady State Isotopic Transient Kinetic Analysis experiment. On the basis of the literature, a kinetic model based on elementary reaction steps, is proposed that is in agreement with the transient data. It appears that the residence time of oxygenated intermediates on the catalyst surface reacting to ethanal is shorter than that of the intermediates reacting to ethanol. Vanadium promotion reduces the time of ethanol

formation, while it enhances the time necessary for ethanal formation. The reaction coefficient of CO insertion is high compared with hydrogenation rates, showing that CO insertion is not a rate-limiting step. Vanadium promotion does not stimulate CO insertion, in the experiment described.

Ethanal formation occurs at least at two different sites. Vanadium promotion stabilizes oxygenated reaction intermediates on the catalyst surface, which results in a decrease of the rate of ethanal desorption. The hydrogenation activity of oxygenated intermediates to ethanol is enhanced by the vanadium promoter, which can be explained by more strongly adsorbed hydrogen.

LITERATURE

1. Katzer J.R., Sleight A.W., Gajardo P., Michel J.B., Gleason E.F. and McMillan S., *Faraday discuss. Chem. Soc.*, 72, 21 (1981).
2. Gilhooley K., Jackson S.D. and Rigby S., *Appl. Catal.*, 21, 349 (1986).
3. Nakajo T., Sano K., Matsuhira S. and Arakawa H., *Chem. Lett.*, 1986, 1557.
4. Ichikawa M., Shikakura K. and Kawai M., in "Heterogeneous Catalysis Related to Energy Problems", Proc. Symp. in Dalian, China, A.08-I (1982).
5. Van den Berg F.G.A., Glezer J.H.E. and Sachtler W.M.H., *J. Catal.*, 93, 340 (1985).
6. Bond G.C. and Richards D.G., *Appl. Catal.*, 28, 303 (1986).
7. Bhasin M.M., Bartley W.J., Ellgen P.C. and Wilson T.P., *J. Catal.*, 54, 128 (1987).

7a Dickson R.S., in "Homogeneous catalysis with compounds of rhodium and iridium", Riedel D. publishing comp. (1985).

7b. Ichikawa M., *J. Catal.*, 56, 127 (1979).

7c. Ichikawa M., *J. Catal.*, 59, 67 (1980).

8. Hackenbruch J., Keim W., Röper M. and Strutz H., *J. Mol. Catal.*, 26, 129 (1984).
9. Koerts. T. and Van Santen R.A., *J. Mol. Catal.*, 70, 119 (1991).
10. Orita H., Naito S. and Tamaru K., *J. Catal.*, 90, 183 (1984).
11. Underwood R.P. and Bell A.T., *Appl. Catal.*, 21, 157 (1986).

11a. Mazzochia C., Tempesti E., Grouchi P., Giuffré L. and Zabderighi L., *J. Catal.*, 111, 345 (1988).

12. Kiennemann A., Breault R. and Hindermann J-P., *J. Chem. Soc., Faraday Trans. I*, 83, 2119 (1987).
13. Jackson S.D., Brandreth J.B. and Winstantley D., *J. Catal.*, 106, 464 (1987).
14. Ichikawa M. and Fukushima T., *J. Chem. Soc., Chem. Comm.*, 1985, 321.
15. Fukushima T., Arakawa H. and Ichikawa M., *J. Phys. Chem.*, 89, 4440 (1985).
16. Agarwal A.K., Wainwright M.S. and Trimm D.L., *J. of Mol. Catal.*, 45, 247 (1988).
17. Sachtler W.M.H., Shriver D.F., Hollenberg W.B. and Lang A.F., *J. Catal.*, 92, 429 (1985).
18. Solymosi F., Tombácz I., Kocsis M., *J. Catal*, 75, 78 (1982).
19. Goodman D.W., *Appl. Surf. Sci.*, 19, 1 (1984).
20. Kip B.J., Smeets P.A.T., Van Wolput J.H.M.C., Zandbergen H., Van Grondelle J. and Prins R., *Appl. Catal.*, 33, 157 (1987).
21. Bastein A.G.T.M., Luo H.Y., Mulder A.A.J.P. and Ponec V., *Appl. Catal.*, 38, 241 (1988).
22. Fukuoka A., Kimura T., Kosugi N., Kuroda H., Minai Y., Sakai Y., Tominaga T. and Ichikawa M., *J. Catal.*, 126, 434 (1990).
23. Fukuoka A., Kimura T., Rao L-F. and Ichikawa M., *Catal. Today*, 6, 55 (1989).
24. Chuang S.C., Pien S-I. and Narayanan R., *Appl. Catal.*, 57, 241 (1990).

25. Chuang S.C., Pien S-I. and Sze C., *J. Catal.*, **126**, 187 (1990).
26. Chuang S.C., Tian Y.H., Goodwin J.G. Jr. and Wender I., *J. Catal.*, **96**, 396 (1985).
27. Sachtler W.M.H. and Ichikawa M., *J. Phys. Chem.*, **90**, 4742 (1986).
28. Chuang S.C., Goodwin J.G. Jr. and Wender I., *J. Catal.*, **92**, 416 (1985).
29. Pijolat M. and Perrichon V., *Appl. Catal.*, **13**, 321 (1985).
30. Fukushima T., Arakawa M. and Ichikawa M., *J. Chem. Soc., Chem. Comm.*, **1985**, 729.
31. Boujana S., Demri D., Cressely J., Kiennemann A. and Hindermann J.P., *Catal. Lett.*, **7**, 359 (1990).
31a. Happel J., Suzuki I., Kokayeff P. and Fthenakis V., *J. Catal.*, **65**, 314 (1982).
31b. Happel J., Chen H.I., Otarod M., Ozawa S., Severdia A.D., Yoshida T. and Fthenakis V., *J. Catal.*, **75**, 314 (1982).
31c. Ozawa S., Yin F., Chew M., Chen H.I. and Happel J., *J. Catal.*, **84**, 156 (1983).
31d. Stockwell M.D. and Bennett C.O., *J. Catal.*, **110**, 354 (1988).
32. Zhang, X. and Biloen P., *J. Catal.*, **98**, 59 (1980).
33. Nwalor J.U., Goodwin J.G. and Biloen P., *J. Catal.*, **117**, 121 (1989).
34. Iyagba E.T., Hoost T.E., Nwalor J.U. and Goodwin J.G., *J. Catal.*, **123**, 1 (1990).
35. Hoost T.E. and Goodwin J.G., *submitted to J. Catal.* on april 12, 1991
36. De Pontes M., Yokomizo G.H. and Bell A.T., *J. Catal.*, **104**, 147 (1987).
37. Siddall J.H., Miller M.L. and Delgass W.N., *Chem. Eng. Commun.*, **83**, 261 (1989).
38. Mori Y., Mori T., Hattori T. and Murakami Y., *Catal. Lett.*, **10**, 165 (1991).
39. Koerts T., Welters W.J.J., Van Santen R.A. , Nonnemann L.E.Y. and Ponec V., Proceedings of the conference on C_1 chemistry, Oslo, (1990), in '*Studies in surface science*' **61**, 235 (1991).
40. Efstathiou A.M. and Bennett C.O., *J. Catal.*, **120**, 137 (1989).
41. Leclercq P.A., Snijders H.M.J., Cramers C.A., Maurer K.H. and Rapp U., *J. of High Res. Chrom.*, **12**, 651 (1989).
42. Yates J.T., Duncan T.M., Worley S.D. and Vaughan R.W., *J. Chem. Phys.*, **70**, 1219 (1979).
43. Davis J.L. and Barteau M.A., *Surf. Sci.*, **187**, 387, (1987).
44. Collman J.P., Finke R.G., Cawse J.N. and Brauman J.I., *J. Am. Chem. Soc.*, **100**, 4766 (1978).
45. Richmond T.G., Basolo F. and Shriver D.F., *Inorg. Chem.*, **21**, 1272 (1982).
46. Koerts T. and Van Santen R.A., *Catal. Lett.*, **6**, 49 (1990).
47. Orita H., Naito S. and Tamaru K., *J. Catal.*, **112**, 167 (1988).
48. Bastein A.G.T.M., Ph.D. Thesis, Leiden University (1988).
49. Hartog A.G. den, Deuz M., Jongerius F. and Ponec V., *J. Molec Catal.*, In Press.
50. Arakawa H., Fukushima T., Ichikawa M., Takeuchi K., Matsuzaki T. and Sugi Y.,*Chem. Lett.*, **1985**, 23.
51. Jackson S.D., Brandreth B.J. and Winstanley D., *Appl. Catal.*, **27**, 325 (1986).
52. Bhore N.A., Sudhakar C., Bischoff K.B., Manogue W.H. and Mills G.A., *Proc. IX I.C.C. Calgary*, **vol. 2**, 594 (1988).
53. Ichikawa M., Lang A.J., Shriver D.F. and Sachtler W.M.H., *J. Am. Chem. Soc.*, **107**, 7216 (1985).
54. Trunschke A., Böttcher H.-C., Fukuoka A., Ichikawa M. and Miessner H., *Catal. Lett.*, **8**, 221 (1991).

4

The reactivity of surface carbon from dissociated carbon monoxide on vanadium promoted rhodium catalysts.

ABSTRACT

The hydrogenation reactivity of surface carbon deposited by CO decomposition was investigated for a rhodium and a rhodium-vanadium catalyst. It appeared that the rate of methanation of reactive surface carbon is decreased by the vanadium promoter. The reactivity towards C_2^+ hydrocarbons is enhanced by this promotion. The relation between more strongly adsorbed carbon atoms and the formation of higher hydrocarbons is suggested. Quantum chemical calculations support the proposal that changes in metal-carbon bond strength have a significantly larger effect on the rate of methanation than on carbon chain growth.

This chapter is published in *Catalysis Letters*, 6, 49 (1990), with co-author Rutger A. van Santen.

INTRODUCTION

Adsorbed carbon atoms on group VIII metals are reaction intermediates [1-6] in the formation of hydrocarbons from synthesis gas. The formation of carbonaceous intermediates from CO disproportionation on these metals has been studied previously [7-9]. On rhodium three types of carbon [10-16] can be produced from CO adsorption at temperatures above 250°C. They can be distinguished in their hydrogenation temperatures and are referred to as C_α, C_β and C_γ. Reactive C_α species can be hydrogenated to methane even at room temperature. C_β is less reactive and can be hydrogenated between 200 and 300°C to methane. C_γ is an unreactive graphitic type of carbon and needs hydrogenation temperatures above 400 °C.

The reactive C_α species are important intermediates when supported on rhodium catalysts. They can react towards methane, C_2-intermediates or C_2O-intermediates. The relative reactivity towards methane is one of the factors determining the maximum selectivity of the catalyst towards other products. In order to understand the promoting action of oxophilic promoters, it is essential to study changes in reactivity of adsorbed carbonaceous intermediates. The influence of vanadium promotion on the reactivity of adsorbed C atoms towards hydrogenation and carbon-carbon coupling on rhodium based catalysts is studied in this chapter.

EXPERIMENTAL

A 3% wt. rhodium catalyst was prepared by incipient wetness impregnation of an aqueous $RhCl_3$ solution on silica (Grace 332, 240 m^2/g, PV=1.6 ml/g). The mean rhodium particle size after reduction is 22 Å as concluded from TEM and CO chemisorption. After drying and reducing the rhodium catalyst at 300°C for 24 hours, vanadium was post impregnated from a solution of NH_4VO_3, (Rh/V=3 mol). This post impregnation did not affect the rhodium particle size. The vanadium caused a reduction of the CO chemisorption capacity of 50-55%. This was independent of the reduction temperature between 200 and 450°C. For further characterization of the catalysts see chapter 2.

Reactive C_α carbon species were created during CO adsorption flowing 10 minutes 55 ml/min of diluted CO with a partial pressure of 0.5% CO in He at 1 atm. over the catalysts. The adsorption temperature was chosen in such a way that the surface coverage of reactive carbon was the same on the Rh and RhV catalysts (respectively 390 and 340°C). This was confirmed with Temperature Programmed Surface Reaction spectroscopy in which 14 percent of the total methane formation occurred at a temperature below 100°C. After CO adsorption

the catalyst was quickly cooled in a helium flow to the temperature were the hydrogenation reactivity was measured.

The hydrogenation rate of the reactive carbon species was studied isothermally in a flow of 55 ml/min of 8% hydrogen in helium at 1 atmosphere. All gases were purified with BTS (reduced copper) and molecular sieve. Analysis was performed with a Quadrupole Mass Spectrometer in which 8 masses could be detected every second.

The influence of reactive carbon on the synthesis gas reaction was studied with transient experiments, in a system in which it was possible beside continually monitoring with a QMS, to store 16 loops of 0.3 ml of reaction gases. The reaction gas samples were analysed afterwards with a gas chromatograph (12 meter of a wide bore plot Q column) as shown in figure 1.

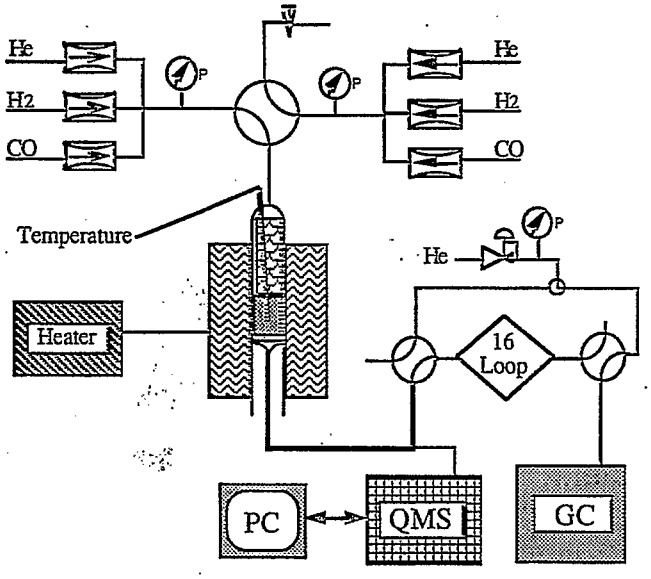

Figure 1. Apparatus for transient response information with time based GC analysis.

The dead volume of the system was reduced as much as possible to avoid mixing of the gases. After creating reactive carbon and cooling to 200°C, the flow over the catalyst was changed to 67% H_2 in He or to synthesis gas ($H_2/CO=2$), with a flow of 15 ml/min, at atmospheric pressure. During the start of the reaction 15 loops of the reaction gases were stored and analysed afterwards. In this way a time based GC experiment could be performed. Such a system is necessary when a mass spectrometer can not separate all components or when it is not possible to measure them quantitatively.

RESULTS

After depositing reactive carbon the hydrogenation activity towards methane was investigated at different temperatures. After switching to the diluted hydrogen flow methane product formation was monitored. Assuming a reaction first order in adsorbed C_α carbon, what is true for low $\Theta_{C\alpha}$, and the hydrogen partial pressure to be constant, the decreasing part of the methanation curve can be used to determine the reaction rate constant. The k values obtained in this way from Rh and RhV catalysts are compared in figure 2.

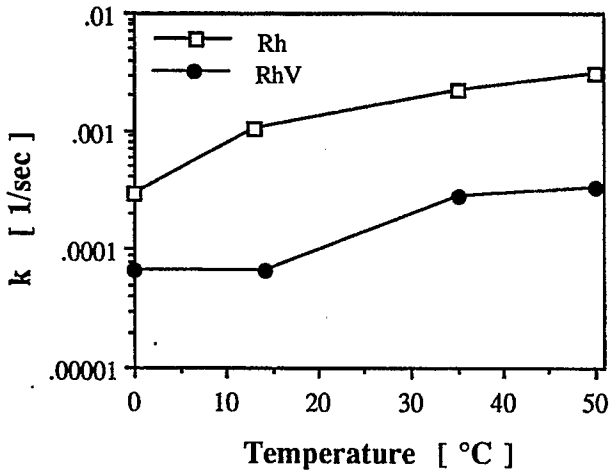

Figure 2. Hydrogenation reactivity coefficient (k) for the hydrogenation of reactive C_α surface carbon species, on Rh and RhV catalyst as a function of the temperature. The same surface coverage of reactive surface carbon is generated from CO dissociation at temperatures above 250 °C. k is expressed in sec^{-1}.

The hydrogenation reactivity of the carbon species on the rhodium catalyst is found to be 7 times higher than that on the vanadium promoted catalyst.

Hydrogenation experiments were also performed at 200°C. The formation of hydrocarbons from reactive carbon during this hydrogenation was studied using the time based GC equipment. In figure 3 the initial concentrations of hydrocarbons are plotted for the Rh and RhV catalyst.

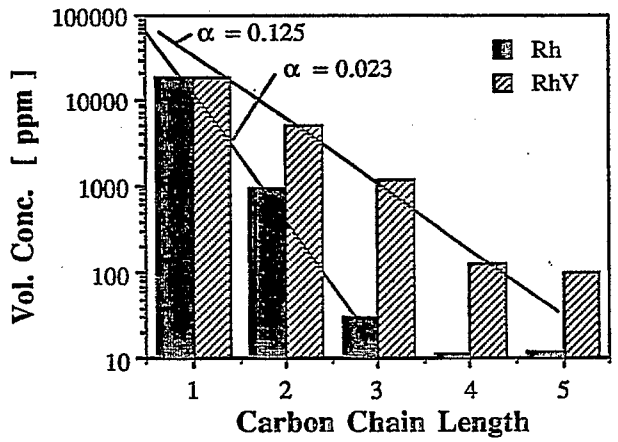

Figure 3. The maximum concentration of hydrocarbons observed at 200°C during the hydrogenation of reactive surface carbon generated from CO, plotted as a function of the carbon chain length.

It is clear that the reactivity of the reactive carbon species towards higher hydrocarbons is increased by the vanadium promoter. This increased reactivity can not be due to a higher concentration of reactive carbon species because the initial $\Theta_{C\alpha}$ was the same on both catalysts. The increased reactivity is due to a changed intrinsic reactivity of the adsorbed CH_x species or to a changed local surface concentration. The alpha values deduced from this Schulz-Flory plot are low and methane is the main product on both catalysts. However, the chance for recombination of carbon fragments is five times larger on the vanadium promoted catalyst.

A similar experiment was performed using synthesis gas instead of the hydrogen helium mixture. The initial formation of hydrocarbons at 200°C during the start of the synthesis gas, with an initial surface concentration of reactive carbon species of about 14 percent, is plotted in figure 4.

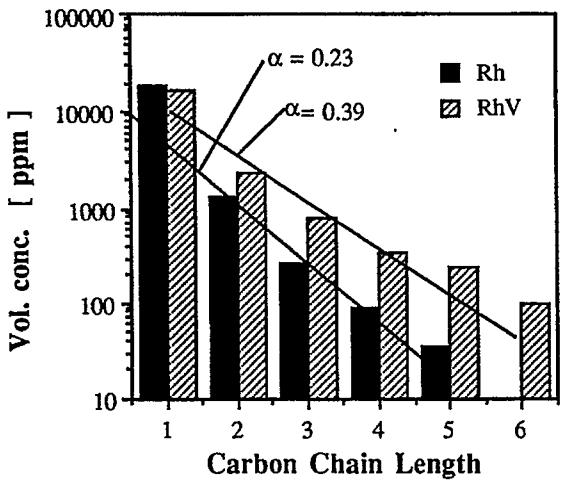

Figure 4. The formation of hydrocarbons during the start of a CO/H_2 reaction at 200 °C after deposition of reactive carbon from CO.

From figure 4 it appears that the rate of initial methane formation is about the same for both catalysts. Again more C_2+ hydrocarbons are produced on the vanadium-promoted catalyst. This implies that the carbon-carbon bond formation rate at the same initial surface coverage of carbon species is enhanced by vanadium promotion. So also during the synthesis gas reaction the higher intrinsic reactivity of the adsorbed carbon species towards C_2+ hydrocarbons is shown.

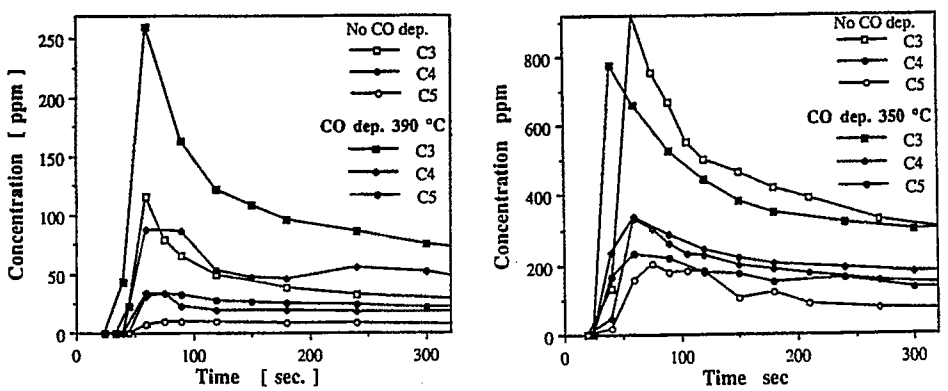

Figure 5. Propane , butane and pentane formation during the start of a reaction with synthesis gas on a reduced catalyst and on a catalyst with 14% of reactive carbon created from CO deposition. a (left): Rhodium. b (right): Rhodium/vanadium.

The rates of hydrocarbon formation during the start of a synthesis gas reaction was compared for catalysts with and without predeposition of reactive carbon. The results for propane to pentane are given in the figures 5a and b. Carbon monoxide adsorbed at 200°C on a rhodium catalyst will not produce reactive carbon on a fully covered rhodium surface. In the presence of hydrogen the temperature of CO dissociation can be lowered [16-19]. Therefore, even at 200°C, hydrocarbons can be produced from synthesis gas. Also without predeposition of carbon the initial formation rate of hydrocarbons is higher than during the steady state reaction that exists after about 30 min. This is due to the fact that the first CO molecules that adsorb on the rhodium surface can be relatively easy dissociated since free metal ensembles necessary for this reaction are present. On a CO covered rhodium surface the amount of free metal ensembles is lower, and therefore the rate of CO dissociation and hydrocarbon formation decreases. When $\Theta_{C\alpha}$ is higher after CO decomposition, more C_3 to C_5 species are produced suggesting that hydrocarbons are formed from the reactive C_α species. When C_α is removed by hydrogenation at 50 °C after CO deposition at 370 °C and before the CO/H_2 reaction at 200 °C, no extra C_2^+ hydrocarbon formation is observed.

For the RhV system it seems that there is no significant difference between the hydrocarbon formation with and without predeposition of CO. Apparently, there is not much difference in the amount of reactive carbon formed at 200°C during the start of a synthesis gas reaction compared to CO decomposition at 340°C. This implies that also in the abundance of hydrogen the formation of reactive carbon on rhodium catalysts is enhanced by the vanadium promoter [20].

From the hydrogenation experiments it appears that vanadium promoter suppresses the reactivity of adsorbed carbon atoms for methanation. This agrees with the results on Ru of Mori et al [19]. They investigated the rate of methanation of a pulse of CO in which k_{CO} and k_{CH_x} could be separately measured. The ratio of k_{CH_x}/k_{CO} for a Ru/Al_2O_3 catalyst was reduced by vanadium and molybdenum promotion. We also compared the reactivity of CO on a ruthenium with a vanadium-promoted ruthenium catalyst in a temperature programmed hydrogenation experiment with adsorbed CO. Only when vanadium was co-adsorbed C_2^+ hydrocarbon formation was observed, indicating a changed selectivity for methanation versus carbon-carbon bond formation.

The difficult step in the hydrogenation of adsorbed C atoms on metal particles is likely related to the bond strength of the adsorbed CH_x intermediates. A slower hydrogenation can be expected with a stronger interaction between the

carbon fragments and the metal surface. This would lead to a higher selectivity for higher hydrocarbons, if carbon-carbon coupling is less affected. This suggestion disagrees with an alternative proposed by Meriaudeau et al [21] who suggested that carbon-carbon bond formation is stimulated by more mobile CH_x fragments on rhodium catalysts, which mobility should be induced by TiO_2 promotion.

The relation between more strongly adsorbed carbon atoms and recombination of carbon fragments was also studied by quantum chemical calculations using the Atom Superposition Electron Delocalization molecular orbital theory as described by Anderson .[22,23]. The ASED method is a semi empirical method, based on Extended Huckel calculation to which a repulsion term is added [24]. Calculations on a 40 atom cluster simulating the (111) surface of an f.c.c. crystal indicate that the activation energy for carbon-carbon coupling is rather insensitive to the metal-carbon bond strength. The influence of the metal-carbon bond strength was simulated by varying the number of valence electrons per metal atom. Table 1 shows the results for the maximal M-CH_x bond strength for different surface carbon fragments, at their favoured adsorption sites, relative to the free metal and CH_x radicals.

Table 1. Adsorption energies in e.V. of CH_x fragments on Ru, Rh and Pd on a f.c.c.(111) metal clusters of 40 atoms as calculated with the ASED method.

Particle	Ru	Rh	Pd
CH_3	-2.70	-2.58	-2.27
CH_2	-4.07	-3.77	-2.93
CH	-5.64	-5.45	-4.46
C	-5.51	-5.47	-4.47

The metal-carbon bond strength decreases going from Ru to Rh to Pd. This result is in agreement with the LCAO calculations of Feibelman [25]. The influence of the metal-carbon bond strength on the recombination of surface CH_x species was studied by comparing the activation energy for carbon-carbon bond formation on the different metals. The reaction path studied was the recombination of a carbon atom adsorbed on three metal atoms with a moving CH_2 fragment as is shown in figure 4 of chapter 5. The potential energy as a function of the carbon-carbon distance projected on the metal surface, is shown in figure 6.

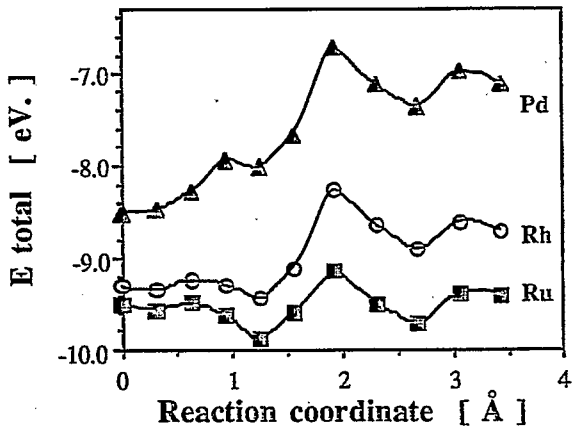

Figure 6. Potential energy during the formation of a carbon-carbon bond on an f.c.c.(111) surface, as a function of the reaction coordinate. The d-band occupation of the metal was varied, while the metal structure and parameters of Ru, Rh and Pd were taken identical.

For palladium the reaction is more exothermic than on rhodium and ruthenium. The created vinylidene species is bonded with one carbon atom to a palladium surface in a on top position, while it is bended in a tilted position bonded with two carbon atoms to the a ruthenium surface as indicated by the small dip in the ruthenium curve at a projected C-C distance of 1.3 Å.

Whereas the metal-carbon bond strength decreases in order Ru > Rh > Pd, the activation energy for carbon-carbon bond formation is not much changed. However, the rate of methane formation from adsorbed carbon fragments, where the metal-carbon bond must be broken, is dependent on the metal-carbon interaction, resulting in a decreased methanation rate at a high M-C interaction. Therefore, a strong metal-carbon interaction favours the carbon chain growth versus methane formation. Experimentally it is found [26,27] that the selectivity for C_2^+ hydrocarbons in synthesis gas conversion reaction decreases from Ru to Pd. So the higher activity of Ru than Rh and Pd in the Fischer-Tropsch reaction is not only due to an enhanced activity in CO dissociation but also due to a changed intrinsic activity for carbon-carbon bond formation versus methanation. At a higher carbon adsorption energy the mean residence time of CH_x fragments is increased that makes the chance for C-C bond formation greater. The discussed favourable chain growth at strong M-C interaction is only valid in a selected range of metal-carbon bond strength. If the interaction of

carbon atoms with the metal surface is too large (as with tungsten), stable carbides can be formed what leads to a strongly reduced catalytic activity in both reactions.

CONCLUSION

Vanadium promotion reduces the rate of methane formation upon hydrogenation of surface carbon on rhodium catalysts due to an enhanced metal-carbon interaction. This effect is accompanied with a higher chain growth probability. Quantum chemical calculations indicate that at a higher metal carbon bond strength the activation energy for methane formation is decreased while the activation energy for carbon-carbon bond formation is much less affected.

LITERATURE

1. M. Araki and V. Ponec, *J. Catal.*, 44 (1976) 439.
2. J.G. McCarty and H. Wise, *J. Catal.*, 57 (1979) 406.
3. A.T. Bell, *Catal. Rev.-Sci. Eng.*, 23 (1981) 203.
4. N.W. Cant and A.T. Bell, *J. Catal.*, 73 (1982) 257.
5. P. Biloen, J.N. Helle, F.G.A. van den Berg and W.M.H. Sachtler, *J. Catal.*, 81 (1983) 450.
6. R.C. Baetzold and J.R. Monnier, *J. Phys. Chem.*, 90 (1986) 2944.
7. J.A. Rabo, A.P. Risch and M.L. Poutsma, *J. Catal.*, 53 (1978) 295.
8. J.G. McCarty and H. Wise, *J. Catal.*, 57 (1979) 406.
9. M. McLaughlin McClory and R.D. Gonzales, *J. Catal.*, 89 (1984) 392.
10. F. Solymosi and A. Erdöhelyi, *Surf. Sci.* ,110 (1981) L630 .
11. F. Solymosi, I. Tombácz and M. Kocsis, *J. Catal.*, 75 (1982) 78.
12. A. Takeuchi and J.R. Katzer, *J. Catal.*, 82 (1983) 351.
13. H. Orita, S. Naito and K. Tamaru, *J. Catal.*, 111 (1988) 464.
14. A.M. Efstathiou and C.O. Bennett, *J. Catal.*, 120 (1989) 118.
15. Gupta N.M., Kamble V.S., Annaji-Rao K. and Iyer R.M., *J. Catal.*, 60, 57 (1979).
16. F. Solymosi, I. Tombácz and M. Kocsis, *J. Catal.*, 75 (1982) 78.
17. T. Mori, H. Masuda, H.Imal , A.Miyamota, R. Hasebe and Y. Murakami, *J. Phys. Chem.*, 87 (1983) 3648.
18. J.H. Siddall, M.L. Miller and W.N. Delgass, *Chem. Eng. Commun.*, 83 (1989) 261.
19. T. Mori, A. Miyamoto, N. Takahash, M. Fukagaya, H. Niizuma, T. Hattori and Y. Murakami, *J. Chem. Soc. Chem. Comm.*, 1984 678.
20. T. Koerts, W. Welters, R.A. van Santen, *J. Catal.*, 133, (1992) in press.
21. P. Meriaudeau, H. Ellestad and C. Naccache, *J. Mol. Catal.* ,17(2-3) (1982) 219.
22. A.B. Anderson, *J. Chem. Phys.*, 62 (1975) 1187.
23. A.B. Anderson, R.W. Grimes and S.Y. Hong, *J. Chem. Phys.*, 91 (1987) 4245.
24. De Koster A., Thesis, Eindhoven (1989).
25. P.J. Feibelman, *Phys. Rev. B.*, 26 (1982) 5347
26. M.A. Vannice, *J. Catal.*, 37 (1975) 462.
27. B.W. Wojciechowski, *Catal. Rev. -Sci. Eng.*, 30 (1988) 629.

5

The reaction path for recombination of surface CH_x species.

ABSTRACT

Using the semi-empirical quantum-chemical calculations the reaction path for carbon-carbon bond formation has been studied on a Rh_{40} cluster simulating an f.c.c. (111) surface. Highly hydrogenated surface carbon fragments are found to have high activation energies for recombination. This is due to repulsion between the hydrogen atoms. The lowest activation energy was found for the recombination of a three fold bonded carbon atom with a CH_2 species, to form a vinylidene surface species. Experimental results are presented, obtained on silica supported Rh, Co and Ru catalysts, which confirm that carbon-carbon bond formation is favourable from CH_x fragments in which the average value of x is about one.

Comparing the reaction for carbon-carbon bond formation on metal clusters simulating ruthenium, rhodium and palladium surfaces, it appeared that the activation energy for carbon-carbon bond formation is rather insensitive for the metal-carbon bond strength. This is not true for methanation of surface carbon atoms, in which the metal-carbon bond has to be broken. This indicates that carbon chain growth is favourable at high metal-carbon interaction, within the discussed range.

This chapter is published in *Journal of Molecular Catalysis*, 70, 119 (1991), with co-author Rutger A. van Santen.

INTRODUCTION

Adsorbed carbon atoms on group VIII metals are important reaction intermediates in the formation of hydrocarbons from synthesis gas [1-6]. The formation of carbonaceous intermediates from CO dissociation on these metals has been studied extensively [7-9]. On rhodium different types of carbon can be produced from CO adsorption at temperatures above 250°C, as has been shown on practical catalysts [10-14], single crystals [15-17] and from quantum chemical studies [18-21]. Recent experiments in our laboratory [22] show that similar carbon surface species can be created from methane decomposition at temperatures between 200 and 600 °C. Three different types of carbonaceous intermediates, distinguishable by their hydrogenation reactivity, can be generated by methane decomposition on reduced supported transition-metal catalysts. Three-fold bonded carbidic surface species such as Ni_3C for nickel [23] have been suggested as the most reactive one for the formation of methane as well as for the recombination of surface carbon fragments [24]. Therefore, this study will concentrate on reactive isolated surface carbon atoms and CH_x species, for the hydrogenation to methane and the formation of a carbon-carbon bond.

Recombination of these carbonaceous species is one of the important reaction steps in Fischer-Tropsch synthesis. Of interest, to the mechanism of carbon-carbon bond formation, is the extent to which carbon fragments are hydrogenated. We will present results of an experimental investigation to determine the value of x of the recombinating CH_x surface fragments. We explored the possibility to create surface CH_x fragments with a known value of x by methane decomposition. Subsequently, carbon-carbon bond formation can be initiated upon hydrogenation of the carbonaceous surface species [22]. First, we will discuss the quantum theoretical results concerning the reaction path and geometry of the recombination of surface CH_x species.

Theoretical studies of interactions of adsorbates with surfaces are subjects of an increasing interest. Here we use the Atom Superposition and Electron Delocalization (ASED) method as introduced by Anderson [27,28] to study the reaction path of elementary reaction steps on metal surfaces. The ASED program is based on the Extended Hückel method [25,26] to which an electron repulsion term is added. Whereas absolute values of calculated adsorption energies of surface fragments have to be treated carefully, it can be useful for a qualitative prediction of electronic trends, geometry of adsorbates and the reaction paths of surface reactions [29]. Currently semi-empirical methods as the ASED method, are the only ones that can be used to study chemical reactivity problems as considered here. Ab initio calculations are still limited to small systems [30,40].

However, a large metal-ensemble of metal atoms, with proper first coordination shells, has to be applied. Also many different reaction paths have to be probed.

The calculations are performed on a rhodium 40 cluster with 29 atoms in the top layer and 11 atoms in the second layer, simulating an f.c.c. (111) surface. Ruthenium and palladium surfaces are simulated from the rhodium surface by respectively adding and subtracting one electron per rhodium atom. Comparing results in this way one can study in isolation the effect of changes in d-orbital occupation, while structure and electron energy parameters remain unchanged.

The implications for carbon-carbon bond formation as found with the ASED calculations will be compared with results obtained from practical model experiments on silica-supported Co, Ru and Rh catalysts.

RESULTS AND DISCUSSION

In a previous study de Koster et al [31] showed that CH_x fragments when interacting strongly with d-valence electrons, optimize hybridization of the s, p carbon electrons, by choosing different adsorption sites when x varies. On the Rh(111) surface a CH_3 fragment will adsorb preferentially on top of a Rh atom, CH_2 adsorbs bridge on two Rh atoms and CH and C will adsorb coordinated to three Rh atoms in a three fold position. However, Yang et al and Siegbahn et al found that CH_3 surface species can be bonded to more than one nickel atom [31a,31b].

The adsorption energies for the carbon fragments on their favourable adsorption sites used in this study are presented in table 1. The distance z above the surface is the position with a minimized energy.

Table 1. Adsorption energies (in eV.) of surface species on Ru, Rh and Pd_{40}(111) surface. Adsorption energies are calculated with respect to the free radicals

Particle	Position	z (Å)	Ru	Rh	Pd
CH_3	1-fold	2.1	-2.70	-2.58	-2.27
CH_2	2-fold	1.5	-4.07	-3.77	-2.93
CH	3-fold	1.3	-5.64	-5.45	-4.46
C	3-fold	1.2	-5.51	-5.47	-4.47
H	1-fold	1.8	-3.89	-3.60	-3.21
CO	3-fold	1.4	-2.46	-2.38	-1.65
O	1-fold	1.4	-6.83	-6.35	-5.08

As also observed by Feibelman [32] and Darling et al [33], the adsorption energy of carbon fragments is decreasing at increasing d-valence occupation. This is due to the filling of anti-bonding orbitals of the metal-adsorbate intermediate, resulting in a decrease of the metal-carbon bond strength. Highly hydrogenated CH_x fragments are supposed to be more mobile due to a decreased metal-adsorbate interaction (see Table 1). Therefore, one has initially been concentrated on the recombination of those CH_x species in which x is 2 or 3. Zheng e.a. [34] studied C-C bond formation between two adsorbed CH_3 radicals on a Co(0001) surface according to the mechanism in fig. 1. No reaction path with an acceptable low activation energy was found.

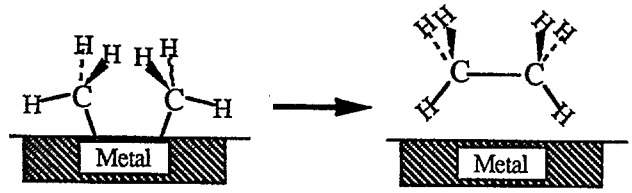

Figure 1. Reaction path of the recombination of two CH_3 radicals as considered by Zheng [34].

De Koster and van Santen [31] studied the co-adsorption of a CH_3 and a CH_2 fragment on different sites with a C-C distance of 1.55 Å. Again no C-C bond formation was found to occur.

We have analysed the co-adsorption of a CH_3 fragment adsorbed on top of a Rh atom together with a CH fragment in a two fold or three fold site, with a C-C distance of respectively 1.34 and 1.55 Å. A significant repulsion between the two fragments occurs. This repulsion can be decreased by 'bending' the hydrogen atom of the CH fragment away from the CH_3 fragment according to fig. 2a, or by 'straining' two hydrogen atoms of the CH_3 fragment (see fig. 2b).

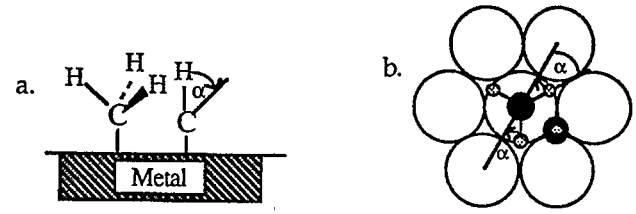

Figure 2. Schematic presentation of distortion of hydrogen atoms in CH_x species. a. Bending of CH. b. Straining in a CH_3 fragment.

The adsorption energy as a function of the distortion angle, as schematically drawn in the figures 2a and 2b, are shown in the figures 3a and 3b respectively.

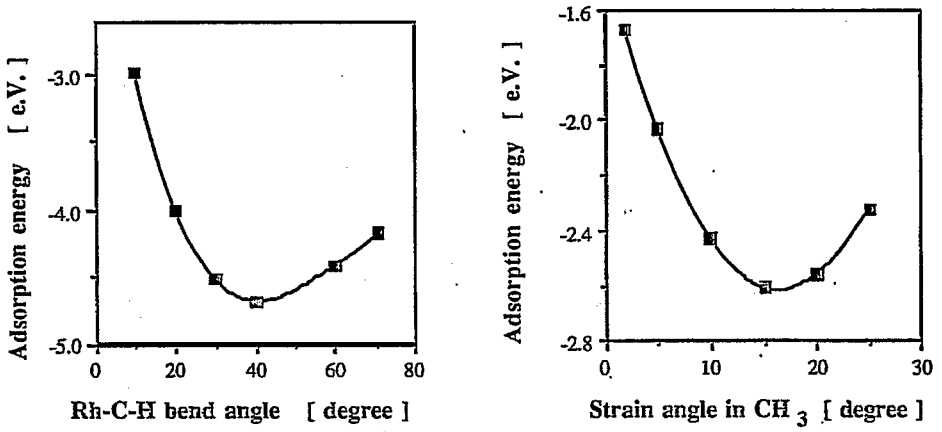

Figure 3. Adsorption energy of a CH_3 and CH fragment at a distance of 1.55 Å according to the geometry of the figures 2a and 2b as a function of the hydrogen distortion angle. a (left): bending b (right): stretching.

The bending of hydrogen atoms to more unfavourable positions for the loosely adsorbed fragments, decreases the total adsorption energy drastically. The energy gain is caused by a loss of steric repulsion of the hydrogen atoms. However still a large activation energy barrier for carbon-carbon bond formation remains, due to steric hindrance of hydrogen atoms. Therefore it is of interest to study also the recombination of carbon fragments without hydrogen atoms as the Rh_3C carbon atom.

The three fold bonded C atom is sp^3 hybridized and has one dangling bond available for the formation of a carbon bond with a moving fragment. Different CH_x species were moved to the carbidic carbon atom according to two different reaction paths (see figure 4).

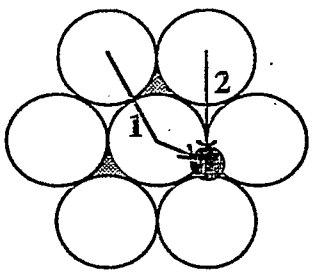

Figure 4. Reaction paths studied for C-C recombination involving a surface carbidic atom (black). Only 7 surface metal atoms are shown.

According to the reaction path 1, an adsorbed CH_x fragment approaches the carbon atom along a one-fold bonded (on top) position, while in reaction path 2 the approaching fragment has a two-fold bonded intermediate. The position of the CH_x fragment was changed in ten steps along the drawn line of the reaction

path. At each position the height above the rhodium surface was changed in steps of 0.2 Å.

In figure 5 the computed potential energy surface plots are drawn as a function of the position of a moving CH_3 and CH fragment in the plain perpendicular to the Rh surface according to reaction path 1.

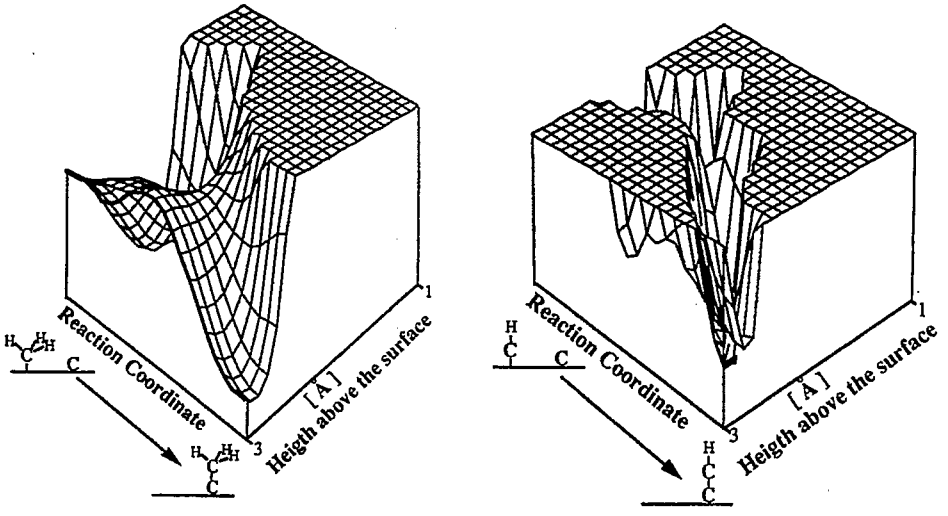

Figure 5. Adsorption energy of the moving surface species as a function of the position of the moving fragment in the plain perpendicular to the Rh surface along reaction path 1. a (left): Recombination of C and CH_3. b (right): Recombination of C and CH.

The height of the saddle-point in figure 5, relative to the initial adsorption energy determines the activation energy for C-C recombination. In table 2 the activation energies are collected for the recombination of different CH_x fragments with a three fold bonded carbon atom according to the reaction path 1 and 2 from fig. 4.

Table 2 shows that the affinity for recombination of a partially hydrogenated carbon fragment with a carbon atom increases with the decreasing activation energy according to CH_3 (1.98 eV) < CH (1.75 e.V.) < C (1.63 e.V.) < CH_2 (0.98 e.V.). Most of the proposed reaction mechanisms are a little exothermic. The subsequent hydrogenation steps become less exothermic when more hydrogen atoms are added to the C_2 fragment. The activation energy for methanation can be considered proportional to the metal-carbon bond strength [41], because this bonding has to be broken.

Table 2. Energy barriers for carbon-carbon bond formation with different moving surface CH_x fragments.

Path	Species [1]	E_{start} [2]	$E_{intm.}$ [3]	E_{end} [4]	E_{ads} [5]	E_{act_1} [6]	E_{act_2} [7]
1	CH_3	-7.86	-6.07	-8.23	-8.05	1.79	1.98
	CH_2	-8.71	-8.26	-9.3	-9.24	0.45	0.98
	CH	-10.24	-8.82	-10.4	-10.92	1.42	2.1
	C	-10.5	-9.31	-9.8	-10.94	1.19	1.63
	H	-9.38	-8.62	-10.95	-9.61	0.76	0.99
	CO	-7.83	-6.5	-7.52	-7.85	1.33	1.35
2	CH_3	-7.8	****	-8.23	-8.05	****	****
	CH_2	-8.74	-8.19	-9.29	-9.24	0.55	1.05
	CH	-10.24	-9.17	-10.4	-10.92	1.07	1.75
	C	-9.76	-9.13	-10.5	-10.94	0.63	1.81
	H	-9.47	-8.49	-10.94	-9.61	0.98	1.12
	CO	-7.83	-6.14	-7.54	-7.85	1.69	1.71

1: Moving Species towards C atom.
2: Adsorption energies of surface fragments in start position: moving species 1-fold.
3: Adsorption energy of activated complex.
4: Adsorption energy after C-C bond formation.
5: Adsorption energy of loose adsorbed species and C atom in favoured adsorption state.
6: Activation energy with respect to the start energies.
7: Activation energy taking the loose surface fragments from table 1 as start energy.
****: CH_3 fragment will desorb.

The reaction path for carbon-carbon bond formation with the lowest activation energy found is the recombination the three-fold bonded surface carbon atom with a moving CH_2 fragment forming a vinylidene surface species. The importance of the CH_2 fragment in relation to the formation of a carbon-carbon bond on heterogeneous catalysts, has been previous proposed by Petit and Brady [42,43] and by Tanaka [44] as well as on homogeneous systems [45,46]. Also it has been demonstrated that vinylidene metal complexes can act as reactive intermediates on ruthenium, by Trost et al [36]. The presence of methylene intermediates on metal surfaces has been demonstrated on ruthenium by George et al [47] and on iron by Chang et al [48]. This indicates that the found reaction path from quantum chemical calculations is in agreement with practical observations.

As demonstrated in chapter 4 (Fig. 6) the activation energy for carbon-carbon bond formation is only weakly dependent on the d-valence band occupation, and is not sensitive to the strength of the metal-carbon interaction. However the activation energy for methane formation from CH_x fragments increases with increasing metal-carbon bond strength. This leads to the conclusion that chaingrowth propagation is favourable at not too low metal-carbon bond interactions. This result is in disagreement with Shustorovich's 'Bond Order Conservation' principle [35,41] deduced from empirical rules of Polanyi [41b]. According to this theory more strongly adsorbed surface carbon must is reactive for carbon-carbon bond formation.

The reaction intermediate in the formation of a carbon-carbon bond has been analysed on a rhodium cluster of 10 atoms from changes in electronic densities. The change in electronic density of the reaction intermediate relative to the single carbon atom, the CH_2 fragment and metal cluster is calculated. Fig. 6 shows the electronic density difference in a plane through the two carbon atoms perpendicular to the rhodium surface.

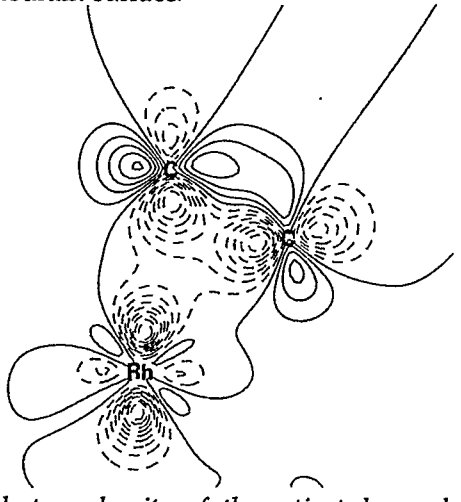

Figure 6. Changes in electron density of the activated complex of a C and CH_2 fragment adsorbed on a Rh_{10} cluster, during recombination, relative to the loose fragments. The dotted line connects points with equal electron density loss; the solid line connects points with the same electron density increase.

The moving CH_2 fragment shows an increase of electronic density in its $p_{x,y}$ orbitals, which are used to initiate C-C bonding. However, the metal-carbon bond of the CH_2 fragment is mainly formed from carbon p_z and s orbitals. Therefore it is proposed that different orbitals are involved in carbon-carbon bond formation and methane formation from carbon surface species. This

partially explains why the activation energy for C-C bond formation changes less than that for methane formation when the metal carbon bond strength increases.

CH_x species with a known average value of x can be deposited by a controlled methane decomposition [22]. Methane was decomposed from a flow of 40 ml/min of 1.8% CH_4 in helium, on a reduced transition-metal catalyst between 200 and 600 °C during 90 seconds. The fraction of methane adsorbed as well as the amount of hydrogen produced were measured with a quadrupole mass spectrometer. This enabled calculation of the average value of x. The average value of x in the CH_x fragments is a function of the adsorption temperature as shown in figure 7.

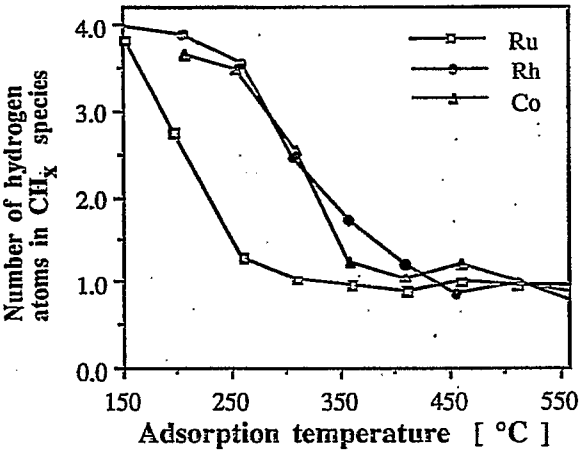

Figure 7. Extent to which methane is decomposed as a function of the methane adsorption temperature on some silica-supported metal catalysts.

Fig. 7 shows that at a higher temperature methane species are decomposed to a larger extent. The calculated effective x values at low temperature (< 200 °C) may be too high due to hydrogen that remains adsorbed on the catalyst surface. In chapter 6 it will be demonstrated that these surface CH_x fragments from CH_4 decomposition can be recombined and hydrogenated to C_2^+ hydrocarbons. The optimum hydrogenation temperature for this process is 95 °C. Here we compare the relative amount of C_2^+ hydrocarbon formation, from surface CH_x fragments with different effective values of x (see Fig. 8).

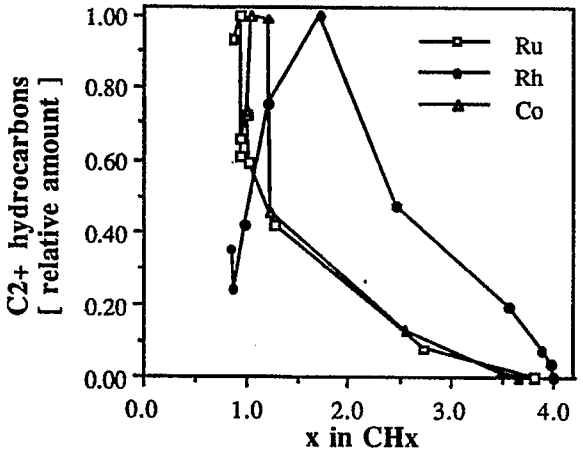

Figure 8. Amount of C_2^+ hydrocarbons formed upon hydrogenation at 95 °C, as a function of the extent of dehydrogenation of the surface CH_x species generated from methane decomposition.

Figure 8 shows that carbon-carbon bond formation is favourable when the surface fragments are largely dehydrogenated. The optimum average value for the CH_x species found in this way is 1 to 1.5. This measured low hydrogen content of the recombinating CH_x fragments is in agreement with that obtained from the quantum chemical calculations. Also Van Barneveld and Ponec [37,37b] suggested this from the incorporation of CH_x fragments generated from the decomposition of different chloro substituted methanes, upon synthesis gas conversion. The order of enhancement of carbon chain-growth was $CHCl_3$ > CH_2Cl_2 >> CH_3Cl, suggesting that carbon-carbon bond formation preferentially occurs from dehydrogenated carbon fragments.

The ASED calculations predict that the performance for carbon-carbon bond formation versus methanation increases with increasing metal-carbon bond strength. This has implications for both the metal as well as the recombinating surface species. For the surface species, the highly dehydrogenated species have a stronger metal-carbon interaction (see table 1), and therefore a higher chance for carbon-carbon bond formation. For the group VIII metals, a decreased d-orbital occupation will lead to a large metal-adsorbate interaction due to a decreased filling of anti-binding orbitals. The increased metal-carbon interaction is expected to result in a higher selectivity for chaingrowth. It can partially explain the larger selectivity for higher hydrocarbon formation on ruthenium compared to that of rhodium or palladium in synthesis gas conversion.

CONCLUSIONS

the predicted trends from ASED calculations on carbon-carbon bond formation, are in good agreement with experimental findings. Carbon-carbon bond formation needs highly dehydrogenated surface CH_x species as reaction intermediates. Surface CH_x species with a large number (2 or 3) of hydrogen atoms, have high activation energies for carbon-carbon bond formation through repulsion between the hydrogen atoms. A high metal-carbon bond strength is favourable for chaingrowth versus methane formation. However, when the metal-carbon interaction becomes too high, stable carbides can be formed that are not easily hydrogenated. Surface carbon fragments with only few hydrogen atoms have a relatively large metal-carbon interaction, which increases the selectivity for C_2^+ hydrocarbon formation.

APPENDIX

Atomic parameters used in the ASED program: principal quantum number (n), ionization potential (V.S.I.P.), orbital exponents (ζ) and respective coefficients (C_1) - only used for d-orbitals.

	s - electrons			p -electrons		
Atom	n	VSIP	ζ	n	VSIP	ζ
H[1]	1	13.6	1.200			
H[2]	1	7.5	1.200			
C	2	20.00	1.658	2	11.26	1.618
O	2	28.48	2.246	2	13.62	2.227
Rh	5	8.09	2.135	5	4.57	2.100

	d -electrons					
	n	VSIP	ζ_1	C_1	ζ_2	C_2
Rh	4	12.50	4.290	0.5807	1.97	0.5685

1 Used for hydrogen atoms in CH_x [31,38].

2 Used for adsorbed hydrogen on the metal surface [39].

LITERATURE

1. Araki M. and Ponec V., *J. Catal.*, 44 , 439 (1976).
2. McCarty J.G. and Wise H., *J. Catal.*, 57 , 406 (1979).
3. Bell A.T., *Catal. Rev.-Sci. Eng.*, 23, 203 (1981).
4. Cant N.W. and Bell A.T., *J. Catal.*, 73, 257 (1982).
5. Biloen P., Helle J.N., Berg F.G.A. van den and Sachtler W.M.H., *J. Catal.*, 81, 450 (1983).
6. Baetzold R.C. and Monnier J.R., *J. Phys. Chem.*, 90, 2944 (1986).
7. Rabo J.A., Risch A.P. and Poutsma M.L., *J. Catal.*, 53, 295 (1978).
8. McCarty J.G. and Wise H., *J. Catal.*, 57, 406 (1979).

9. McLaughlin M., McClory M. and Gonzales R.D., *J. Catal.*, **89**, 392 (1984).
10. Solymosi F. and Erdöhelyi A., *Surf. Sci.*, **110**, L630 (1981).
11. Solymosi F., Tombácz I. and Kocsis M., *J. Catal.*, **75**, 7 (1982).
12. Takeuchi A. and Katzer J.R., *J. Catal.*, **82**, 351 (1983).
13. Orita H., Naito S. and Tamaru K., *J. Catal.*, **111**, 464 (1988).
14. Efstathiou A.M. and Bennett C.O., *J. Catal.*, **120**, 118 (1989).
15. Gorodetskii V.V. and Nieuwenhuis B., *Surf. Sci.*, **105**, 299 (1981).
16. Castner P., and Somorjai G.A., *Surf. Sci.*, **83**, 60 (1979).
17. Castner P., and Somorjai G.A., *Surf. Sci.*, **103**, L134 (1981).
18. Blyholder G., *J. Chem. Phys.*, **68**, 2772 (1964).
19. Yin-Sheng X. and Xiao-Le H., *J. Mol. Catal.*, **33**, 179 (1985).
20. De Koster A., Jansen A.P.J., Geerlings J.J.C. and Van Santen R.A., *Farad. Disc. Chem. Soc.*, **87**, 263 (1989).
21. Santen R.A. van, Koster A. de and Koerts T., *Catal. Lett.*, **7**, 1 (1990).
22. Koerts. T. and Santen R.A. van, *J. Chem. Soc., Chem. Comm.*, **1991**, 1281.
23. Kuijpers, E.G.M., Breedijk, A.K., Wal, W.J.J. van den & Geus, J.W., *J. Catal.*, **81**, 429 (1983).
24. Koerts T. and Van Santen R.A., *Catal. Lett.*, **6**, 49 (1990).
25. Baerends E.J., Ellis D.E. and Ros P., *Chem. Phys.*, **2**, 41 (1973).
26. Hoffman R., *J. Chem. Phys.*, **39**, 1397 (1963).
27. Anderson A.B., *J. Chem. Phys.* **62**, 1187 (1975).
28. Anderson A.B., R.W. Grimes and S.Y. Hong, *J. Chem. Phys.* **91**, 4245 (1987).
29. Hoffman R., "*Solids and Surfaces, a chemists view of bonding in Extended Structures*", VCH Publishers Inc., New York, (1988).
30. Low J.J. and Goddard W.A., *J. of Am. Chem. Soc.*, **106**, 8321 (1984).
31. Koster A. de and Santen R.A. van, *J. Catal.*, **127**, 141 (1991).
31a. Yang H. and Whitten J.L., *J. Am. Chem. Soc.*, **113**, 6442 (1991).
31b. Siegbahn P.E.M., Blomberg M.R.A. and Bauschlicher C.W. Jr. J., *Chem. Phys.*, **81**, 2103 (1984).
32. Feibelman P.J., *Phys. Rev. B*, **26** , 5347 (1982).
33. Darling G.R., Joyner R.W. and Pendry J.B., *Chem. Phys. Lett.*, submitted.
34. Zheng C., Apeloig Y. and Hoffman R., *J. Am. Chem. Soc.*, **110**, 749 (1988).
35. Shustorovich E., *Catal. Lett.*, **7**, 107 (1990).
36. Trost B.M., Dyker G. and Kulawiec R.J., *J. Am. Chem. Soc.*, **112**, 7809 (1990).
37. Barneveld W.A.A., and Ponec V., *J. Catal.*, **88**, 382 (1984).
37b. Ponec V. and Van Barneveld W.A.A., ACS meeting Honolulu (1979), I&EC product & research & development, vol. 18, p. 268.
38. Koster A. de and Santen R.A. van, *Surf. Sci.*, **233**, 366 (1990).
39. Santen R.A. van, *Recueil des Trav. Chem. des Pays Bas*, **101**, 121 (1982).
40. Swang O., Faegri K., Gropen O. and Wahlgren U., in "*Natural gas conversion*", ed. Holmen A. et al, 191 (1991), Elsevier, Amsterdam.
41. Shustorovich E., *Adv. Catal.*, **37**, 101 (1990).
41b. Evans M.G. and Polanyi M., *Trans. Farad. Soc.*, **34**, 11 (1938).
42. Petit R.C. and Brady R., *J. Am. Chem. Soc.*, **102**, 6181 (1980).
43. Petit R.C. and Brady R., *J. Am. Chem. Soc.*, **103**, 1287 (1981).
44. Tanaka K-I., Yaegashi I. and Aomoura K., *J. Chem Soc. Chem. Comm.*, 938 (1982).
45. Herrmann W.A., Bauer C., Plank J., Kalcher W., Speth P. and Ziegler M.L., *Angew. Chem., Int. Ed. Engl.*, **20**, 193 (1981).
46. Summer C.E. Jr., Riley P.E., Davis R.E. and Petit R., *J. Am. Chem. Soc.*, **102** , 1752 (1980).
47. George P.M., Avery N.R., Weinberg W.H. and Tebbe F.N., *J. Am. Chem. Soc.*, **105** , 1393 (1983).
48. Chang S-C., Kafafi Z.H., Hauge R.H., Billups W.E. and Margrave J.L., *J. Am. Chem. Soc.*, **107** , 1447 (1985).

6

Hydrocarbon formation from methane by a low temperature two step reaction sequence.

ABSTRACT

At atmospheric pressure thermodynamics limit the direct conversion of methane to higher hydrocarbons to temperatures above 1200 K. Converting methane at lower temperatures requires at least two different steps occurring at different conditions. Here we report such a low temperature conversion route towards ethane, propane, butane and pentane without using oxygen. The overall reaction consists of two steps. Methane is dissociatively adsorbed on a group VIII transition-metal catalyst at a temperature between 300 and 600 °C resulting in surface carbonaceous species and hydrogen. In the second step the carbonaceous intermediates produce small alkanes upon hydrogenation around 100 °C. The maximum yield to C_nH_{2n+2} (n>1) obtained on a Ru catalyst is 13%.

Parts of this chapter have been or will be published: *J. Chem. Soc., Chem. Comm.*, 1991, 1281, with co-author Rutger A. van Santen and *J. Catal.*, accepted, with co-authors Marc J.A.G. Deelen and Rutger A. van Santen.

INTRODUCTION

One of the intriguing problems in heterogeneous catalysis is the direct conversion of methane into other useful products. Methane activation is difficult because methane is a thermodynamic stable product with a noble gas like configuration. The strong tetrahedral C-H bonds (435 kJ/mol [1]) offer no magnetic moments or polar distortions to facilitate chemical attack. This makes methane less reactive than nearly all products of its conversion. Especially, in the selective oxidation of methane [2] this limits methane conversion to occur at low conversion level to maintain reasonable selectivity. Current practice to convert natural gas into higher hydrocarbons proceeds by the indirect route in which natural gas is first converted to synthesis gas at a high temperature [3]. Subsequently, hydrocarbons can be produced in a low temperature exothermic process from synthesis gas, either by Fischer-Tropsch synthesis [4,5] or via methanol and the Methanol To Gasoline process [6]. Direct methane conversion, like pyrolysis to acetylene and benzene [7], can only operate at temperatures above 1200 K [8,9]. At those very high temperatures graphite is much more stable than any hydrocarbon. Oxidative coupling of methane to ethene has been proposed as an alternative route [10-14]. This reaction can result in C_2^+ hydrocarbon yields up to 25% when performed at temperatures around 1100 K. To increase the catalyst lifetime and the selectivity for ethene, there is need for lower reaction temperatures [15,16].

A process to convert methane in several steps but all occurring at lower temperatures might have potential advantages. Of interest are recent experiments demonstrating that hydrocarbon formation is possible at low temperature, once methane is activated. Kazanski and co-workers [17] activated methane on a molybdenum catalyst by photo chemisorption at pressures between 0.4-50 torr at room temperature. Upon desorption in vacuum, ethene, ethane and propane were detected. Ceyer and co-workers [18] decomposed pre-adsorbed methane on a Ni(111) single crystal surface by a krypton bombardment at 47 K under ultra high vacuum conditions (P=5.10-6 torr). These authors reported the selective desorption of benzene around 250 °C, formed from surface carbon fragments from methane. Tanaka et al [19] created surface CH_x fragments by dissociative methane adsorption around 430 °C on cobalt catalyst. They succeeded in creating small amounts of ethene during hydrogenation and suggested that adsorbed CH_2 species are the precursor for ethene formation.

Here we report the formation of C_2 to C_6 alkanes from methane at atmospheric conditions in a two step route in which methane is thermally activated. At a temperature between 450 and 800 K methane is decomposed by a reduced group VIII metal catalyst into hydrogen and adsorbed surface

carbonaceous species (1). In a second reaction step a particular surface carbonaceous intermediate produces hydrocarbons upon hydrogenation at 300-400 K (2).

$2\,CH_4 + 6\,M \rightarrow 2\,M_3C + 4\,H_2$	(1)	M = zero-valent transition metal
$2\,M_3C + 3\,H_2 \rightarrow C_2H_6 + 6\,M$	(2)	
	+	
$2\,CH_4 \rightarrow C_2H_6 + H_2$	(3)	$\Delta G°_{(1000\ K)} = 71.0$ kJ/mol

Thermodynamics.

The conversion of methane into ethane and hydrogen is thermodynamically not allowed in one reaction step [20], due to the positive change in Gibbs free energy. Therefore the introduction of oxidants like O_2 or Cl_2 has been used to convert the liberated hydrogen into H_2O or HCl. This lowers the change in Gibbs free energy to respectively -121.6 and -130.6 kJ/mol. A different approach is to split the overall reaction (3) into two reaction steps occurring at different conditions. In such a two step procedure the thermodynamic limitation can be circumvented as illustrated in fig. 1. This is shown for the case that the reaction sequence involves formation of bulk cobalt carbide as intermediate.

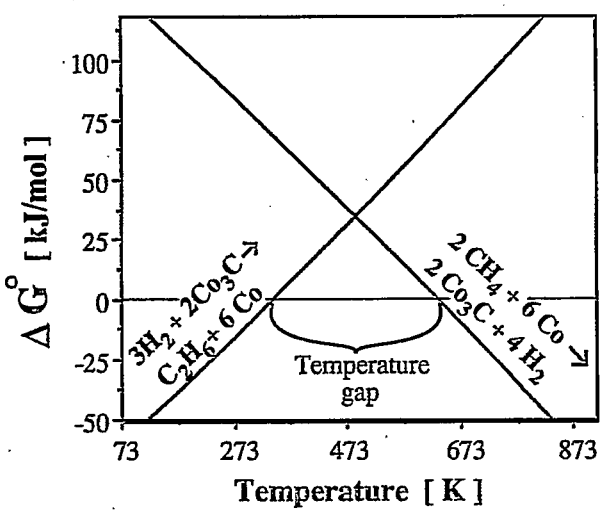

Figure 1. Standard Gibbs free energy as a function of the temperature for the decomposition of methane on cobalt and the hydrogenation of cobalt carbide to ethane.

The decomposition of methane on cobalt forming bulk cobalt carbide is endothermic while the change in entropy is negative. This reaction is only possible at temperatures above 632 K at standard concentrations and pressures. The hydrogenation of bulk cobalt carbide to form ethane is exothermic and the change in entropy is negative. Therefore this reaction is favoured at low temperatures and can only occur below 347 K. There is no common temperature at which both reaction steps (1) and (2) can occur, so the temperature gap of 283 K is a thermodynamic stipulation. This temperature gap can be decreased by increasing the methane pressure during adsorption, increasing the hydrogen pressure in the second step and by working at low conversion level.

The heat of formation of surface carbides is normally higher than that of bulk carbides. This will shift the lines in figure 1 to a lower temperature. The temperature where the change in Gibbs free energy is negative depends on the heat of formation of the surface carbides. For a negative Gibbs free energy the reaction temperature should be above the equilibrium temperature for step 1, while it should be under the equilibrium temperature for step 2, as shown in figure 2.

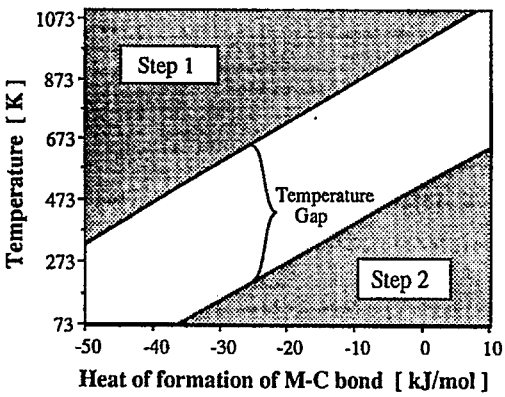

Figure 2. Equilibrium temperatures for methane decomposition into surface carbides (dashed line) and hydrogenation of surface carbide to ethane (straight line) as a function of the metal carbon bond strength. The gray areas show the regions were reaction is possible. The equilibrium temperatures are calculated according to $T_{eq.}=\Delta H°/\Delta S°$. *$\Delta H°$ and $\Delta S°$ are taken of the gas phase products at 298 K.*

The metal-carbon bond interaction determines the working temperature areas for each metal catalyst and should be roughly between -60 and 20 kJ/mol. The heat of formation of surface carbide is estimated by Shustorovich [21] for

some transition metals. For iron the metal carbon bond is about -117 kJ/mol that is too high (see fig. 2), for copper the metal carbon bond relative to graphite is 53 kJ/mol that is too low. Nickel (4 kJ/mol) and cobalt (around 50 kJ/mol) have intermediate values and have in principle capabilities for performing the desired reaction sequence. Of course catalyst morphology, type of surface carbon as well as promoters can influence the metal carbon bond strength, and are therefore important parameters.

Instead of working in a temperature cycle it is also possible to perform the reaction isothermally and work in a pressure swing as recently indicated by Belgued et al [22]. These authors decomposed methane on a ruthenium and platinum catalyst into adsorbed surface CH_x fragments and hydrogen and subsequently, they hydrogenated those fragments in a pure hydrogen flow in which C_2^+ hydrocarbons were detected up to C_7. They were able to perform up to 90 cycles per hour. However to overcome the $\Delta G°$ of 71 kJ/mol one is limited to very low product concentrations, as shown in fig. 3. The pressure equilibrium constants are given by equations 4 and 5.

$$\frac{(p_{H_2})^2}{p_{CH_4}} = \exp\left[\frac{-\Delta G°_{step\,1}}{RT}\right] \qquad (4)$$

$$\frac{p_{C_2H_6}}{(p_{H_2})^3} = \exp\left[\frac{-\Delta G°_{step\,2}}{RT}\right] \qquad (5)$$

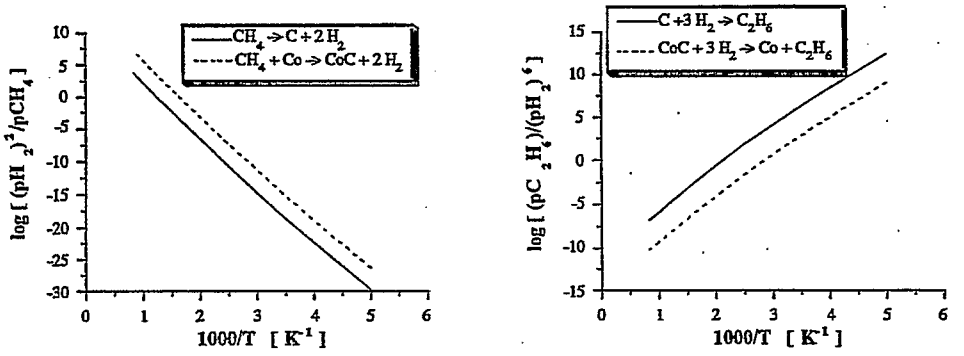

Figure 3. The ratio of the equilibrium partial pressures as a function of the temperature. Left: the decomposition of methane. Right: the formation of ethane. The plots are calculated for graphite and bulk cobalt carbide with equation 4 and 5.

The equilibrium pressure constants in fig. 3 determine the maximum concentration of gaseous products in the two reaction steps. This means for example that at 400 K the maximum methane conversion into graphite and hydrogen is $4 \cdot 10^{-6}$.

Dissociative methane chemisorption.

Methane decomposition on transition metal surfaces is an activated process and the activation energies found vary from 25 to 60 kJ/mol [23-30]. These activation energies are quite low compared to those of e.g. CO dissociation, while the temperatures at which methane decomposition occurs with a useful yield is normally higher then that for CO that has a higher activation energy. This is due to the very low sticking coefficient for dissociative methane adsorption. The mechanism of dissociative methane adsorption is not fully understood. From surface science studies on platinum [31], it appeared that the surface temperature does not influence the methane sticking coefficient. Molecular beam studies showed that high methane translation energies perpendicular to a metal surface enhance the methane dissociation probability greatly [31,32]. Also increased internal vibrations were shown to enhance the methane sticking probability [27,28]. The mechanism for methane dissociation may involve quantum tunnelling of a proton as the rate determining step [31-33]. The large isotope effect for CD_4 is consistent with this mechanism [34,37]. Beckerle at al [25] proposed a mechanism which they called "chemistry with a hammer". In this mechanism adsorbed methane molecules are activated at low temperature by collisions with other particles. It implies that the total pressure is important. Trevor et al [35] studied methane decomposition on Pt metal clusters of different size and concluded that the methane decomposition rate is highest at clusters of 2 - 5 atoms. One metal atom is not able to dissociate CH_4, while in bigger clusters (>6 atoms) the platinum atoms have higher coordination, reducing the CH_4 decomposition rate. This agrees with results of Kuijpers et al [36] on silica-supported nickel catalysts. They showed that methane decomposition is most efficient on small nickel particles.

EXPERIMENTAL

Catalyst.

Transition-metal catalysts were prepared by incipient wetness impregnation of preshaped silica (Grace 332, surface area=300 m^2/g, mesh size=100, pore volume=1.6 ml/g) with an aqueous solution of the metal nitrates or chlorides. The catalysts were dried at 110 °C. The ruthenium catalyst was prepared from $RuCl_3$ and was treated after drying in a H_2/CO flow for 30 min at 250 °C to increase its CO chemisorption capacity. The catalysts were characterized with Transmission Electron Microscopy and CO chemisorption.

Method.

The reactions were performed in a micro flow reactor that consisted of a quartz tube with an internal diameter of 10 mm. For each experiment 300 mg of the catalyst was placed in the reactor and was reduced in situ between 350-550 °C in a diluted hydrogen flow. Methane decomposition was performed from a flow of 45 ml/min of diluted methane. Typically, a pulse of 3 minutes of 0.5 % methane in helium was given at 450 °C. The diluted methane flow contained no detectable amounts of ethane or other hydrocarbon impurities (less than 0.5 ppm). After methane decomposition, the catalyst was cooled in 100 seconds below 200 °C to avoid 'ageing' of the surface carbon species. After cooling, surface carbon was hydrogenated to higher hydrocarbons in a flow of 22.4 ml/min of hydrogen at 1 atm. around 100 °C. The surface carbon created from methane was characterized with a Temperature Programmed Surface Reaction (TPSR) in a flow of 22.4 ml/min of 8% hydrogen in helium. Product analysis was performed on line with a quadrupole mass spectrometer (type: PGA 100 from Leybold) or with a gas chromatograph (CP 9000 from Chrompack) using a widebore column (plot Q) of 25 meters isothermal at 220 °C at an inlet pressure of 100 kpa. With the GC system every 20 sec. a sample could be taken, which analyzed the hydrocar-bons C_1 to C_5.

RESULTS AND DISCUSSION

Methane decomposition.

The activity for methane decomposition into adsorbed surface carbonaceous species and hydrogen, was studied for a silica-supported ruthenium, rhodium and cobalt catalyst, as a function of the temperature (see fig. 4).

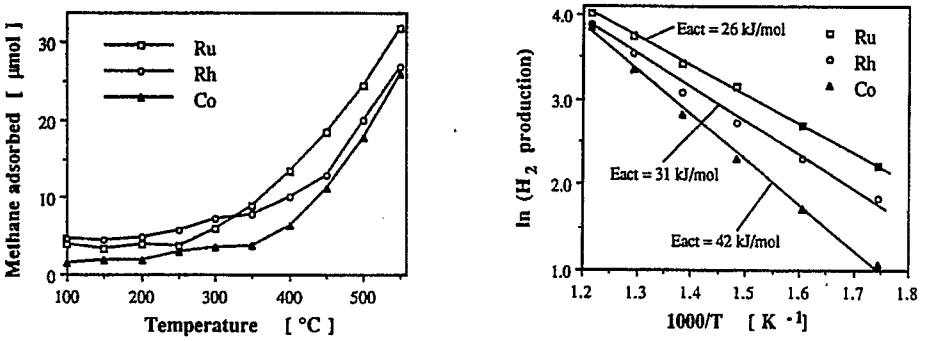

Figure 4. Left: Fraction of methane adsorbed from a methane pulse of 3 min. of 0.5% CH_4 in He as a function of the temperature on a 5%Ru, 3%Rh and 10%Co catalyst. Right: Arrhenius plot of the hydrogen production.

Already at 100 °C a small amount of methane is adsorbed as was also observed by Kuijpers et al on nickel catalysts [29]. At that low temperature no hydrogen desorption takes place. Above 300 °C the sticking coefficient for methane chemisorption increases. The activation energies can be calculated from the amount methane adsorbed as well as from hydrogen produced as a function of the temperature (fig. 4b). The activation energy is 26 kJ/mol for ruthenium, 31 kJ/mol for rhodium and 42 kJ/mol for the cobalt catalyst in the temperature range 350-500 °C. The ratio of hydrogen produced to methane adsorbed is 1.4 to 1.7 at temperatures between 400 and 500 °C, indicating that the adsorbed carbon species can contain hydrogen atoms, or that not all hydrogen desorbs from the catalyst. The methane decomposition rate appeared strongly dependent on the carbon surface coverage. Increasing the carbon coverage from 0 to 0.5 drastically decreased the rate of methane dissociation. Our measurements support the observation that small metal particles are favourable for methane decomposition [35,36].

For the reduced transition metals studied the order of methane activation is Co, Ru, Ni, Rh > Pt, Re, Ir > Pd, Cu, W, Fe, Mo. This corresponds with the order of activity for the methane deuterium exchange reaction [37,38]. According to the Bond Order Conservation principle [39,21] the activation energy for methane decomposition is expected to be lower for metals with stronger M-C bonds. So, for metals in the same row of the periodic table it is expected that the order for methane decomposition is Fe>Co>Ni>Cu. However the results presented show an optimum at nickel and cobalt. This indicates that the

activation energy also depends on the surface metal-metal bond strength as predicted by the modified Bond Order Conservation principle [40].

Similar as with dissociative CO adsorption [41,42], CH_4 decomposition on reduced transition metals around 450 °C results in different surface carbonaceous surface species. They are distinguishable by their hydrogenation reactivity as is shown in the temperature programmed surface reaction plot of figure 5.

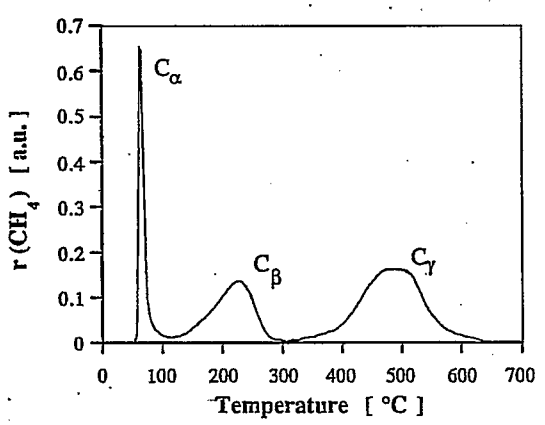

Figure 5. Temperature programmed hydrogenation of surface carbon species created by methane decomposition on a 3 wt.% silica supported rhodium catalyst at 400 °C.

A very reactive surface carbon species generated from CH_4 decomposition can be hydrogenated at 50 °C or even below room temperature to methane. This surface carbonaceous intermediate is called C_α. It has been identified with surface characterization techniques like AES and SIMS on foils and single crystals as a carbidic type of carbon [44-46,32]. Bell and co-workers [47-50] studied the nature of various carbon species with NMR on a silica supported ruthenium catalyst. They showed that the C_α phase has only metal atoms in its first coordination shell [47]. The presence of subsurface carbon can not be excluded. Our quantum chemical calculations indicate that such carbidic carbon atoms are adsorbed in hollow sites, being bounded to three or more surface metal atoms [52,53]. The C_α phase has been studied previously when generated from CO [54-57], and is responsible for higher hydrocarbon formation [58,59]. The mechanism of higher hydrocarbon formation from surface carbon from methane follows a Schulz-Flory like distribution (see fig. 9).

A less reactive surface species (C_β) can be hydrogenated between 100 and 300 °C. During the hydrogenation of C_β only traces of higher hydrocarbons up to C_6 were detected. The C_β species from CO as identified by Duncan et al [47,60] on ruthenium can be separated in $C_{\beta 1}$ and $C_{\beta 2}$ that differ in their mobility. These authors showed that in this carbon phase both C-C, M-C and C-H interactions are present. Therefore, C_β is most likely an amorphous phase. After H_2/CO reaction Winslow et al [49,50] were able to observe C-H stretch frequencies with FT-IR spectroscopy. We have seen by FT-IR spectroscopy that after methane adsorption at 450 °C the C-H stretch frequencies totally disappeared from carbonaceous surface species adsorbed on a reduced ruthenium catalyst.

At temperatures above 400 °C the low reactive C_γ reacts to produce only methane. The C_γ surface species consist likely of a graphitic phase consisting of adsorbed connected six member rings. This carbon phase is probably located partially on the silica support as indicated by CO chemisorption measurements.

Because only the reactive C_α type carbon has reasonable selectivities for C_2^+ hydrocarbon formation upon hydrogenation, it is desirable to have high selectivities for C_α during methane decomposition. We have studied several parameters of CH_4 decomposition like adsorption temperature, adsorption time, methane concentration and ageing time, which could influence the selectivities in the surface carbon formation. One of the parameters that appeared to be crucial is the carbon surface coverage, remaining after methane decomposition.

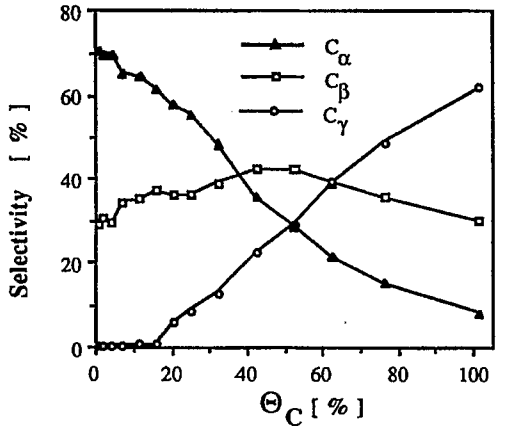

Figure 6. Distribution of carbon types as a function of the carbon surface coverage on a 5%Ru/SiO_2 catalyst. Different carbon coverages were created by varying the methane adsorption time at 460 °C.

Figure 6 shows that only at low carbon surface coverage high selectivities for reactive C_α type carbon is obtained. The selective formation of reactive carbidic type carbon is related with the catalyst's ability to form three-fold bonded carbon species like Ni_3C [51]. At carbon coverages above 80% methane is mainly converted into unreactive graphitic type of surface carbon. The distinction between C_β and C_γ was not obvious for all the catalysts. However, with increasing surface coverage, the deposited carbon species becomes always less reactive.

From the methane decomposition experiments, a tentative reaction scheme can be formulated for the transformation of surface carbon to methane.

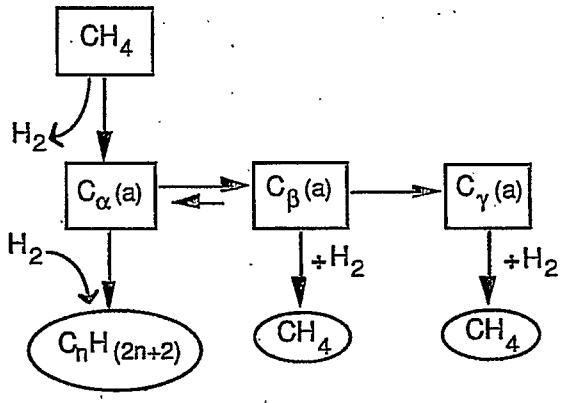

Figure 7. Model for transformation of surface carbon species on transition metal catalysts.

Methane is initially decomposed into carbidic C_α. This type of surface carbon can be transformed rapidly into C_β. C_β can be partially converted back into C_α. This model is in agreement with the one of Bell and co-workers [50,47] who also indicated that these carbon types can be in dynamic equilibrium. C_β can be transformed into the unreactive C_γ, a process called ageing. This process is irreversible and its rate depends on the temperature [42,42a]. It is not clear whether C_α can also be directly transformed into C_γ.

Hydrogenation reaction of surface carbon species to alkanes.

The second reaction step is the hydrogenation of surface carbon to produce C_2^+ hydrocarbons. Fig. 8 shows the products formed as a function of the hydrogenation time after the reaction gas is switched from helium to hydrogen at 95 °C.

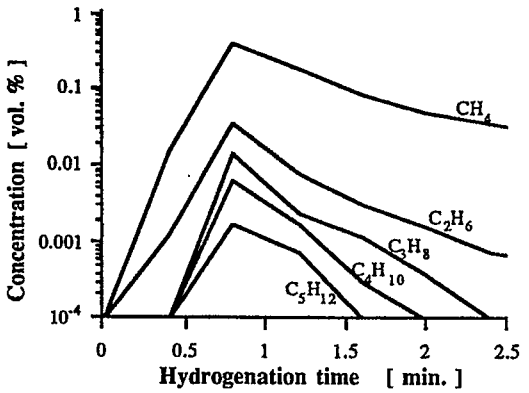

Figure 8. Hydrogenation of surface carbon created from methane decomposition at 450 °C, on a 10 wt.% cobalt catalyst, as a function of the hydrogenation time. For butane and pentane the sum of the iso- and n- products is shown.

By integrating the curves from fig. 8 during the first 6 minutes, the amount of hydrocarbon formed can be calculated. This leads to the product selectivity, which is calculated on carbon efficiency. The hydrocarbon selectivity follows a Schulz-Flory like distribution, indicating that adsorbed surface C_xH_y species can either be hydrogenated to $C_xH_{(2x+2)}$ or grow further to an adsorbed $C_{(x+1)}H_z$ species. The chain growth probability α determines the amount of C_2^+ hydrocarbons formed. Figure 8 shows that the concentration of every subsequent hydrocarbon is about a factor of ten lower, indicating that α is about 0.1.

As predicted by thermodynamics, the temperature at which C_α is hydrogenated is an important parameter, determining the selectivity for the formation of C_2^+ hydrocarbons.

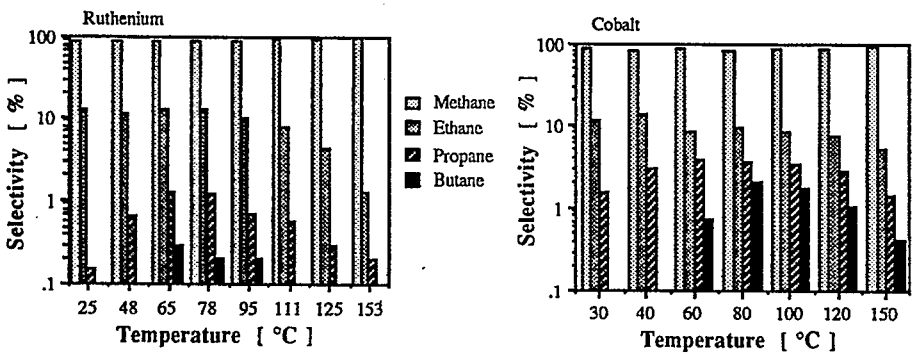

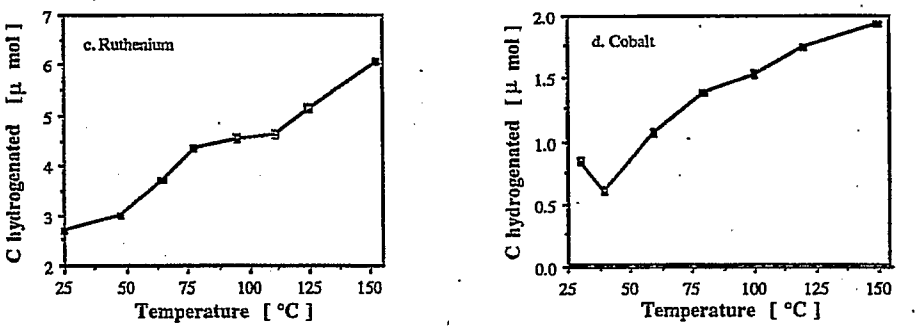

Figure 9. *Figure 9a and b on the previous page show product distributions as a function of the hydrogenation temperature. Surface carbon deposited from methane at 450 °C. 9c and d show the amounts of surface carbon that is hydrogenated. Left: Ruthenium. Right: Cobalt.*

Figure 9 shows the selectivities for C_2^+ hydrocarbon formation upon hydrogenation of surface carbon species generated from methane decomposition. At room temperature most of the surface carbon is hydrogenated to methane, 12 % is hydrogenated to ethane and only a trace of propane is formed. Increasing the temperature results in the hydrogenation of more surface carbon species (see fig. 9b). On small metal particles different adsorption sites exist for carbon atoms, having slightly different metal-carbon interactions. The stronger adsorbed carbon atoms are hydrogenated at higher temperature and have higher probabilities for C-C bond formation versus methanation upon hydrogenation [61,62]. Therefore the selectivities for propane and butane increase when the temperature is raised above 25 °C.

Figures 9c and 9d show that more surface carbon becomes hydrogenatable at temperatures above 130 °C. At that temperature also "unselective" C_β is hydrogenated. This decreases the selectivity for C_2^+ hydrocarbons. At temperatures above 180 °C also hydrogenolysis may transform some ethane back into methane, which explains why short contact times are favourable for high ethane selectivities. At temperatures above about 200°C the formation of higher hydrocarbons is thermodynamically forbidden and the surface carbon removed with hydrogen results in nearly only methane.

The optimum temperature for the formation of C_2^+ hydrocarbons depends on both the selectivity as well as on the amount of surface carbonaceous intermediates hydrogenated. The optimum is around 95 °C for ruthenium and cobalt catalyst. The highest C_2^+ hydrocarbon selectivities were obtained at short contact times and high hydrogen partial pressures: a residence time of 1.4 sec., at

a p_{H_2} of 1 atm. Higher hydrogen flow increase the C_2^+ hydrocarbon selectivity on ruthenium as also found by Belgued et al [22] on platinum. However, this is accompanied by a lower product concentrations and a less effective use of hydrogen.

The addition of some CO in the hydrogen reaction gas, to decrease the rate of methane formation, decreased the formation of higher hydrocarbons even more. However, when respectively 8 and 24 μmol CO were co-adsorbed around 40 °C with surface carbon from methane, the formation of methane and ethane remained the same during hydrogenation at 95 °C while 20-40% more C_3 - C_5 hydrocarbons was formed.

Reduced transition metal catalysts were compared in their ability to form C_2^+ hydrocarbons from methane. The catalysts were characterized with CO chemisorption and Transition Electron Microscopy. Methane adsorption occurred from a pulse of 3 min of 0.5% CH_4 in He at 460 °C. The selectivity for the hydrocarbons formed during hydrogenation at 95 °C was measured as well as the amount of hydrogenated surface carbon at that temperature (see table 1).

Table 1. Product distribution of the hydrogenation reaction of reactive surface carbon at 460 °C on reduced silica supported transition metal catalysts.

	Particle size		Hydrocarbon selectivity in %				
Catalyst	CO/M[1]	nm[2]	CH_4	C_2H_6	C_3H_8	C_4H_{10}	μmol[3]
10%Co	2.2 (73)	8.5	79.6	11.3	6.11	2.92	8.0
5%Ru	35 (4.0)	5.5	80.5	15.8	2.69	1.00	7.10
10%Ni	13 (12)	9.2	89.3	7.3	1.89	1.40	16.8
3%Rh	55 (2.2)	2.2	95.8	4.12	0.09	0	3.4
4%Pt	104 (0.8)	1.4	89.7	10.3	0	0	0.55
5% Re	6.4 (24)	3.8	91.3	8.4	0.23	0	0.96
4%Ir	30 (4.6)	3	98.4	1.3	0	0.29	0.95

1 Percent chemisorption CO per metal atom. In brackets the calculated particle size in nm assuming that every surface metal atom adsorbs 1 CO in a pyramid model.

2 As measured with TEM.

3 mmol surface carbon hydrogenated at 95 °C.

Most of the butane was n-butane but also i-butane was detected. No branched products were detected, except for some small traces of propylene on cobalt. On cobalt and ruthenium also pentane formation was observed. The metal particle size as measured with TEM and CO chemisorption do not agree for all catalysts especially not for cobalt, rhenium and nickel. This is ascribed to

the reduction of the metal is not complete. Especially the cobalt and rhenium catalyst are difficult to reduce. The metal-silica interface probably contains unreduced metal ions [63]. Only cobalt catalysts with a metal loading above 1 % were able to chemisorb CO after reduction and were able to produce higher hydrocarbons in the two step procedure. The real metal particle size is determined by TEM while the active reduced surface area is measured by CO chemisorption.

The ruthenium and cobalt catalysts are more selective towards higher hydrocarbon formation than rhodium, iridium, platinum and nickel. At 550 °C reduced iron, tungsten, molybdenum and copper catalysts were not suitable for the step wise transformation of methane into ethane. These results can be explained by considering the metal-carbon bond strength, which determines the chance for C-C bond formation versus hydrogenation, as we recently suggested [61,62,53]. This relation has been tested for group VIII transition metals (see table 2).

Table 2. Group VIII transition-metal catalysts with their chain growth probability α to form C-C bonds upon hydrogenation at 95 °C.

Cr	Mn	Fe	Co	Ni	Cu
-	-	0	0.20	0.09	0
Mo	Tc	Ru	Rh	Pd	Ag
0	-	0.15	0.02	0	-
W	Re	Os	Ir	Pt	Au
0	0.03	-	0.007	0.06	-

- Not measured

Going to the right in one row of the Periodic Table, the electron occupation of the metal d-valence band increases and the metal-carbon bond strength decreases [40,41]. This is due to an enhanced occupation of the antibonding orbitals of the M-C orbitals [64,65,53]. At increasing electron occupation of the d-valence band the chain propagation probability drops from 0.2 for cobalt to 0.09 for nickel and becomes zero for copper. However, for iron, with an even higher metal-carbon bond interaction, no formation of C_2^+ hydrocarbons occurs. No surface carbon can be hydrogenated at low temperature is formed on iron catalysts, as shown in the temperature programmed hydrogenation plot of figure 10.

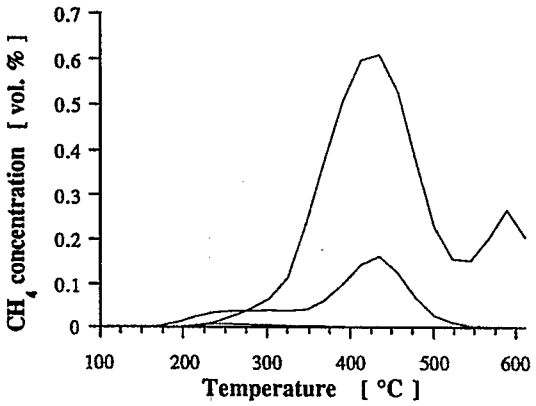

Figure 10. Hydrogenation of surface carbon species from methane on a 10% Fe/SiO2 catalyst with different surface carbon loading of 0.55, 8.9 and 53.6 μmol surface carbon. Different carbon surface coverages were created by varying the methane adsorption time at 500 °C.

Iron binds its surface carbon too strong and no surface carbon is hydrogenated below 200 °C. Thermodynamically ethane formation is only possible at low hydrogenation temperatures (see fig. 1 and 2) and therefore iron catalysts are not suitable for this reaction sequence, although they are known as good Fischer-Tropsch catalysts [68]. Only around 250 °C some ppm of ethane was detected.

So, the transition metals of row three and four of the Periodic Table show a volcano like curve in their behaviour to form C_2^+ hydrocarbons from surface carbon species. Ruthenium and cobalt are found to be optimum in their metal carbon bond strength. In the fifth row platinum is an exception. The optimum in the third row is expected at rhenium due to a similar M-C bond strength as ruthenium and cobalt.

Both alkali as well as other oxygen containing promoters have been shown to influence the metal carbon bond strength [66,67] and can therefore be expected to play an important role in changing the selectivity. We have tested the influence of basic (MgO) and acidic (V_2O_5) catalyst supports. These supports do not improve the catalytic performance of the metal particles. The results obtained on alumina (Ketjen, CK-300) were a little better than on silica.

Carbon-carbon bond formation is a structure sensitive reaction in a similar way as the opposite reaction: hydrogenolysis. Therefore, larger metal particles are expected to show a higher carbon-carbon bond formation. The selectivity for C_2^+

hydrocarbons was increased when a ruthenium catalyst was sintered, indicating that larger particles are indeed favourable for carbon-carbon bond formation.

The overall yield of the formation of C_2^+ hydrocarbons from methane is controlled by the conversion of methane during its decomposition, the selectivity for C_α surface carbon formation and the chain growth probability upon hydrogenation. These parameters are a function of the 'carbon' surface coverage, which is C atoms adsorbed relative to CO chemisorption capacity.

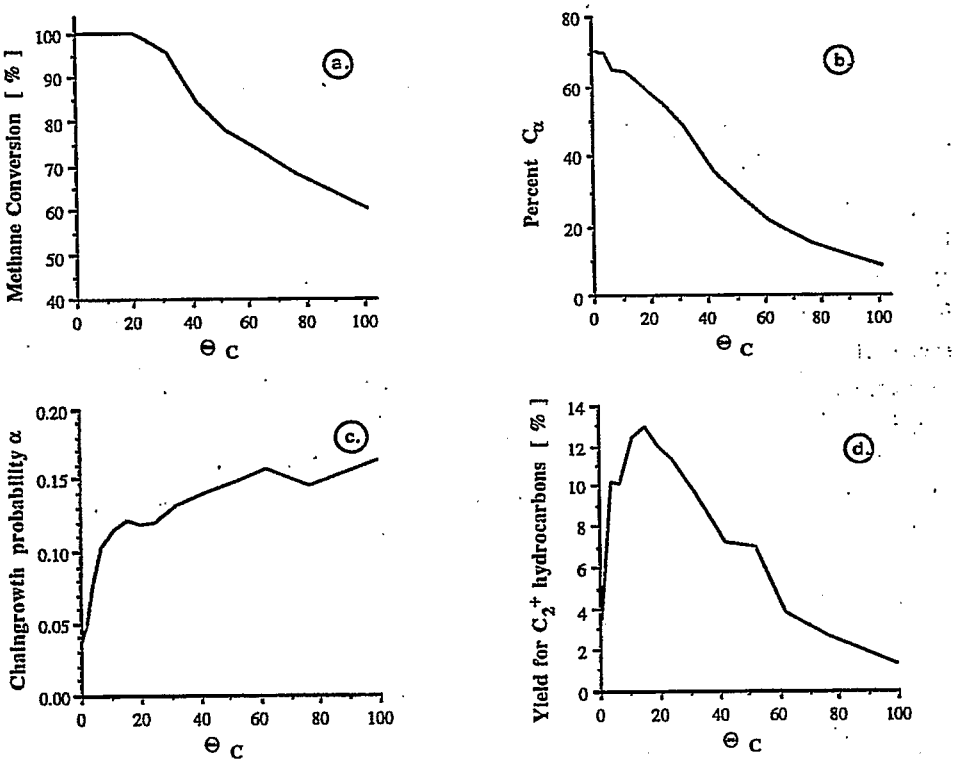

Figure 11. Methane decomposition at 450 °C followed by hydrogenation at 95 °C on a 5% Ru/SiO_2 catalyst. Different 'carbon' surface coverages were created by varying the adsorption time. a: Methane conversion upon adsorption. b: Fraction of C_α type carbon. c: Chain growth probability. d: Overall yield for the formation of C_2^+ hydrocarbons.

The rate of carbon-carbon coupling is low at very low carbon surface coverages (fig. 11c). By raising the carbon surface coverage, the chain growth probability increases to 0.15 at a mono-layer carbon coverage. However at surface coverages above 20% the selectivity for the formation of C_α carbon drops (fig.

11b). Therefore, the optimum overall yield for the formation of C_2^+ hydrocarbons from methane is reached at a surface coverage of only 0.18. The maximum yield for C_2^+ hydrocarbon from methane is 13% which is a true yield because the methane conversion during adsorption is 100%, under the conditions used, until a carbon surface coverage of 25% is reached (fig 11a).

The overall yield of 13% is of the same order as that obtained with high temperature pyrolysis. Oxidative coupling can result in a yield that is nearly twice as high.

CONCLUSION

Thermodynamic temperature limitations for methane conversion to higher hydrocarbons can be circumvented using a two step process. We have indicated the theoretical and practical conditions for a new way of methane conversion to small alkanes and hydrogen without using oxidants. In such a process carbon-carbon bond formation occurs upon hydrogenation from a specific surface carbon intermediate, generated by thermal decomposition of methane. The selective formation of this carbidic reaction intermediate is favoured at low carbon surface coverages. The carbon-carbon bond formation mechanism is similar to the process responsible for the chain growth in the Fischer-Tropsch reaction. The metal carbon bond strength in this process is important and is optimum for the cobalt and ruthenium catalysts used.

The interesting features of the presented methane conversion route are the relative low operation temperatures applied without the use of expensive oxidants. However, practical implications are not to be expected in the near future due to the difficulties induced by the temperature swing, and the low hydrocarbon concentrations obtained.

LITERATURE

1. Golden D.M. and Benson S.W., *Chem. Rev.*, 69, 125 (1969).
2. Pitchai, R. and Klier K., *Catal. Rev. -Sci. Eng.*, 28, 13 (1986).
3. Rostrup-Nielsen, J.R. in '*Catalysis, Science and Technology* ', Vol. 5 (eds. Anderson, J.R. and Boudart, M.) Springer, Berlin, 1984.
4. Vannice, M.A., *Catal. Rev. -Sci. Eng.*, 14, 153 (1976).
5. Pichler H., *Advances in catalysis,*, 4, 271 (1952).
6. Chang C.D., in '*Natural Gas Conversion* ', (edt. Holmen A., Jens K-I. and Kolboe S.), Elsevier, Amsterdam (1991).
7. Zwet, van der G. P., Hendriks, P. A. J. M. and van Santen, R. A., *Catal. Today*, 4, 365 (1989).
8. Kirk, R.E. and Othmer, D.F., in '*Encyclopedia of Chemical Technology* ' 3rd edn, Vol. 1, 180, (eds. Grayson, M. and Eckroth D.), (Wiley Interscience, New York, 1984).
9. Geerts J. W. M. H., Ph. D. Thesis, Eindhoven (1990), p.35.
10. Keller G.E. and Bahsin M.M., *J. Catal.*, 73, 9 (1982).

11. Hinsen, W. and Bearns, M., *Chem. Ztg.*, **107**, 223 (1983).
12. Ito, T., Wang, J-X., Lin, C.H. and Lunsford, J.H., *J. Am. Chem. Soc.*, **107**, 5062 (1985).
13. Sofranko J. A., Leonard J. J. and Jones C. A., *J. Catal.*, **103**, 302 (1987).
14. Otsuka K., Jinno K. and Morikawa A., *Chem. Lett.*, **1985**, 499.
15. Heinerman, H., Somorjai, G.A., Pereira, P. and Lee, S.H., *Catal. Lett.*, **6**, 255 (1990).
16. Roos J. A., Bakker A. G., Bosch H., Van Ommen J.G. and Ross J. R. H., *Catal. Today.*, **1**, 133 (1978).
17. Shelimov, B. N. and Kazansky, V.B., *J. Chem. Soc., Faraday Trans. I*, **83** , 2381 (1987).
18. Yang, Q.Y., Johnson, A.D., Maynard, K.J. and Ceyer, S.T., *J. Am. Chem. Soc.*, **111**, 8748 (1989).
19. Tanaka K-I., Yaegashi I. and Aomoura K., *J. Chem Soc., Chem. Comm.*, 938 (1982).
20. Amenomiya Y., Goledzinowski M., Birss V., Galsuszka J. and Sanger A. R., *Catal. Rev. - Sci. Eng.*, **32**, 63 (1990).
21. Shustorovich E., *Adv. Catal.*, **37**, 101 (1990).
22. Belgued M., Amariglio H., Pareja P., Amariglio A. and Saint-Juste J., *Nature*, **352**, 789 (1991).
23. Bond, G. C. in '*Catalysis by metals* ' (Acad. Press, New York, 1962).
24. Lee M.B., Yang Q.Y. and and Ceyer S.T., *J. Chem. Phys.*, **85**, 1693 (1986).
25. Beckerle J.D., Yang Q.Y., Johnson A.D. and Ceyer S.T., *J. Chem. Phys.*, **86**, 7236 (1987).
26. Tavares M.T., Bernardo C.A., Alstrup I., Rostrup-Nielson J.R., *J. Catal.*, **100**, 545 (1986).
27. Brass S.G. and G. Ehrlich, *Surf. Sci.*, **191**, L819 (1987).
28. Brass S.G. and G. Ehrlich, *Surf. Sci.*, **187**, 21 (1987).
29. Kuijpers E. G. M., Jansen J. W., Van Dillen A. J. and Geus J. W., *J. Catal.*, **72**, 75 (1981).
30. Sun Y.K. and Weinberg W.H., *J. Vac. Sci. Technol., A*, **8**, 2445 (1990).
31. Schoofs G.R., Arumainayagam C.R., McMaster M.C. and Madix R.J., *Surf. Sci.*, **215**, 1 (1989).
32. Sault A. G. and Goodman D. W., *Advances in Chem. Phys.*, **76**, 153 (1989).
33 Rettner C. T., Pfnür H. E. and Auerbach D. J., *Phys. Rev. Lett.*, **54**, 2716 (1985).
34. Kay B. D. and Coltrin M. E., *Surf. Sci.*, **198**, L375 (1988).
35. Trevor D. J., Cox D.M. and Kaldor A., *J. Am. Chem. Soc.*, **112**, 3742 (1990).
36. Kuijpers E. G. M., Breedijk A. K., Van der Wal W. J. J. and Geus J. W., *J. Catal.*, **72**, 210 (1981).
37. Frennet, A., *Cat. Rev.-Sci. Eng.*, **10**, 37 (1974).
38. Kemball, C., *Adv. Catal.*, **11**, 223 (1959).
39. Shustorovich E., *Surf. Sci.*, **176**, L863 (1986); Shustorovich E., *Catal. Lett.*, **7**, 107 (1990).
40. Van Santen R. A., *Recl. Trav. Chim. Pays Bas*, **109**, 59 (1990).
41. Solymosi, F. and Erdöhelyi, A., *Surf. Sci.*, **110**, L630 (1983).
42. Gupta N.M., Kamble V.S., Annaji Rao K. and Iyer R.M., *J. Catal.*, **60**, 57 (1979).
43. Mc Carty J.G. and Wise H., *J. Catal.*, **57**, 406 (1975).
44. Niemantsverdriet, J.W. and Langeveld, A.D. van, *Catalysis*, 769 (1987).
45. Van Langeveld A. D. and Niemantsverdriet J. W., *Surf. Sci. Interface Anal.*, **9**, 215 (1986).
46. Goodman D. W., Kelley R. D., Madey T. E. and Yates J. T. Jr., *J. Catal.*, **63**, 226 (1980).
47. Duncan T. M., Winslow P. and Bell A. T., *J. Catal.*, **93**, 1 (1985).
48. Duncan T. M., Winslow P. and Bell A. T., *Chem. Phys. Lett.*, **102**, 163 (1983).
49. Winslow P. and Bell A. T., *J. Catal.*, **91**, 142 (1985).
50. Winslow P. and Bell A. T., *J. Catal.*, **86**, 158 (1984).
51. Schouten F. C., Ph. D. Thesis, Utrecht (1979).
52. De Koster A. and Van Santen R. A., *J. Catal.*, **127**, 141 (1991).
53. Koerts T. and Van Santen R. A., *J. Mol. Catal.*, **70**, 119 (1991).

54. Mori T., Miyamoto A., Takahash N., Fukagaya M., Hattori T. and Murakami Y., *J. Phys. Chem.*, 90, 5197 (1986).
55. McCarty J.G. and Wise H., *J. Catal.*, 57, 406 (1979)
56. Koerts T., Welters W. J. J. and Van Santen R. A., *J. Catal.*, in press (1991).
57. Rabo J. A., Risch A. P. and Poutsma M. L., *J. Catal.*, 53, 295 (1978).
58. Biloen P. and Sachtler W. M. H., *Adv. catal.*, 30, 165 (1981).
59. Winslow P. and Bell A. T., *J. Catal.*, 94, 385 (1985).
60. Duncan T. M., Reimer J. A., Winslow P. and Bell A. T., *J. Catal.*, 95, 305 (1985).
61. Koerts, T. and Van Santen, R. A., *Catal. Lett.*, 6, 49 (1990).
62 Van Santen R. A., De Koster A. and Koerts T., *Catal. Lett.*, 7, 1 (1990).
63. Van der Grift C. J. G., Ph. D. Thesis, Utrecht 1990.
64. Feibelman P.J., *Phys. Rev. B*, 26(10), 5347 (1982).
65. Darling G.R., Joyner R.W. and Pendry J.B., in 'Structure and reactivity of surfaces', (Editor C. Morterra), Elsevier Amsterdam (1989).
66. Ichikawa M., Fukushima, T. and Shikakura, K., *8th ICC Berlin*, Vol. II, 69 (1984).
67. Mross W. D., *Catal. Rev. -Sci. Eng.*, 25, 591 (1983).
68. Dry M. E., in 'Applied Industrial Catalysis', vol. 2, (ed. B. E. Leach), Academic press, p.167, (1983).

7

Homologation of olefins with methane on transition metal catalysts.

ABSTRACT

Methane addition to olefins is demonstrated using silica supported ruthenium and cobalt catalysts in a reaction cycle consisting of three reaction steps. First, methane and an olefin are adsorbed separately at different temperatures. Subsequently, the adsorbed carbonaceous surface species are hydrogenated to higher homologues. Using $^{13}CH_4$ it is shown that propane and butane are formed both by self homologation of ethene and propene respectively, and by methane incorporation.

Parts of this chapter have been or will be published: *J. Chem. Soc., Chem. Comm.*, **1992**, 345, with co-author Rutger A. van Santen; *J. Am. Chem. Soc.*, accepted, with co-authers Piet A. Leclercq and Rutger A. van Santen.

INTRODUCTION

Methane conversion into higher hydrocarbons is of world wide interest. One route is the reaction of methane with alkenes to higher homologues. Below 500 K the alkylation of olefins with methane, to an alkane with one extra carbon atom is thermodynamically possible in one step, for ethene and propene [1]. This reaction has been found to occur using superacids as catalysts [2]. Syskin and Mayer [3] converted methane ethene mixtures to propane with about 40-60% selectivity using TaF_5-HF at 40 °C and 1 MPa. Olah used super acids immobilized on alumina [4,5]. At 70 °C he reached a conversion of 38% with respect to ethene with a feed of CH_4:C_2H_6 of 9:1 mol/mol. Olah et al [6] showed in a reaction with $^{13}CH_4$ and $^{12}C_2H_4$ under mild conditions, that $^{13}C^{12}C^{12}C$ propane is formed selectively, when the methane/ethene ratio is above 100. According to Scurell [7] however, it is not totally clear that these systems are truly catalytic and some fluorine loss may occur during the reaction. Although the solid superacids [8,9] used are much more environmental friendly than homogeneous acids, the use of HF to activate these systems remains a drawback. Therefore, it is of interest to perform this reaction on heterogeneous catalysts.

The direct conversion of methane with ethene has not yet been realized on heterogeneous metal catalysts. Indirect conversion routes have been proposed on nickel catalysts. Löffler et al [10] carried out a reaction with methane and cyclo-pentene to benzene and toluene at 310 °C. They repeated the reaction with $^{13}CH_4$ and were not able to detect incorporation of ^{13}C into the reaction products. However when the nickel oxide catalyst was reduced at a higher temperature with $^{13}CH_4$ before the reaction, ^{13}C incorporation in benzene and toluene could be demonstrated to a modest extent. Ovales et al [11] reported the conversion of methane with propene to iso-butane at 350 °C on a silica-supported nickel catalyst. They reduced the nickel oxide catalyst at 600 °C for 8 hours before the reaction. When the methane was substituted by nitrogen, the butane yield decreased, a process which is reversible. At 350 °C the thermodynamics is not favourable for the reaction of methane and propene to butane.

One of the main problems in the conversion of methane together with olefins on transition metals is the low sticking coefficient of dissociative methane adsorption compared with that of alkene adsorption. The chance that methane is dissociatively adsorbed in the presence of ethene is very small and methane will not become a selective reactant. Therefore, methane should not be adsorbed together with other reactants, but in a separate step. To achieve this, we developed a catalytic cycle in which the reactants are adsorbed separately at different temperatures (see fig. 1).

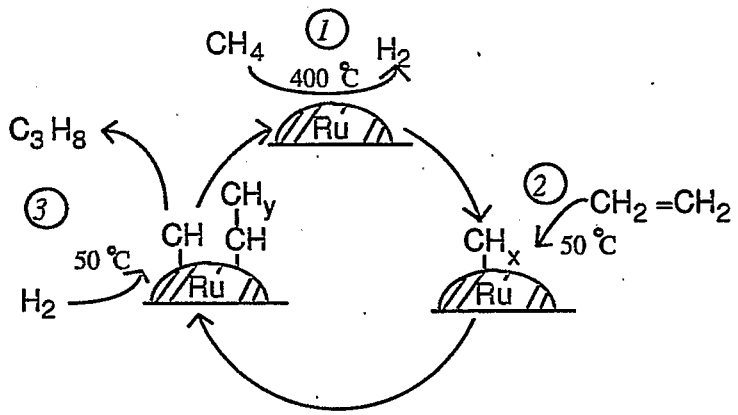

Figure 1. Reaction cycle for the step wise conversion of methane and an olefin to a higher homologue.

In the first step methane is dissociatively adsorbed on a reduced transition metal catalyst at a temperature between 100 and 550 °C. In the second step an olefin is co-adsorbed together with surface carbon from methane at a temperature between 20 and 100 °C. In the third step both hydrocarbon fragments are hydrogenated forming a higher homologue.

This reaction sequence provides an overall new reaction path for alkylation reactions using methane. Here we discuss the results for the reaction of methane with ethene, acetylene and propene to form propane and butane respectively. To prove that methane is really incorporated in the reaction products, the reactions were repeated with ^{13}C labelled methane.

EXPERIMENTAL

Catalysts

A 5 wt.% ruthenium catalyst and a 10 wt. % cobalt catalyst were prepared by incipient wetness impregnation of Grace 332 type silica (300 m^2/g, pore volume=1.65 ml/g, mesh size 75-125) with an aqueous solution of $RuCl_3$ (Drijfhout, Amsterdam) and $Co(NO_3)_2 \cdot 6\ H_2O$ (Merck), respectively. The catalysts were dried at 110 °C and reduced before each experiment in situ between 400 and 550 °C. The ruthenium catalyst was treated in a synthesis gas flow (H_2/CO=2 at 1 bar) for 30 min at 250 °C to increase its chemisorption capacity. The metal particle size as determined with Transmission Electron Microscopy was 5.5 nm for the ruthenium and 8.5 nm for the cobalt catalyst. The active metal surface areas as derived from CO chemisorption (CO/Ru=30% and CO/Co=2.2%) indicate incomplete reduction of the cobalt catalyst.

Experimental conditions

For each experiment 300 mg of the catalyst was placed in the reactor which consisted of a quartz tube (i.d. 10 mm). Methane adsorption was performed at 450 °C from a methane pulse of 90 sec. of 0.5 % CH_4 in helium in a flow of 22.4 ml/min. After methane adsorption the catalyst was cooled in helium as quickly as possible to a temperature between 25 and 150 °C to avoid 'ageing' of the surface carbon: typically the temperature was decreased within 100 sec. to 150 °C. Ethene, acetylene or propene were adsorbed from pulses of 1.4 μmol, between 25 and 150 °C. Subsequently, the adsorbed carbonaceous surface species were hydrogenated in a flow of 22.4 ml/min hydrogen at ambient pressure at the same temperature as the olefin adsorption. After this hydrogenation the temperature was raised at a rate of 20 °C/min to 550 °C in the same hydrogen flow, to remove carbonaceous residues. After cooling to 450 °C the cycle was repeated.

Analysis

During the first two minutes of hydrogenation, 15 times 0.2 ml of the reaction gases were stored in a 16 loop multi-position valve (Chrompack type ST34). The stored reaction gases were injected in a GC (CP 9000, Chrompack) and the reaction products were separated on a widebore plot Q column (25 m * 0.53 mm i.d.).

For the experiments with labelled methane (99% $^{13}CH_4$ from Cambridge Isotope Laboratories), the stored reaction gases were separated on the same column which was connected (splitless) with a coupling unit ('Graphpack-3D-Saulenverbinder' from Gerstel) to a fused silica.capillary of 2 meter (i.d. 100 μm). This capillary was directly introduced in the ion chamber of a high resolution mass spectrometer [12]. During the analyses the masses between 10 and 60 Dalton were scanned every 1.5 second. For each component about 10-20 mass spectra were taken to calculate the average peak ratios. From these peak ratios the fraction of each labelled product was calculated (see appendix). From the mass spectra the position of the ^{13}C atom incorporated could be deduced.

RESULTS

During the methane pulse at 450 °C all the methane is adsorbed on the ruthenium catalyst resulting in a carbon surface coverage of about 20%. On the cobalt catalyst 60% of the methane pulse, is adsorbed. During the adsorption of ethene, acetylene and propene between 25 and 150 °C, not all the reactants are adsorbed. A part of the olefin was auto-hydrogenated to the paraffin. Especially when no methane was pre-adsorbed alkane desorption was detected. Figure 2 compares the fractions of carbon adsorbed from a pulse of 1.4 μmol ethene on a

reduced ruthenium catalyst, with a pulse after pre-adsorption of 6.6 µmol methane at 450 °C.

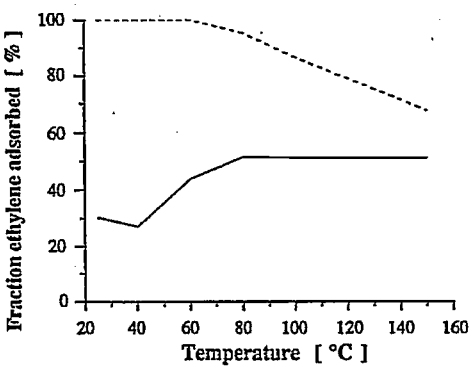

Figure 2.
Fraction of ethene adsorbed on the reduced ruthenium catalyst before (solid line) and after methane adsorption at 450 °C (dashed line) as a function of the ethene adsorption temperature.

The fraction of adsorbed ethene is increased when surface carbon from methane is present on the catalyst surface. On the ruthenium catalyst more methane formation is observed during ethene adsorption than on cobalt. Above 100 °C methane is the only product desorbing from the ruthenium catalyst, while it is mainly ethane at the cobalt catalyst.

After the adsorption steps on the ruthenium catalyst 6.6 µmol carbon from methane and 2.8 µmol carbon atoms from ethene (1 pulse) is present on the catalyst surface. For the cobalt catalyst these figures are 4.0 and 1.7 µmol respectively, due to the incomplete adsorption from the pulse. The amount of adsorbed carbonaceous surface species, which can be hydrogenated at a particular hydrogenation temperature, is shown in fig. 3 for the cobalt catalyst.

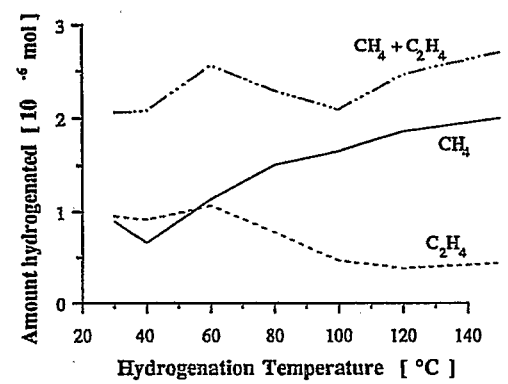

Figure 3.
Total amount of carbonaceous material that is hydrogenated (in µmol C) after separate methane and ethene adsorption and their co-adsorption on the cobalt catalyst as a function of the hydrogenation temperature. (6.6 µmol methane pulsed at 450 °C; 1.4 µmol ethene pulsed at the hydrogenation temperature).

At a hydrogenation temperature above 100 °C most of the desorbing hydrocarbons originate from methane. Around 50 °C the formed hydrocarbons originate from about the same amounts of ethene and methane.

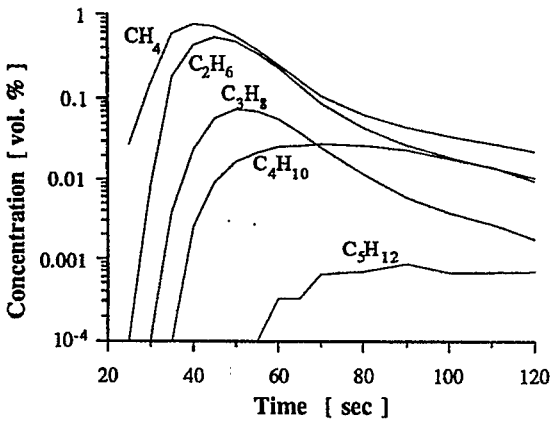

Figure 4. Products formed during the hydrogenation at 40 °C of adsorbed methane (6.6 μmol at 450 °C) and ethene (1.4 μmol at 40 °C) on the ruthenium catalyst at 40 °C as a function of the hydrogenation time.

Figure 4 depicts hydrocarbon formation from surface carbon as a function of the exposure time to hydrogen at 40 °C, during the first two minutes. By integrating these curves the selectivity can be calculated. It is shown in fig. 5 and is expressed in carbon efficiency. For butane and pentane the iso- and n-product are taken together. Mainly the linear hydrocarbons are formed.

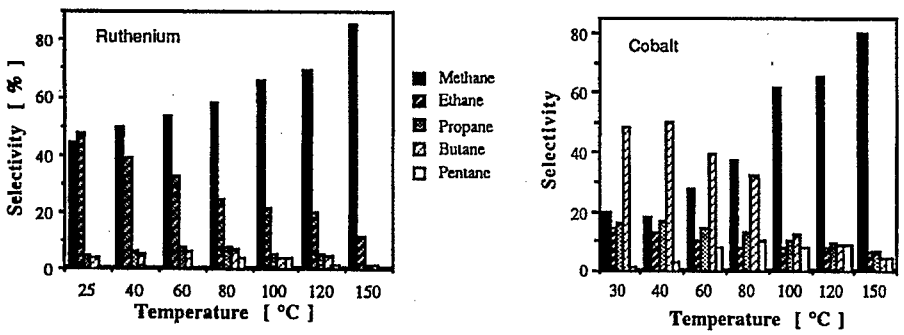

Figure 5. Product selectivity during the hydrogenation of adsorbed methane (at 450 °C) and ethene (1 pulse at stated temperature) as a function of the temperature. left: Ruthenium. right: Cobalt.

On cobalt, at low ethene adsorption and hydrogenation temperature, the selectivity to butane is remarkably high due to ethene dimerization. Increasing the hydrogenation temperature the methane selectivity increases due to enhanced hydrogenolysis. The selectivity for the interesting reaction product propane is not a strong function of the temperature and has its maximum of 19 % at 40 °C on the cobalt catalyst.

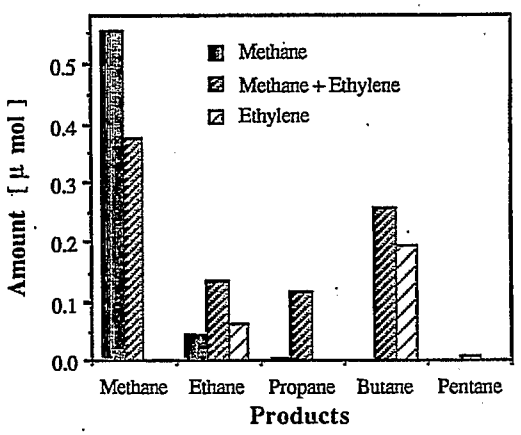

Figure 6. Product formation upon hydrogenation at 40 °C of adsorbed methane (T_{ads}=450 °C), adsorbed ethene (1 pulse at 40 °C) and their co-adsorption, on cobalt.

Figure 6 compares the amount of products formed during hydrogenation, after separate methane and ethene adsorption and their co-adsorption. As previously demonstrated [13-17], surface carbon from methane alone can be hydrogenated to C_2^+ hydrocarbons. However, most of the dissociatively adsorbed methane reacts back towards methane. When ethene is co-adsorbed, the amount of methane formed is reduced and propane formation becomes significant. This indicates a reaction between adsorbed C_1 species from methane and co-adsorbed ethene forming propane. The ability to form propane from adsorbed methane and ethene was tested for different metal catalysts. The order of the selectivity for propane formation is Co, Ru > Pt, Rh, Ni > Re, Fe. Here only the results of the cobalt and ruthenium catalyst are discussed.

As indicated in Table 1, propane formation is also possible from adsorbed ethene via hydrogenolysis and homologation, resulting in methane and propane. Such a disproportionation reaction has been extensively studied by Basset and co-workers [18-20]. To distinguish this reaction from methane incorporation into adsorbed ethene, experiments with ^{13}C labelled methane were performed. Therefore 6.6 µmol of $^{13}CH_4$ was pulsed at 450 °C over the

catalyst and 5.2 μmol unlabelled ethene, acetylene or propene were co-adsorbed at 50 °C. The product selectivities of the experiments performed under those conditions are shown in table 1.

Table 1. Product selectivity during hydrogenation at 50 °C of adsorbed olefins with and without pre-adsorbed methane at 450 °C.

Adsorbates	Methane	Ethane	Propane	Butane [1]	Pentane [1]	Ratio i/n C_4
Ruthenium						
$CH_4+C_2H_4$	34	45	10	11	0.4	0.066
C_2H_4	20	71	5	4.4	0	0.067
$CH_4+C_2H_2$	34	36	14	16	0	0.056
C_2H_2	8.3	54	12	25	0.9	0.044
$CH_4+C_3H_8$	24	29	36	10	1	0.082
C_3H_8	36	34	25	4.9	0.3	0.052
Cobalt						
$CH_4+C_2H_4$	10	12.5	17	53	6.5	0.030
C_2H_4	5.7	18	11	61	4.5	0.024
$CH_4+C_2H_2$	33	21	16	26	4.8	0.072
C_2H_2	6.9	19	12	53	8.1	0.053
$CH_4+C_3H_8$	11	3.2	54	26	6.1	0.164
C_3H_8	1.9	3.5	66	19	10	0.077

[1] Sum of iso and n product.

The reaction was repeated using $^{13}CH_4$ and the products were analysed for the presence of ^{13}C atoms. Of interest is the fraction of ^{13}C incorporated in the alkylated reaction products. This was measured for the different labelled isotopes and is shown in Table 2.

The labelled carbon atom from methane is added to adsorbed acetylene, ethene and propene resulting in a product with one ^{13}C atom from methane and ^{12}C atoms from the olefin, as indicated from the underlined figures in Table 2. As deduced from the fragment mass spectra, the labelled ^{13}C atom in the singly labelled products is the primary atom in propane and butane. The reaction products propane and butane are also formed exclusively from ^{12}C atoms from the adsorbed olefin due to auto-homologation. Apparently, $^{13}C_1$ surface species from methane compete with $^{12}CH_x$ species generated by olefin hydrogenolysis for carbon incorporation.

Table 2. Relative frequency of different ^{13}C isotopically labelled reaction products. The results are weighted averages of the analyses of 6 to 13 loops. (For calculations see appendix).

	Methane	Ethane			Propane		
Precursor	$^{13}CH_4$	$^{12}C_2$	^{12}C-^{13}C	$^{13}C_2$	$^{12}C_3$	$^{12}C_2$-^{13}C	^{12}C-$^{13}C_2$
Cobalt							
Acetylene	95	83	2	12	41	51	0.02
Ethene	99	89	0	12	40	58	0.7
Propene	98	61	9	30	98	1.1	0.3
Ruthenium							
Acetylene	94	88	4	8	51	47	1
Ethene	75	95	1	4	36	62	1.7
Propene	92	89	5	6	93	5.3	0.8

	n-Butane			
Precursor	$^{12}C_4$	$^{12}C_3$-^{13}C	$^{12}C_2$-$^{13}C_2$	^{12}C-$^{13}C_3$
Cobalt				
Acetylene	79	14	5.2	2.2
Ethene	82	8.2	8.8	0.6
Propene	26	73	0.7	0.4
Ruthenium				
Acetylene	85	11	4.4	0
Ethene	81	10	7.8	0.6
Propene	50	47	1.9	1.3

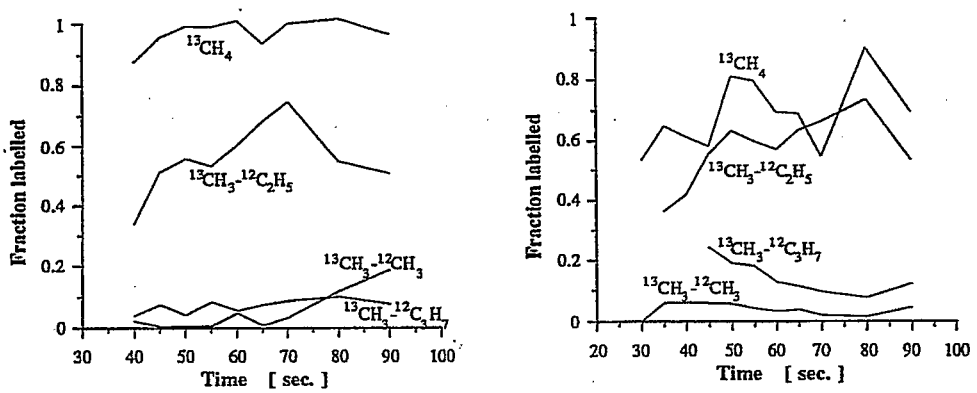

Figure 7. The fraction of each product consisting of one ^{13}C atom as a function of the hydrogenation time, for the step-wise reaction of ^{13}C methane with unlabelled ethene. a (left): Cobalt. b (right): Ruthenium.

Figure 7 shows the ^{13}C incorporation as a function of the hydrogenation time. The fraction of ^{13}C in propane is a slight function of the hydrogenation time. The fraction of ^{13}C in the reaction product increases a little in time as measured for nearly all the experiments of labelled methane incorporation.

DISCUSSION

Hydrocarbon adsorptions

Dissociative methane adsorption can result in three types of surface carbonaceous species which differ in their hydrogenation temperature [16,17]. Under the particular methane adsorption conditions used here, about 60 % of the surface carbon species from methane on Ru and 40 % on Co consist of reactive carbidic C_α which is able to react below 100 °C with hydrogen to hydrocarbons. The less reactive C_β and unreactive C_γ species can be removed during temperature programmed hydrogenation. Up to a hydrogenation temperature of about 240 °C some C_2^+ hydrocarbon formation is observed, while at higher temperatures only methane is formed.

The differences in adsorption probability of olefins with and without the pre-adsorption of methane (fig. 2) might suggest a direct interaction between adsorbed surface carbon and the co-adsorbed olefin. However, concerning the ethene adsorption mechanism this appears not to be the case. The mechanism of adsorption of ethene on reduced transition metals has been extensively studied on single crystals [21-23]. Chemisorbed ethene looses one or more hydrogen atoms at temperatures above room temperature, and is adsorbed like an ethylidyne (CCH_3), vinylidyne (CCH_2) or acetylide (CCH) species [24]. Due to the low temperature the resulting surface hydrogen does not desorb but is used to hydrogenate other ethene molecules to ethane in an auto-hydrogenation reaction. The desorbing products consist of only methane and ethane, no trace of ethene was detected at low ethene surface concentrations. When surface carbon from methane is present the resulting surface hydrogen atoms from ethene are used to form CH, CH_2 or CH_3 surface species, instead of forming ethane from ethene. This decreases the formation of ethane and enhances the fraction of atoms from ethene that remains adsorbed.

Hydrogenation

The optimum temperature for hydrogenation of surface carbon depends on the amount of surface species that can be hydrogenated and on the product selectivity (figs. 3, 4 and 5). In general, at low hydrogenation temperature (<60°C), the selectivity to propane and butane is high while at a hydrogenation temperature above 80 °C, more surface carbon can be hydrogenated. The

optimum hydrogenation temperature is about 50 °C. This was the temperature chosen for the experiments with labelled methane. At this temperature about equimolar amounts of adsorbed methane and olefins are hydrogenated on both catalyst systems. These amounts correspond to a carbon surface coverage of about 11 % for both methane and alkene (normalised on the CO chemisorption capacity). At higher carbon surface coverages, surface carbon becomes less reactive due to the enhanced formation of C_β [17].

Table 1 shows that upon hydrogenation of adsorbed olefins, the selectivity for methane formation is higher on ruthenium than on cobalt. This result is in agreement with earlier reports [25,26], where it was indicated that ruthenium is the most active metal for hydrogenolysis. At 50 °C the clean surface of the well reduced ruthenium catalyst has a remarkably high activity for hydrogenolysis.

The higher rate of hydrogenolysis on ruthenium does not lead to an enhanced selectivity for homologation compared to cobalt. At the hydrogenating conditions (50 °C and 10 kPa H_2) the thermodynamics are in favour for methane formation instead of homologation.

Cobalt has a high selectivity of 64 % for ethene dimerization, whereas it is only 4% on ruthenium. The selectivity for dimerization of acetylene is higher than that of ethene on ruthenium. This supports previous suggestions on the same catalyst, indicating that the recombination of carbon surface fragments is most effective from hydrogen deficient adsorbates [31].

Experiments with labelled methane

Table 2 shows that labelled methane can be incorporated into co-adsorbed olefins, resulting in the reaction products propane and butane. This demonstrates alkylation of olefins with methane according to the reaction cycle in fig. 2. However, 30-50 % the homologated olefins contain only ^{12}C, and thus originate entirely from the initial olefin. This means that C-C bond formation from C_1 intermediates, generated from methane deposition or from alkene hydrogenolysis, occurs with about the same probability. Because the surface concentrations of the reacting methane and olefin fragments are the same, this indicates that the C_1 intermediates involved are very similar.

Some additional experiments were done to study the influence of the olefin hydrogenation temperature and the ratio of adsorbed methane/olefin. When less ethene was pulsed and the ethene adsorption and hydrogenation temperature were decreased to 25 °C, the fraction of singly labelled ^{13}C propane increased to 76 % on the ruthenium catalyst. Due to the lower temperature the rate of hydrogenolysis decreased. This reduced the amount of $^{12}C_1$ surface fragments, resulting in an enhanced fraction of propane from ^{13}C methane and ^{12}C ethene. The rate of hydrogenolysis is much lower on the cobalt catalyst. At 25

°C no methane formation is observed when adsorbed ethene is hydrogenated. However, in the reaction of $^{13}CH_4$ with ethene, only 66 % of the propane formed is singly labelled and still 30 % consists of only ^{12}C from ethene. This suggests that either ethene reacts towards propane and methane, or that singly labelled propane can exchange its ^{13}C carbon atom with a ^{12}C from ethene, resulting in ^{12}C-^{13}C ethene. ^{12}C-^{13}C ethene is not found in the reaction gas, but it can be dimerized to singly or doubly labelled butane, which butanes are formed in a low fraction.

The absence of singly ^{13}C labelled propane, when propene is co-adsorbed with labelled methane, and the absence of singly labelled ethane when ethene is co-adsorbed, indicate that the metathesis reaction (see fig. 8), or other routes of carbon scrambling, are slow on both ruthenium and cobalt compared to hydrogenolysis, carbon-carbon bond formation and hydrogenation.

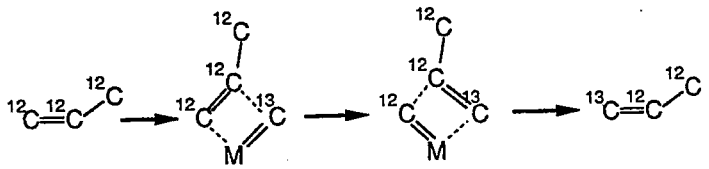

Figure 8. Metathesis mechanism according to which ^{12}C propene could exchange a carbon atom with an adsorbed ^{13}C atom from methane. The hydrogen atoms are not drawn. M symbolizes an active site consisting of one or more metal atoms.

The metathesis reaction between ^{13}C surface carbon and an olefin as proposed in fig. 8 does not occur and is therefore very slow compared to hydrogenolysis and carbon-carbon bond formation at 50 °C and 100 kPa H_2. Hence, non-labelled butane is not formed from two propene molecules via metathesis, resulting in ethene and butene, but via hydrogenolysis and homologation. This result is in agreement with measurements of Tanaka at al [27-30] on MoO_x catalysts. They demonstrated that surface carbon species involved in metathesis are different from the intermediates active in the Fischer-Tropsch reaction.

It is possible to calculate the selectivity for hydrogenolysis and homologation of the adsorbed olefins in the presence of ^{13}C from methane from tables 1 and 2, by not taking into account the molecules containing ^{13}C atoms. The selectivity pattern appeared to be about the same as that of the solely adsorbed olefins. This indicates that the selectivities for hydrogenolysis, homologation and dimerization are not influenced by surface carbon species from methane. In particular for hydrogenolysis this was unexpected, because surface carbon species should decrease the amount of free metal ensembles,

necessary for hydrogenolysis. Apparently the carbon surface coverages applied are too low to change the mentioned rates significantly.

Iso- / n-butane ratio

During the hydrogenation of carbonaceous intermediates from methane and olefins at 50°C, the selectivity for butane formation varies from 5-60 %. Most of the butane is n-butane but also some i-butane is formed. In relation to iso-butane formation, differences in the mechanistic formation routes are of interest. A comparison of the fraction of ^{13}C in n-butane and i-butane in the hydro-genation reaction of adsorbed ^{13}C with ethene or propene is given in Table 3.

Table 3. Percentage of singly ^{13}C labelled i- and n-butane.

Precursors	Cobalt		Ruthenium	
	i-C_4	n-C_4	i-C_4	n-C_4
$^{13}CH_4 + C_2H_4$	50-70	14	60-80	15
$^{13}CH_4 + C_3H_6$	40-80	73	30-50	45

Due to the low selectivity, the fraction of ^{13}C in iso-butane could not be determined with great accuracy. The incorporation of ^{13}C in iso-butane formed from ethene is more dominant than in n-butane, because the later is mainly formed by dimerization of ethene. Iso- and n-butane are not in a dynamic equilibrium and their routes of formation are probably different. For the incorporation of ^{13}C in propene to form i- and n-butane no significant differences were found. This indicates that surface carbon generated from propene dissociation reacts similarly as surface carbon from methane.

When more carbidic surface carbon is present on the surface together with adsorbed propene species, the ratio of i/n -butane increases from 0.08 to 0.16 on cobalt (see table 1). This indicates that in the formation of iso-butane a carbidic carbon atom is involved. The ratio of i/n butane from only surface carbon from methane is higher (0.30) than that with co-adsorbed propene. Adsorbed propene reacts mainly towards n-butane.

The ratio of i/n -butane is even lower on the ruthenium than on the cobalt catalyst. These low ratios are typical distributions of the Fischer-Tropsch (F.T.) synthesis in which ruthenium mainly produces the linear alkanes [32,33]. This indicates that the mechanism of carbon-carbon bond formation between ethene and carbidic surface carbon from methane, are very similar to that occurring in F.T. synthesis. In the F.T. reaction added ethene in the feed has been shown to

incorporate into hydrocarbons [34-36]. The formation of adsorbed ethene has been suggested to be one of the slow steps, for chain propagation and therefore added ethene can serve as chain growth initiator [37,38]. Our results are in agreement with these observations: more surface carbon from methane undergoes carbon-carbon bond formation when ethene is co-adsorbed.

Yields

The overall yield for the reaction of methane and ethene to propane according to the proposed reaction cycle depends on: fraction of methane adsorbed, fraction of ethene adsorbed, amount of surface carbon hydrogenated at the hydrogenation temperature, selectivity to propane and the fraction of propane consisting of only one ^{13}C atom from methane. Taking all these factors into account, the yield for the reaction of $^{13}CH_4$ with adsorbed ethene is 2.8% on the basis of pulsed methane and 4.5 % on the basis of pulsed ethene on the ruthenium catalyst. The ethene yield can be increased by increasing the methane/ethene ratio. The yield on methane basis is about 3 times higher than that in superacid catalysed alkylation [6], while it is about 6 times lower on ethene basis.

CONCLUSIONS

The incorporation of methane into alkenes in the presence of hydrogen on transition metal catalysts, can be performed using a reaction cycle in which methane is separately adsorbed. In this way methane can be used as an alkylating agent. This is demonstrated for the incorporation of methane into ethene, acetylene and propene. The reaction products propane and butane can be formed via also auto-homologation. The comparable reaction rates of self-homologation and methane incorporation indicate that the C_1 intermediates involved are similar; they are both related to the CH_x fragments active in the Fischer-Tropsch reaction.

The exchange of carbon atoms according to a metathesis reaction does not occur on the ruthenium or cobalt catalyst. The cobalt catalyst has a remarkably high selectivity for dimerization of adsorbed ethene.

APPENDIX

Calculation of isotopic distributions from mass spectra.

An alkane with n carbon atoms either ^{12}C or labelled ^{13}C, can have n+1 differently labelled isotopes: unlabelled, singly ^{13}C labelled up to n times labelled alkane (not taking into account the different positions of the ^{13}C atom). It is possible to calculate the fraction of each differently labelled isotope from a mass spectrum. This is not trivial because the mass spectrum of the unlabelled alkane disturbs an easy calculation [39]. Here we present an algorithm that deduces these fractions from the measured mass spectra. Propane is taken as an example, while problems are identical for C_n with n>3. Propane can have four types of different labelled isotopes: $^{12}C_3$, $^{12}C_2$-^{13}C, ^{12}C-$^{13}C_2$ and $^{13}C_3$. Their relative frequency are indicated with f_1 to f_4. To calculate f_1 to f_4 one has to know the reference mass spectrum of unlabelled propane and that of the labelled mixture. It is assumed that the "isotope effect" [39] does not influence the fragmentation process. A part of the reference spectrum m_1 to m_7, have relative intensities I_1 to I_7 as shown in figure A1.

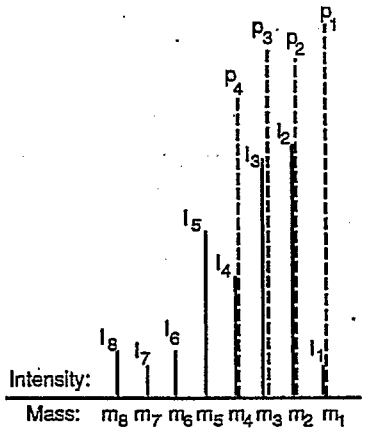

Figure A1.
Reference mass spectrum with intensities I_i at mass m_i. The intensities of the peaks p1 to p4 from the labelled mixture at mass m1 to m4 are shown by the dashed lines.

From the measured peaks p_1 to p_4 of the labelled mixture, one can calculate the fractions f_1 to f_4. Each of the measured intensities p is the sum of the fraction multiplied by the intensity of the unlabelled component. This follows from figure A1 and is shown in equation (1).

$$p_1 = I_1f_1 + I_2f_2 + I_3f_3 + I_4f_4 \qquad (1)$$

This can be written in matrix form for all the 4 peaks measured (2).

$$\begin{pmatrix} p_1 \\ p_2 \\ p_3 \\ p_4 \end{pmatrix} = \begin{pmatrix} I_1 & I_2 & I_3 & I_4 \\ I_2 & I_3 & I_4 & I_5 \\ I_3 & I_4 & I_5 & I_6 \\ I_4 & I_5 & I_6 & I_7 \end{pmatrix} \cdot \begin{pmatrix} f_1 \\ f_2 \\ f_3 \\ f_4 \end{pmatrix} \qquad (2)$$

The fractions f_1 to f_4 are calculated from the inverse matrix (M^{-1}) containing the intensities I_1 to I_7 from equation (2).

$$\vec{f} = M^{-1} \cdot \vec{p} \tag{3}$$

Finally the fractions f_i (i=1..4) are normalized according to (4).

$$f_i = \frac{f_i}{\sum_{i=1}^{4} f_i} \tag{4}$$

In principle from any n peaks from the mass spectrum of C_nH_{2n+2} this calculation can be performed, however experimental errors are relative low when differences between intensities in the reference spectrum are large. Therefore we used the masses m/z 44-47 for propane, m/z 30-32 for ethane and m/z 31-29 for the C_2 fragment of propane. By comparing the analyses of the C_2 and the C_3 fragments of propane it could be concluded that in the singly labelled product mainly the primary atom is labelled.

LITERATURE

1. Scurrell M.S., *Appl. Catal.*, **32**, 1 (1987).
2. Siskin M., *J. Am. Chem. Soc.*, 98, 5413 (1976).
3. Siskin M. and Mayer I., U.S. Patent 4 094 924 (1987) (Exxon research).
4. Olah G.A., U.S. Patent 4 373 109 (1983).
5. Olah G.A. and Schlosberg R.H., *J. Am. Chem. Soc.*, 90, 2726 (1968).
6. Olah G.A., Felberg J.D. and Lammertsma K., *J. Am. Chem. Soc.*, **105**, 6529 (1983).
7. Scurrell M.S., *Appl. Catal.*, **34**, 109 (1987).
8. Arata K., *Adv. in Catal.*, **37**, 165 (1990).
9. Olah G.A., *Angew. Chem., Int. Ed. Engl.*, **12**, 173 (1973).
10. Löffler I.D., Maier W.F., Andrade J.G., Thies I. and von Ragué Schleyer P., *J. Chem. Soc., Chem. Comm.*, **1984**, 1177.
11. Ovales C., Leon V., Reyes S. and Rosa F., *J. Catal.*, **129**, 368 (1991).
12. Leclerque P.A., Snijders H.M.J., Cramers C.A., Maurer K.H. and Rapp U., *J. of High Res. Chrom.*, **12**, 651 (1989).
13. Tanaka K-I., Yaegashi I. and Aomoura K., *J. Chem Soc. Chem. Comm.*, **1982**, 938.
14. Yang, Q.Y., Johnson, A.D., Maynard, K.J. and Ceyer, S.T., *J. Am. Chem. Soc.*, **111**, 8748 (1989).
15. Belgued M., Amariglio H., Pareja P., Amariglio A. and Saint-Juste J., *Nature*, **352**, 789 (1991).
16. Koerts T. and van Santen R.A., *J. Chem. Soc., Chem. Comm.*, **1991**, 1281.
17. Koerts T. and van Santen R.A., *J. Catal.*, accepted; chapter 6 of this thesis
18. Rodriguez E., Leconte M., Basset J-M., Tanaka K. and Tanaka K-I., *J. Am. Chem. Soc.*, **110**, 275 (1988).
19. Rodriguez E., Leconte M., Basset J-M., *J. Catal.*, **131**, 457 (1991).
20. Leconte M., Theolier A., Rojas D. and Basset J.M., *J. Am. Chem. Soc.*, 106, 1141 (1984).

21. Hills M.M., Parmeter J.E., Mullins C.B. and Weinberger W.H., *J. Am. Chem. Soc.*, 108, 3554 (1986).
22. Zaera F., *J. Am. Chem. Soc.*, 111, 4240 (1989).
23. Hills M.M., Parmeter J.E. and Weinberger W.H., *J. Am. Chem. Soc.*, 92, 7215 (1986).
24. Salmerón M. and Somorjai G.A., *J. Phys. Chem.*, 86, 341 (1981).
25. Sinfelt J.H., *Adv. in Catal.*, 23, 91 (1973).
26. Gao S. and Schmidt L.D., *J. Catal.*, 115, 356 (1989).
27. Tanaka K. and Tanaka K-I., *J. Chem. Soc., Chem. Comm.*, 1984, 1626.
28. Tanaka K., Tanaka K-I., Takeo H. and Matsumura C., *J. Chem. Soc., Chem. Comm.*, 1986, 33.
29. Tanaka K. and Tanaka K-I., *J. Chem. Soc., Farad. Trans. I.*, 83, 1859 (1987).
30. Tanaka K. and Tanaka K-I., *J. Chem. Soc., Chem. Comm.*, 1983, 259.
31. Koerts T. and Van Santen R.A., *J. Mol. Catal.*, 70, 119 (1991).
32. McCandlish L.E., *J. Catal.*, 83, 362 (1983).
33. Joyner R.W., *Catal. Lett.*, 1, 307 (1988).
34. Morris S.R., Moyes R.B., Wells P.B. and Whyman R., *J. Catal.*, 96, 23 (1985).
35. Smith D.F., Hawk C.O. and Golden P.L., *J. Am. Chem. Soc.*, 52, 3221 (1930).
36. Adesina A.A., Hudgins R.R. and Silveston P.L., *Appl. Catal.*, 62, 295 (1990).
37. Mims C.A. and McCandlish L.E., *J. Phys. Chem.*, 91, 929 (1987).
38. Mims C.A., McCandlish L.E. and Melchior M.T., *Catal. Lett.*, 1, 121 (1988).
39. Millard B.J., in *"Quantitative Mass Spectrometry"*, Ad. Heyden & Son Ltd., London (1978).

8

General Conclusions

This study has been concentrated on two reactions both related with carbon-carbon bond formation on transition metal catalysts. The first concerns the influences of a vanadium promoter on the kinetics of elementary reaction steps upon synthesis gas conversion on a rhodium catalyst. The second is related to the general problem of initiating a carbon-carbon bond between two methane molecules. Both reactions occur via reactive C_1 surface intermediates. These surface species were created from CO and CH_4 respectively. Mainly transient kinetic techniques were used which were combined with some quantum chemical calculations.

The understanding of bimetallic catalysts in which a noble metal is promoted with a less noble metal oxide is of great interest. Such a system has been considered here for CO hydrogenation. The influence of a vanadium promoter on the formation and intrinsic reactivity of CH_x species adsorbed on rhodium catalysts, for hydrogenation, chaingrowth and CO insertion, has been investigated. On rhodium catalysts a very reactive C_1 intermediate was found to be formed from dissociative CO adsorption. The formation of this surface species was found to be enhanced by vanadium promotion, which lowers the activation energy for CO dissociation. This effect is proposed to be a structure like effect in which vanadium generates free sites for CO dissociation by the creation of oxygen vacancies, necessary for CO dissociation. Free rhodium metal atoms are important for CO dissociation; the optimum CO coverage for CO dissociation on the rhodium catalyst lies between 0.2 and 0.3.

Due to the vanadium promoter the surface C_1 species are less reactive for hydrogenation to methane and have an increased probability for chaingrowth. This effect has been explained using semi-emperical quantum-chemical calculations. It is suggested that stronger adsorbed carbon atoms are less reactive for methanation, while the activation energy for carbon-carbon bond formation is much less affected. This results in the conclusion that stronger adsorbed surface carbon is favourable for chaingrowth. This has also implications to the recombinating surface CH_x species. Highly dehydrogenated surface carbon fragments are stronger adsorbed and have a higher affinity for carbon-carbon bond formation. The optimum average value found for x of the recombinating CH_x fragments is about one. This low value is due to an enhanced steric repulsion of hydrogen atoms in the recombination of CH_x fragments in which x=2 or 3.

The reaction coefficient for CO insertion into adsorbed CH_x fragments, is not enhanced by vanadium. This step is not rate determining and seems to be in a kind of equilibrium with the adsorbed CH_3CO surface species. The vanadium promoter stabilizes such oxygenated intermediates. The hydrogenation rate of these surface species is slow, and is enhanced by vanadium. The order in hydrogen during this hydrogenation is drastically decreased, which may indicate stronger adsorbed hydrogen induced by vanadium.

The second reaction studied, was the conversion of methane via surface carbon to higher hydrocarbons. Dissociative methane adsorption can result similar as CO dissociation in three different types of carbonaceous surface species. They can be distinguished in their hydrogenation temperature. The most reactive carbidic type of surface carbon, reactive below 100 °C, and could be formed on supported Co, Ni, Ru, Rh, Pt, Ir and Re catalysts. This surface carbon is most suitable for carbon-carbon bond formation. A less reactive surface carbon is formed on most catalysts, reacting between 200 and 300 °C to mainly methane. Only small amounts of higher hydrocarbons up to hexane are formed from this amorphous like carbon. At temperatures above 400 °C an unreactive graphitic type of surface carbon is formed that produces only methane upon hydrogenation above 400 °C. These surface carbon types can be distinguished also in their reactivity with oxygen to CO_2.

Of importance is the discovery of the reactive C_1 intermediate by dissociative methane adsorption, that is able to produce C_2^+ hydrocarbons upon hydrogenation. This has led to a new route of methane conversion to hydrocarbons. The theoretical and practical conditions for such a route are

described in chapter 6. Thermodynamic analysis show that methane decomposition has to occur at a temperature of 280 °C higher than the hydrogenation temperature of surface carbon to C_2^+ hydrocarbons. Practical data show that methane decomposition can be carried out at 450 °C while the optimum hydrogenation temperature of surface carbon is about 100 °C on Ru and Co. Different metal catalysts have been tested, showing that in the same row of the periodic table, the less noble zero valent transition metals, which bind the carbidic surface carbon more strongly, show a larger carbon chain growth probability. However if the metal-carbon bond interaction becomes too large (Fe, W), stable carbides can be formed that can not be hydrogenated at the required low temperature. The optimum metals found for the step wise conversion are the well know Fischer-Tropsch metal catalysts Co and Ru. The mechanism of carbon-carbon bond formation between the surface CH_x species is very similar to that occurring in the Fischer-Tropsch reaction, as indicated by the product distribution.

The selective formation of the favourable reactive C_1 intermediate generated by methane decomposition, is high at low carbon surface coverages. At high surface carbon surface coverages (near mono-layer), mainly unreactive graphitic carbon is formed. The overall yield for the formation of C_2^+ hydrocarbons from methane depends on the methane conversion during adsorption, the selectivity for carbidic type carbon and on the selectivity for C_2^+ hydrocarbons upon hydrogenation. The maximum yield obtained on a ruthenium catalyst was 13 %. This yield is about the same as that obtained with selective oxidation or with pyrolysis. Yields obtained with oxidative coupling can be nearly twice as high.

The main problems for practical implications of the two step conversion route are due to the large difference in operation temperature between the two steps, imposed by the thermodynamics. Further the hydrogen conversion and the selectivity for C_2^+ hydrocarbon formation are low, while the separation of the reaction gases, H_2, CH_4 and C_2^+ hydrocarbons, is difficult. Therefore this route needs still a lot of exploration. The advantage of the proposed conversion route is the relative low operation temperatures applied: 450 °C compared with 800 °C for commercial synthesis gas production. Further the process does not require expensive oxidative reagentia.

The reactive carbon atoms from methane also can be used to form carbon-carbon bonds with co-adsorbed olefins, as was shown in chapter 7. The problem of performing a direct reaction between methane and e.g. ethene to propane, on

transition metal catalysts, is related to the large differences in sticking probability for dissociative adsorption. Methane will not be adsorbed together with ethene on a metal surface. Therefore methane is adsorbed in a separate step at a higher temperature. Subsequently ethene is coadsorbed at a lower temperature (50 °C) were propane can be formed upon hydrogenation of the adsorbed carbonaceous intermediates. ^{13}C labelled methane was used to demonstrate that methane can be incorporated into coadsorbed olefins, and can hence be used for alkylation reactions on supported metal catalysts. Compared to the ethylation of methane using superacids, the presented heterogeneous route is more environmental friendly and has a higher yield on methane basis. The disadvantage is related with the low olefin yield due to olefin hydrogenation and hydrogenolysis.

It has not been realized to use the surface CH_x fragments from methane in a step wise route for CO insertion, resulting in ethanal or ethanol. The formation of ethanol is slow and therefore not suitable for the proposed transient conversion route.

In heterogeneous catalysis one commonly uses the great advantage of operating under steady state conditions. However by introducing transient steps like a temperature change or pressure change, it is shown that new routes for methane conversion can be found. The principle new aspect of the proposed conversion route is the idea to use the catalyst also as intermediate reactant at the same time. In methane oligomerization the positive change of $\Delta G°$ could be circumvented in the presented two step route. In the methane addition to olefins, methane and olefin coadsorption was realized on transition metals, which is necessary for the creation of a carbon-carbon bond.

Samenvatting

Dit proefschrift beschrijft de reaktiviteit van oppervlaktekool-intermediairen op gedragen groep VIII metaalkatalysatoren. Katalytische reakties met koolwaterstoffen verlopen veelal via geadsorbeerde reaktie-intermediairen. Het bestuderen van de aard en reaktiviteit van dergelijke oppervlakte-intermediairen is van wezenlijk belang voor de heterogene katalyse. Een veel voorkomende belangrijke elementaire reaktiestap in de petrochemische industrie, is de vorming van een binding tussen twee koolstofatomen. Het vormen van een dergelijke binding, betekent meestal de vorming van meer waardevolle produkten. Er zijn veel voorbeelden van industriële processen waarbij een koolstof-koolstof-binding tot stand komt. Deze kunnen verlopen volgens allerlei soorten reaktie-intermediairen. De in dit proefschrift gepresenteerde studie beperkt zich tot de vorming van koolstof-koolstof-bindingen op gedragen groep VIII metaalkatalysatoren. Met name Fischer-Tropsch-achtige reakties die via geadsorbeerde CH_x intermediairen kunnen verlopen, zijn bestudeerd. Twee reakties staan daarbij centraal. De eerste is de omzetting van synthesegas naar koolwaterstoffen, ethanal en ethanol over rhodiumkatalysatoren. De tweede reaktie beschrijft een methode voor de omzetting van methaan naar hogere koolwaterstoffen.

Synthesegas reakties

Als reaktie op de oliecrisis in de zeventiger jaren, werd een algemene route ontworpen om koolstofhoudende verbindingen om te zetten via synthesegas (een mengsel van CO en waterstof) in benzine. Synthesegas kan worden omgezet naar methanol, naar koolwaterstoffen en naar produkten als ethanal en ethanol. Deze laatste reaktie, wordt gekatalyseerd door rhodium waarbij oxydische overgangsmetalen worden toegevoegd om de aktiviteit en selektiviteit te verhogen. Dergelijke additieven worden promotoren genoemd. De precieze werking van promotoren is een essentieel punt in de heterogene katalyse. In deze studie is de invloed van een oxydische metaalpromotor op een rhodiumkatalysator bestudeerd, waarbij met name is gekeken naar de invloed op de reaktiviteit van oppervlakte-intermediairen. Er is uitgegaan van het bekende mechanisme dat tijdens synthesegasreakties plaats kan vinden (zie figuur 1). Hierbij neemt het CH_x intermediair een centrale plaats in.

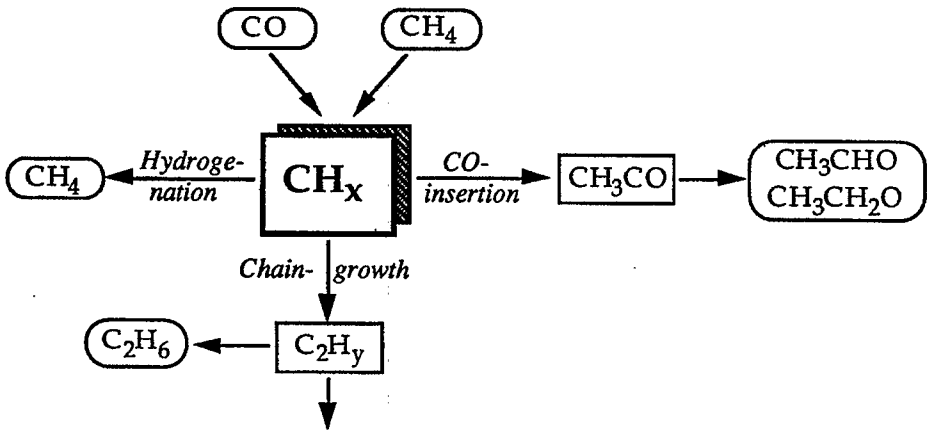

Figuur 1. Elementaire reaktie stappen die een geadsorbeerd CH_x intermediair kan ondergaan tijdens synthese gas reakties.

Het mechanisme in figuur 1 toont dat de reaktiviteit van het geadsorbeerde CH_x intermediair mede bepalend is voor de uiteindelijke produktverdeling. Gekozen is voor rhodium als katalysator, omdat dit metaal zowel de hydrogenering tot methaan, de koolstofketengroei als CO-insertie katalyseert. De invloed van de modelpromotor, vanadium, is onderzocht op de reaktiviteit van oppervlakte-intermediairen voor deze elementaire reaktiestappen alsmede voor CO dissociatie.

De vorming van geadsorbeerd C vanuit CO bleek versneld te worden door rhodium katalysatoren te promoteren met vanadium. De aktiveringsenergy voor CO dissociatie wordt hierdoor aanzienlijk verlaagd, zoals bleek uit transiënte modelexperimenten. Voor het promotiemechanisme wordt verondersteld dat vanadium vrije plaatsen, mogelijk zuurstofvakatures, op het oppervlak creëert. Deze zijn nodig om CO te laten dissociëren. De hydrogenering van het karbidische oppervlakte-intermediair naar methaan, wordt vertraagd door de aanwezigheid van vanadium, terwijl de ketengroeikans toeneemt. Vanadium wordt verondersteld de bindingssterkte van oppervlaktekool te kunnen vergroten. Dit vergroot de verblijftijd van CH_x intermediairen op het oppervlak en vergroot de kans voor de vorming van een koolstof-koolstof binding. De CO insertie in geadsorbeerde CH_x fragmenten is bestudeerd met transiënte experimenten met isotopisch gemerkt ^{13}CO. Hieruit bleek dat de reaktiecoëfficiënt voor deze stap niet vergroot wordt door vanadium. Verder bleek vanadium in staat, zuurstofhoudende oppervlakte-intermediairen te stabiliseren. Hierbij wordt de hydrogeneringssnelheid van deze intermediairen naar ethanol, vergroot.

Methaankonversie

Het tweede bestudeerde onderwerp is gerelateerd aan het algemene probleem een koolstof-koolstof binding te initiëren tussen twee methaan-moleculen. Er bestaat veel interesse om methaan om te zetten in beter transporteerbare en meer waardevolle koolwaterstoffen. Methaan is echter uiterst onreaktief door z'n edelgas-achtige konfiguratie met sterke, apolaire C-H bindingen. Direkte routes voor methaankonversie zoals oxydatieve-koppeling, selektieve-oxydatie en pyrolyse worden nog niet commercieel uitgevoerd. In huidige processen wordt methaan in meerdere stappen omgezet met water of zuurstof, in synthese gas, dat vervolgens kan worden omgezet in b.v. benzine. De omzetting naar synthesegas is duur en vindt plaats bij hoge temperatuur. Er is daarom interesse in alternatieve methoden om methaan om te zetten in koolwaterstoffen met twee of meer koolstofatomen.

De opzet voor de manier van methaanomzetting, vloeit voort uit de ontdekking dat uit CO een zeer reaktief karbidisch oppervlaktedeeltje gevormd kan worden dat koolstof-koolstofkoppeling kan ondergaan. Een dergelijk reaktie-intermediair blijkt eveneens uit methaan gevormd te kunnen worden. Er zijn twee routes opgesteld om via dit intermediair methaan te konverteren naar C_2^+ koolwaterstoffen, hetgeen is weergegeven in de onderstaande figuren.

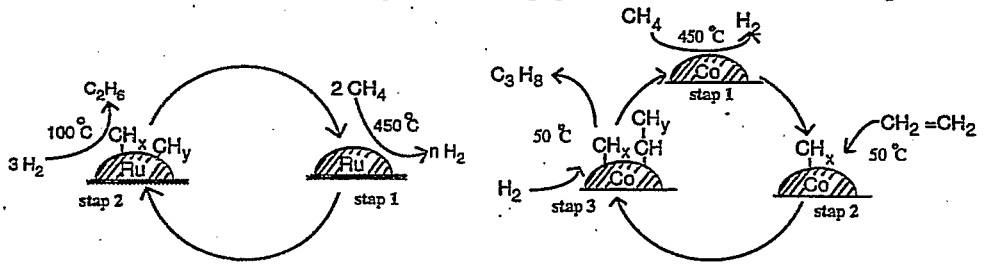

Figuur 2. Reaktie paden voor het omzetten van methaan in hogere koolwaterstoffen. Links: methaan dimerizatie of oligomerizatie. Rechts: methaan inbouw in etheen.

In de eerste stap wordt methaan ontleedt bij 450 °C op een gereduceerde groep VIII metaalkatalysator in oppervlaktekool en waterstof. Dit resulteert in drie verschillende soorten oppervlaktekool, die te onderscheiden zijn in hun hydrogeneringsreaktiviteit. De meest reaktieve is een karbidische oppervlakte-kool die al bij 50 °C reageert. Een minder reaktieve kool, reageert tussen de 200 en 300 °C met waterstof tot methaan waarbij spoortjes hogere alkanen tot hexaan gevormd worden. Dit is een amorf-achtige kool waarbij waarschijnlijk koolstof-koolstof-interakties aanwezig zijn. Bij temperaturen boven de 400 °C reageert een onreaktief grafitische kool tot methaan. De meest reaktieve, karbidisch oppervlaktekool heeft de beste eigenschappen voor het vormen van een

koolstof-koolstofbinding in een reaktie met waterstof. De optimale hydrogeneringstemperatuur voor de vorming van C_2^+ koolwaterstoffen is 100 °C voor Ru en Co. De maximale opbrengst voor C_2^+ koolwaterstoffen, behaald met een rutheniumkatalysator, is 13% en is van dezelfde grootte-orde als die verkregen met selectieve-oxydatie en pyrolyse.

Hetzelfde type oppervlaktekool kan ook een binding aangaan met een gecoadsorbeerd olefine, zoals is weergegeven in figuur 2b. Dan wordt na methaanadsorptie bij 450 °C een olefine geadsorbeerd bij lage temperatuur (50 °C) om hydrogenolyse van het olefine tegen te gaan. Bij deze temperatuur kan, in de aanwezigheid van waterstof, het olefine met een oppervlakte C_1 fragment van methaan reageren, waarbij een alkaan ontstaat met een extra koolstofatoom. De reaktiecycli kunnen probleemloos herhaald worden, indien opgewarmd wordt in waterstof om minder reaktieve koolresten te verwijderen.

De methaankoppelingsreaktie zoals uitgevoerd in stappen, geeft inzicht in het mechanisme van de vorming van een koolstof-koolstofbinding zoals die plaats kan vinden bij de Fischer-Tropschreaktie. Dit mechanisme is eveneens bestudeerd met semi-empirische, quantum-chemische berekeningen. De resultaten komen overeen met praktische metingen. De twee belangrijkste konklusies zijn dat sterker gebonden oppervlaktekool gunstig is voor de koolstofketen-groeikans en dat oppervlakte CH_x fragmenten met weinig waterstofatomen beter koppelen door een lagere repulsie tussen deze atomen.

In de heterogene katalyse streeft men meestal naar processen die continu verlopen. Door de introduktie van transiënte stappen, zoals een verandering in temperatuur en waterstofdruk, zijn alternatieve methaanconversieroutes gevonden. Hierbij is de katalysator gelijktijdig een intermediair reaktant. Bij methaanoligomerizatie kan daarmee de positieve $\Delta G°$ voor direkte methaankonversie, omzeild worden, indien het temperatuurverschil tussen de twee stappen 285 °C is. Bij methaaninbouw in een olefine wordt door de aparte methaanadsorptie, de gezamenlijke adsorptie van methaan en een olefine gerealiseerd. Dit is een voorwaarde voor het vormen van een koolstof-koolstofbinding. Op deze wijze is een alternatieve omzetting gevonden voor de bestaande route die gebruik maakt van corrosieve superzuren. De omzetting via heterogene katalysatoren is milieuvriendelijker.

Het aantrekkelijke van de nieuwe routes om methaan om te zetten in hogere koolwaterstoffen, is dat deze plaats vinden bij lagere temperaturen dan die van huidige commerciële routes, zonder gebruik te maken van oxydatieve reagentia. Praktische uitvoering van deze route is voorlopig niet aantrekkelijk door het grote temperatuurverschil tussen de twee reaktiestappen en de lage produktconcentraties.

Curriculum Vitae

Tijs Koerts werd geboren op 27 april 1964 in Haarlem. In 1983 werd aan het Rhedens Lyceum te Rozendaal het eindexamen VWO afgelegd. In datzelfde jaar begon hij met zijn scheikundestudie aan de rijksuniversiteit te Utrecht. Zijn keuzevakken waren informatica en fysische chemie. Tijdens zijn onderzoeksjaar in de vakgroep Anorganische Chemie en Katalyse, werd onderzoek verricht aan niet-selectieve methaanoxydatie over met lanthaan gestabiliseerde koperkatalysatoren. In mei 1988 werd in deze vakgroep bij Prof. J.W. Geus het doctoraalexamen behaald. Tijdens zijn studie was hij gedurende ruim een jaar aktief als studentassistent op het eerstejaarsprakticum (0.5 aanstelling).

Vanaf juni 1988 was hij in dienst bij SON/NWO bij de vakgroep Anorganische Chemie en Katalyse op de Technische Universiteit te Eindhoven, alwaar een promotie-onderzoek werd verricht. Dit onderzoek betrof de vorming en reaktiviteit van C_1-oppervlakte-intermediairen op overgangsmetaalkatalysatoren, waarvoor hij in juni 1991 van DSM de 2^e prijs voor Chemie en Technologie kreeg. De resultaten van het, bij Prof. Dr. R.A. van Santen uitgevoerde onderzoek, zijn in dit proefschrift vastgelegd, waarop hij 19 juni 1992 hoopt te promoveren.

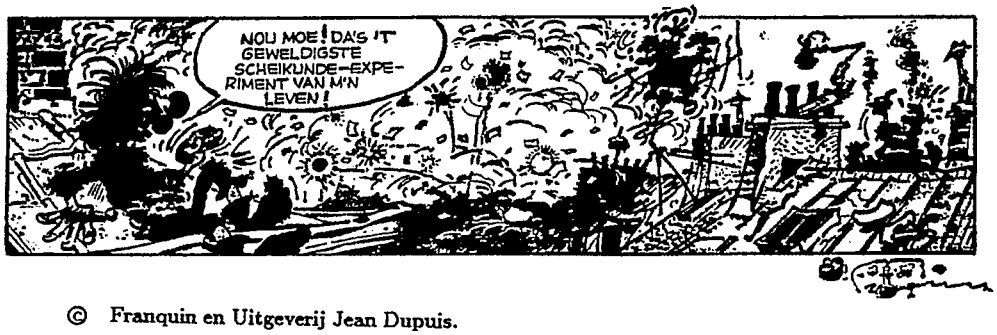

U.S. DEPARTMENT OF COMMERCE
Technology Administration
National Technical Information Service
Springfield, VA 22161 (703) 605-6000